Sodium/amino Acid Cotransporters from the SLC6 Family localizing to the luminal Membrane of Kidney and Intestine

Dissertation
zur
Erlangung der naturwissenschaftlichen Doktorwürde
(Dr. sc. nat.)

vorgelegt der
Mathematisch-naturwissenschaftlichen Fakultät
der
Universität Zürich

von

Elisa Romeo
aus
Italien

Promotionskomitee
Prof. Dr. Esther Stoeckli (Vorsitz)
Prof. Dr. François Verrey (Leitung der Dissertation)
Prof. Dr. Richard Warth

Zürich, 2006

Dedicata a
mio marito Andrea
per essermi sempre vicino,
sostenermi ed amarmi
e
alla mia piccola Ashlee Nya
che mi regala ogni giorno un'emozione nuova

TABLE OF CONTENTS

SUMMARY

Ingested dietary proteins are cleaved into small oligopeptides and single amino acids that are then absorbed across small intestine enterocytes. Similarly, small oligopeptides and single amino acids are reabsorbed across kidney proximal tubule epithelial cells to prevent their loss in the urine. The first step of this transcellular transport is the influx across the luminal brush border membrane that is mediated by symporters (cotransporters) and antiporters (exchangers). The basolateral efflux of amino acids from the epithelial cells into the extracellular space is mediated by (a) facilitated diffusion pathway(s) and exchangers.

The main focus of my doctoral thesis was the system B^0 transport, which mediates the sodium-driven uptake of a broad range of neutral amino acids into epithelial cells of small intestine and kidney proximal tubule. For many years, the B^0 transport system remained molecularly unidentified and only to some extent functionally characterized. The first B^0-type transporter was identified in 2004 by Broer's group. This transporter called B^0AT1 (broad range neutral amino acid transporter 1) belongs to the mouse gene family Slc6 (SLC6 in human) of Na^+-(and Cl^-)-dependent (neurotransmitter) transporters. Its function as Na^+-dependent neutral amino acid cotransporter was demonstrated by flux- and electrophysiological measurements of transporter expressed in *Xenopus laevis* oocytes. Unlike other members of the SLC6 family, its function does not depend on the presence of Cl^-, as expected for system B^0. The orthologue human gene SLC6A19 localizes to chromosome 5p15.33 and its defect was shown by us together with others to cause Hartnup disorder, an autosomal recessive condition characterized by an increase in the urinary excretion of neutral amino acids. This amino aciduria is often asymptomatic but can be accompanied by pellagra-like skin rash, attacks of cerebellar ataxia and other neurological or psychiatric symptoms.

Two quite similar human transporters called XT2 (Xtrp2) and XT3 (Xtrp3) have been identified earlier and represent the products of the genes SLC6A18 and 20. Together with B^0AT1, they form a separate cluster within the SLC6 family. One of these genes, SLC6A18, is localized on chromosome 5p15.33, just next to SLC6A19, whereas SLC6A20 is on chromosome 3p21.3. In the mouse genome, there are two SLC6A20-related genes arranged sequentially on chromosome 9 that probably have arisen from a duplication that took place after the evolutionary separation of rodents and primates. The

first of these gene products identified in mice was named XT3, whereas the second one, XT3s1, is 90% identical to it but resembles, in terms of primary structure and tissue distribution, more human XT3. In human, the single XT3 gene gives rise by alternative splicing to two isoforms. One of these human XT3 isoforms and the rodent XT3s1 have been shown in 2005 to correspond to system imino, that transports L-Pro as well as some other substrates such as pipecolate and N-methylated amino acids (e.g. MeAIB and sarcosine) with a high apparent affinity and have correspondingly been renamed SIT1 or Imino^{B}.

The original studies on the still orphan transporter XT2 and mouse XT3 showed that their mRNAs are expressed in kidney and possibly also in small intestine. Expression experiments of XT2 and mouse XT3 in *Xenopus laevis* oocytes and in other expression systems have not revealed their function. A recently published study on a XT2 knock out mouse showed that these mice loose some glycine in their urine and possibly little quantities of other neutral amino acids as well, suggesting that this transporter might similarly to B^{0}AT1 transport amino acids.

In the first part of my doctoral thesis, I focused on the production of a knockout mouse for XT3. Because of several technical problems, this project was discontinued after few months.

Our interest moved then to the question of the putative role of these four B^{0}AT1-related gene products in mouse. Therefore, we localized their expression by quantifying their mRNAs in different tissues using real time RT-PCR and tested their localization at the protein level in kidney and intestine using Western blotting an immunofluorescence. Furthermore, we tested in C57BL/6J mice subjected to low and high sodium diets or treatments inducing metabolic acidosis and alkalosis whether the regulation of these transporters at the mRNA and protein level in kidney plays a role. Because these different treatments did not influence the expression of any of the transporters tested we concluded that they essentially play a constitutive role.

Quantitative real-time RT-PCR showed that the mRNAs of the four B^{0}AT-cluster members are abundant in kidney, whereas only those of B^{0}AT1 and XT3s1/SIT1 are elevated in small intestine. In brain, the XT3s1/SIT1 mRNA was more abundant than the other B^{0}AT-cluster mRNAs. We showed by immunofluorescence that all four mouse B^{0}AT-cluster transporters localize, with differential axial gradients, to the brush border

membrane of proximal kidney tubule and, with the possible exception of XT3, also of intestine. Deglycosylation and Western blotting of brush border proteins demonstrated the glycosylation and confirmed the luminal localization of B^0AT1, XT2 and XT3.

Taken together, the work performed during this PhD thesis has contributed to the characterization of the formerly orphan Slc6 transporters of the B^0AT cluster. In particular, the localization studies have clarified the precise distribution of B^0AT1 and the related transporters in the brush border membrane of kidney proximal tubule and small intestine. Furthermore, these studies have shown that the B^0AT cluster transporters are constitutive elements of amino acid reabsorbing epithelia, subjected only to moderate regulatory changes, and set the basis for the detailed *in vivo* analysis of the mouse transporter XT2 (Slc6a18).

ZUSAMMENFASSUNG

Mit der Nahrung aufgenommene Proteine werden in kleine Oligopeptide und Aminosäuren gespalten, welche anschliessend im Dünndarm absorbiert werden. In ähnlicher Weise werden solche Oligopeptide und Aminosäuren im proximalen Tubulus der Niere über Epithelzellen reabsorbiert, um deren Ausscheidung mit dem Urin zu verhindern. Der erste Schritt dieses transzellulären Transportes ist die Aufnahme der Aminosäuren über die luminale Bürstensaummembran, was durch Symporter (Cotransporter) und Antiporter (Austauscher) gewährleistet wird. Der basolaterale Efflux der Aminosäuren aus den Epithelzellen in den extrazellulären Raum wird sowohl durch erleichterte Diffusion als auch durch Austauscher vermittelt.

Der Hauptaspekt dieser Arbeit richtete sich auf das B^0-Transportsystem, welches die Natrium-abhängige Aufnahme von neutralen Aminosäuren in Epithelzellen des Dünndarms und des proximalen Tubulus in der Niere vermittelt. Während vieler Jahre blieb das B^0-Transportsystem molekular unbekannt und war nur teilweise funktionell charakterisiert. Der erste B^0-artige Transporter wurde von der Arbeitsgruppe Bröer im Jahr 2004 identifiziert. Dieser Transporter, B^0AT1 („broad range amino acid tranporter 1“), gehört der Mausgenfamilie Slc6 (human SLC6) der Na^+-(und Cl^-)-abhängigen (Neurotransmitter) Transporter an. Mittels Expression in *Xenopus laevis* Oozyten und nachfolgenden Flux- und elektrophysiologischen Messungen wurde gezeigt, dass es sich bei B^0AT1 um einen Na^+-abhängigen Cotransporter, der neutrale Aminosäuren transportiert, handelt. Anders als bei anderen Mitgliedern der Slc6-Familie und als für das System B^0 erwartet, hängt dessen Funktion nicht von der Anwesenheit von Chlorid ab. Das orthologe, humane Gen SLC6A19 ist auf dem Chromosom 5p15.33 lokalisiert. Es konnte von uns, zusammen mit anderen Gruppen, gezeigt werden, dass ein Defekt in diesem Gen zur autosomal-rezessiven Hartnup Krankheit führt, welche durch eine erhöhte Ausscheidung von neutralen Aminosäuren im Urin charakterisiert ist. Diese Aminosäureausscheidung verläuft oft asymptomatisch, kann aber von einem „pellagra“-ähnlichen Hautausschlag, zerebellaren Ataxie-Attacken und anderen neurologischen oder psychiatrischen Symptomen begleitet werden.

Zwei ganz ähnliche humane Transporter, XT2 (Xtrp2) und XT3 (Xtrp3), wurden schon früher identifiziert und entsprechen den Genprodukten SLC6A18 und SLC6A20.

Zusammen mit B^0AT1 bilden diese einen separaten Cluster in der Familie SLC6. Eines dieser Gene, SLC6A18, ist gleich neben SLC6A19 auf dem Chromosom 5p15.33 lokalisiert, während SLC6A20 auf Chromosom 3p21.3 zu finden ist. Im Mausgenom befinden sich zwei dem SLC6A20 verwandte Gene hintereinander auf dem Chromosom 9. Diese sind wahrscheinlich durch eine Duplikation entstanden, die nach der evolutionären Trennung von Nagern und Primaten stattgefunden hat. Das erste dieser in der Maus identifizierten Genprodukte wurde XT3 genannt. Das zweite Genprodukt, XT3s1, ist zu 90 % identisch mit dem XT3, ähnelt aber bezüglich der Primärstruktur und der Gewebeverteilung mehr dem humanen XT3. Beim Menschen existieren in Folge von alternativem Splicing des einzigen XT3-Gens zwei Isoformen. In 2005 wurde gezeigt, dass die eine dieser beiden humanen Isoformen sowie das murine XT3s1 dem Imino-System angehören, das L-Pro sowie einige andere Substrate wie Pipecolate und N-methylierte Aminosäuren (z. B. MeAIB und Sarcosin) mit einer hohen apparenten Affinität transportiert. Daher wurden diese Transporter in SIT1 oder $Imino^B$ umbenannt.

Studien an den Orphantransportern XT2 und XT3 (Maus) ergaben, dass deren mRNAs in der Niere und möglicherweise im Dünndarm exprimiert werden. Die Expression von XT2 und Maus-XT3 in *Xenopus laevis* Oozyten und anderen Expressionssystemen führte zu keinem Ergebnis bezüglich der Funktion dieser Transporter. Eine kürzlich erschienene Studie an XT2 Knock-out-Mäusen ergab, dass diese Tiere Glycin und möglicherweise kleine Mengen anderer neutraler Aminosäuren im Urin ausscheiden, was nahe legen könnte, dass dieser Transporter, ähnlich dem B^0AT1, neutrale Aminosäuren transportiert.

Im ersten Teil meiner Doktorarbeit konzentrierte ich mich auf die Herstellung einer Kock-out-Maus für XT3. Aufgrund verschiedener technischer Probleme wurde dieses Projekt nach wenigen Monaten beendet.

Unser Interesse wandte sich in der Folge der Untersuchung der mutmasslichen Rolle dieser vier B^0AT1-verwandten Genprodukte in der Maus zu. Wir lokalisierten die Expression dieser Gene einerseits mittels RT-PCR, wobei die mRNA-Mengen in verschiedenen Geweben quantitativ bestimmt wurden, und andererseits mittels Western Blot Analyse und Immunfluoreszenz, wobei die Expression der Proteine in Niere und Darm untersucht wurde. Im weiteren wurde untersucht, ob diese Transporter in der Niere unter gewissen Bedingungen auf der Stufe der mRNA bzw. des Proteins reguliert

werden, indem C57BL/6J Mäuse einer natriumarmen bzw. -reichen Diät unterworfen oder in einer Weise behandelt wurden, dass eine metabolische Azidose bzw. Alkalose induziert wurde. Da die unterschiedlichen Behandlungen keinen Einfluss auf die Expression eines dieser Transporter hatte, schlossen wir daraus, dass diese im Wesentlichen eine konstitutive Rolle spielen.

Die quantitative Real-time RT-PCR ergab, dass die mRNAs aller vier Mitglieder des B^0AT-Clusters reichlich in der Niere vorkommen, während im Dünndarm nur diejenigen von B^0AT1 und XT3s1/SIT1 erhöht waren. Im Gehirn war XT3s1/SIT1 mRNA reichlicher vorhanden als die übrigen mRNAs des B^0AT-Clusters. Mit Hilfe der Immunfluoreszenz konnten wir nachweisen, dass alle vier Transporter des Maus B^0AT-Clusters in der Bürstensaummembran des proximalen Nierentubulus exprimiert wurden, wobei die Expression der einzelnen Transporter in den Segmenten S1-3 entlang des Tubulus unterschiedlich war. Mit etwaiger Ausnahme von XT3 wurden die Transporter auch im Darm nachgewiesen. Deglykosylierungs-Experimente und Western Blot Analysen von Bürstensaummembran-Proteinen konnten die Glykosylierung der Transporter nachweisen sowie die luminale Lokalisierung von B^0AT1, XT2 und XT3 bestätigen.

Zusammenfassend lässt sich sagen, dass diese Arbeit sehr zur Charakterisierung der bisherigen Slc6 Orphantransporter des B^0AT-Clusters beigetragen hat. Speziell die Lokalisierungsstudien haben die präzise Verteilung von B^0AT1 und dessen verwandten Transportern in der Bürstensaummembran des proximalen Tubulus in der Niere und des Dünndarms verdeutlicht. Im weiteren zeigten diese Untersuchungen, dass die Transporter des B^0AT-Clusters konstitutive Elemente von Aminosäure-reabsorbierenden Epithelien sind, nur moderaten regulatorischen Veränderungen unterliegen, und die Basis für die detaillierte *in vivo* Analyse des Maus-Transporters XT2 (Slc6a18) bilden.

INTRODUCTION

1. General aspects of nutrition

The survival of all living organisms strictly depend on a source of energy, required from cells to carry out all functions connected with life. Animals get their energy from ingestion of food, which is mainly constituted by proteins, carbohydrates and lipids. To be used by the cells, these compounds, which are usually macromolecules, need to be cleaved into smaller molecules. Specific sets of enzymes in the mouth, stomach and intestine are responsible for cleavage of large molecules, in order to facilitate their entry in the cells.

Inside the cells two types of chemical reactions occur: synthetic (anabolic) and breakdown (catabolic). Synthetic reactions are those in which molecules are linked together to form a more complex compound while breakdown reactions are those in which a complex compound is split into simpler molecules. One important difference between them is that anabolic (synthetic) reactions generally require energy (endothermic), whereas catabolic reactions generally produce it (exothermic). In fact, one important function of catabolic reactions is to liberate energy.

1.1 Protein metabolism

A major component of food is protein. The proteins ingested as part of our diet are not the same proteins required by the body, nor can large molecules be absorbed from the gut. Therefore, these proteins are digested and their components, amino acids, di- and tripeptides, are absorbed into the blood stream.

Proteins are the main constituent of nitrogen metabolism, which is as important as carbohydrate and lipid metabolism (Figure 1). Proteins make up the structural tissue for muscles and tendons, transport oxygen, haemoglobin, catalyze all biochemical reactions as enzymes, and regulate reactions as hormones. Our body must be able to synthesize the many proteins, amino acids, and other non-protein nitrogen containing compounds

needed for growth, replacement, and repair. Proteins in excess are used to supply energy or build reserves of glucose, glycogen, or lipids.

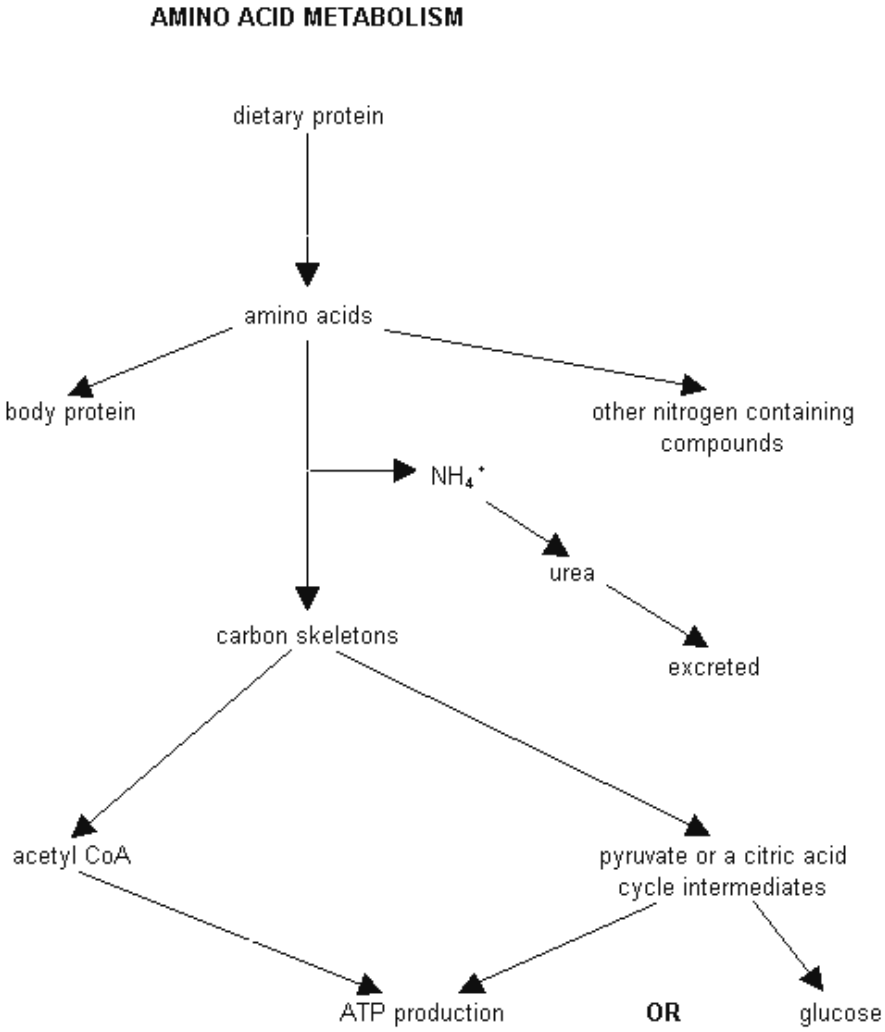

Figure 1. Amino acid metabolism. The scheme shows the fate of dietary proteins after their breakdown to single amino acid. For details, see the text.

The "nitrogen or amino acid pool" is a grand mixture of amino acids available in the cell derived from dietary sources or the degradation of protein. Since proteins and amino acids are not stored in the body, there is a constant turnover, some proteins being synthesized while others degraded. For example, some liver and plasma proteins have a half-life of 180 days or more, while some enzymes and hormones may be recycled in a matter of minutes or hours. Each day, some amino acids are catabolized producing energy and ammonia. The ammonia is mostly converted to urea and excreted from the body and represents a drain on the nitrogen pool. A nitrogen balance is achieved by a

healthy person when the dietary intake is balanced by the excretion, mostly as urea wastes. If nitrogen excretion is greater than the nitrogen content of the diet, the person is said to be in negative nitrogen balance. This is usually interpreted as an indication of tissue destruction. If the nitrogen excretion is less than the content of the diet, a positive nitrogen balance indicates a net formation of protein.

Amino acids are divided into two classes depending on whether they can be synthesized in the human body (non-essential amino acids) or whether they must be supplied in the diet (essential) (Table 1).

Non-essential amino acids	Essential amino acids
Alanine	Tryptophan
Asparagine	Lysine
Aspartate	Methionine
Cysteine	Phenylalanine
Glutamate	Threonine
Glutamine	Valine
Glycine	Leucine
Proline	Isoleucine
Serine	Histidine (only in children)
Tyrosine	Arginine (only in children)

Table 1. Essential and non-essential amino acids. The twenty classical proteogenic amino acids are divided in two classes depending on the ability of human beings to synthesize them. Two essential amino acids, histidine and arginine, are considered so only for children and not for adults.

Non-essential amino acids are synthesized from the products of their catabolism - i.e. acetyl CoA, pyruvate or the relevant citric acid cycle intermediate. The amino group is donated by glutamate and added by transamination reactions.

Eight amino acids are generally regarded as essential for humans: tryptophan, lysine, methionine, phenylalanine, threonine, valine, leucine, isoleucine. Two others, histidine and arginine are essential only in children.

The distinction between essential and non-essential amino acids is somewhat unclear, as some amino acids can be produced from others. The sulfur-containing amino acids, methionine and homocysteine, can be converted into each other but neither can be synthesized from scratch in humans. Likewise, cysteine can be only made from homocysteine. So, for convenience, sulfur-containing amino acids are sometimes considered a single pool of nutritionally-equivalent amino acids. Likewise, arginine, ornithine, and citrulline, which are interconvertible by the urea cycle, are considered a single pool.

The essential amino acids are synthesized in microorganisms (bacteria and yeasts) and passed through the food chain until they reach us in our diet. One of the pathways essential to life that is carried out by bacteria is the "fixation" of atmospheric nitrogen initially as inorganic nitrate and ultimately as amino groups in amino acids. Higher organisms cannot perform this function.

Amino acids are used in the body for synthesis of proteins, purines and pyrimidines (components of nucleotides), catecholamines (adrenaline and noradrenalin), neurotransmitters, histamine and porphyrins (the central oxygen binding component of haemoglobin). The synthesis of new proteins is very important during growth. In adults new protein synthesis is directed towards replacement of proteins as they are constantly turned over. Production of other components is also extremely important for nucleic acids synthesis, for interorgan communication, for central and peripherical nervous system activity and for many other processes.

Moreover, amino acids are used as a biological fuel. About 10% of energy production in humans is from amino acids. The percentage is much higher in carnivores, whose diet contains much protein.

2. Amino acid absorption in intestine

2.1 The gastrointestinal tract

The gastrointestinal tract consists of both the series of hollow organs stretching from the mouth to the anus and the several accessory glands and organs that add secretions to these hollow organs. Each of these organs, separated from each other at key locations

by sphincters, has evolved to serve a specialized function. The mouth and oropharynx are responsible for chopping food into small pieces, lubricating it, initiating carbohydrate and fat digestion, and propelling the food into the esophagus. The esophagus acts as a conduit to the stomach, which temporarily stores food and initiates digestion by churning and by secreting proteases and acid. The small intestine continues the work of digestion and is the primary site for the absorption of nutrients. The large intestine reabsorbs fluids and electrolytes and stores the fecal matter before expulsion from the body. The accessory glands and organs include the salivary glands, pancreas and liver. The pancreas secretes digestive enzymes into the duodenum, in addition to secreting HCO_3^- to neutralize gastric acid. The liver secretes bile, which the gallbladder stores for future delivery to the duodenum during a meal. Bile contains bile acids, which play a key role in the digestion of fats.

A cross section through a generic piece of stomach or intestine shows the characteristic layered structure of mucosa, submucosa, muscle and serosa (Figure 2A).

The mucosa consists of the epithelial layer, as well as an underlying layer of loose connective tissue known as the lamina propria, which contains capillaries, enteric neurons, and immune cells (e.g. mast cells), as well as a thin layer of smooth muscle known as the lamina muscularis mucosae. The surface area of the epithelial layer is amplified by several mechanisms. Most cells have microvilli on their apical surfaces. In addition, the layer of epithelial cells can be evaginated to form villi or invaginated to form glands (or crypts) (Figure 2B). Finally, on a grosser scale, the mucosa is organized into large folds.

The submucosa consists of loose connective tissue and larger blood vessels. The submucosa may also contain glands that secrete material into the GI lumen.

The muscle layer, the muscularis externa, includes two layers of smooth muscle. The inner layer is circular whereas the outer layer is longitudinal. These muscles are responsible for peristalsis, which is a progressive wave of relaxation, followed by contraction. Enteric neurons are present between these two muscles layers.

The serosa is an enveloping layer of connective tissue that is covered with squamous epithelial cells.

2.2 Digestion of proteins

Digestion involves the conversion of dietary food nutrients to a form that the small intestine can absorb. For carbohydrates and lipids, these digestive processes are initiated in the mouth by salivary and lingual enzymes: amylase for carbohydrates and lipase for lipids; protein digestion is initiated in the stomach by gastric proteases. Digestion is completed in the small intestine by the action of both pancreatic enzymes and enzymes at the brush border of the small intestine. Pancreatic enzymes, which include lipase, chymotrypsin and amylase, are critical for the digestion of lipids, proteins and carbohydrates respectively. The enzymes on the luminal surface of the small intestine complete the digestion of carbohydrates and proteins.

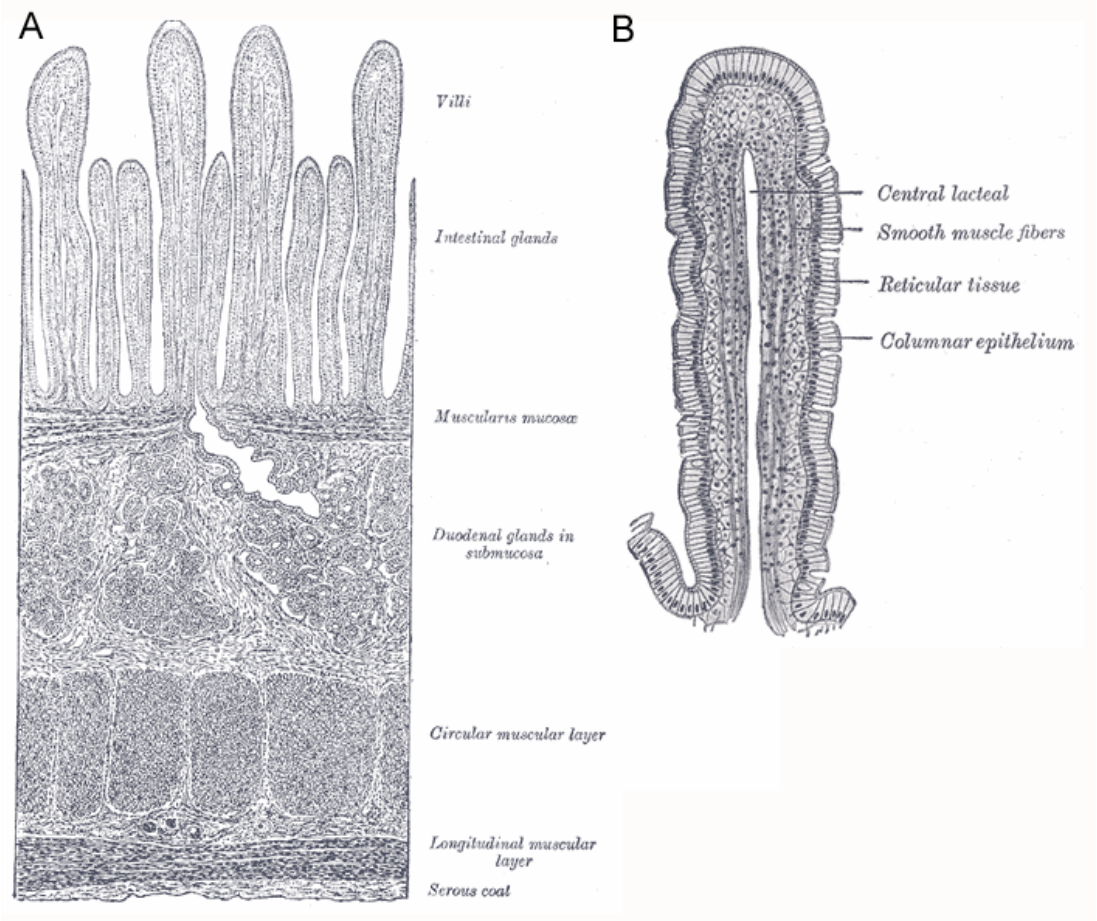

Figure 2. The small intestine. A. The drawing shows the different layers of intestinal wall. B. A drawing of a intestinal villus with its structure. The columnar epithelium is formed by enterocytes and goblet cells. For details see text. (http://www.bartleby.com/107/248.html).

Dietary proteins are a major component of food and they are usually ingested as large polypeptides, which are broken down to individual amino acids or short peptides before being absorbed into the blood stream.

Large polypeptides ingested with the diet undergo a first cleavage in the stomach where hydrochloric acid denatures their structure exposing the peptide bonds to the digestive enzymes. Hydrochloric acid also converts the inactive form of the enzyme pepsinogen to its active form pepsin. Pepsin cleaves proteins into smaller polypeptides and some amino acids. The digestion of proteins continues in the small intestine, where proteolytic enzymes produced by the pancreas and activated such as trypsin, chymotrypsin, carboxypeptidases and others are released. Trypsin cleaves peptide bonds next to the amino acids lysine and arginine. Chymotrypsin cleaves peptide bonds next to the amino acids phenylalanine, tryptophan, tyrosine, methionine, asparagine, and histidine. Carboxypeptidases cleave amino acids from the acid (carboxyl) ends of polypeptides. Other proteases are for instance elastase and collaganase that cleave polypeptides into smaller polypeptides and tripeptides, aminopeptidases that cleave amino acids from the amino ends of small polypeptides (oligopeptides) and tripeptidases that cleave tripeptides to dipeptides and amino acids.

2.3 Amino acid absorption

The cells of the small intestine absorb amino acids and have peptidase enzymes on their surface that split most of the dipeptides and tripeptides into single amino acids. Amino acids are then co-transported into enterocytes with Na^+, through a variety of specialized amino acid transporters, like heterodimeric transporter family (Dave et al., 2004), ATB^0 (Avissar et al., 2001; Kekuda et al., 1997), B^0AT1 (Broer et al., 2004), the IMINO-system transporter SIT1 (Kowalczuk et al., 2005; Takanaga et al., 2005) and many others (Ganapathy, 1994; Ganapathy, 2001). Di- and tri-peptides and some amino acids are co-transported with H^+ by members of the PEPT family (SLC15) (Ganapathy, 1994; Ganapathy, 2001; Leibach and Ganapathy, 1996; Liang et al., 1995) and PAT1 (SLC36) respectively (Anderson et al., 2004).

Cells lining the intestinal mucosa are specialized polarized cells (Figure 3) (Madara and Trier, 1986). The distinct feature of these epithelial cells is the asymmetric distribution of macromolecules and organelles both in cytoplasm and in two plasma membrane domains (Achler et al., 1989; Drenckhahn and Dermietzel, 1988).

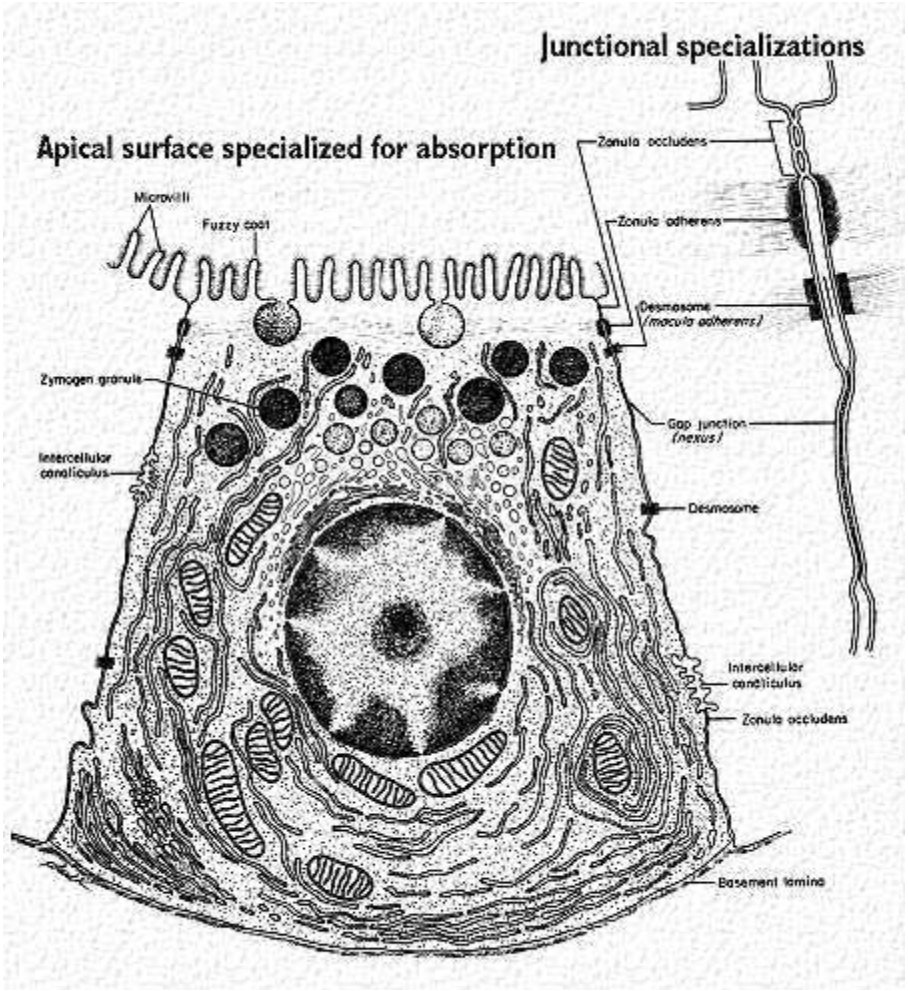

Figure 3. Polarized cell. The drawing shows some features of polarized cells lining the intestinal mucosa and the proximal kidney tubule. The apical surface is kept distinct from the basolateral one by the presence of specialized junctions (tight junctions). (http://www.cytochemistry.net/Cell-biology)

The polarized phenotype of the cell is mainly dependent on actin cytoskeleton, spectrin-based membrane skeleton and microtubules (Burgess et al., 1987). Tight junctions also have a fundamental role during development of cell surface polarity, since they form an intramembrane diffusion fence that restricts diffusion of lipids in the plasma membrane. They form the limit between the apical and the basolateral membrane domain of the polarized epithelial cells that have distinct protein and lipid compositions. The apical

membrane domain, facing the external milieu (lumen), is characterised by specialised structures such as microvilli (Mooseker, 1985; Mooseker et al., 1984). The presence of microvilli greatly increases the absorptive surface of these cells.
Besides tight junctions, other junctional complexes such as adherent junctions and desmosomes are responsible for the maintenance of the structure of the epithelial monolayer and the polarity of the cells.

3. Amino acid reabsorption in kidney

3.1 Anatomy and physiology of the kidney

The kidneys serve three essential functions. They function as filters, removing metabolic products and toxins from the blood and excreting them through the urine. They also play a key homeostatic role by regulating the body's fluid status, electrolyte balance, and acid-base balance. Finally, kidneys produce hormones involved in erythrogenesis, calcium metabolism and regulation of blood pressure and blood flow. The mammalian kidneys perform certain functions that in lower vertebrates are shared by other organs such as the skin and bladder of amphibians, the gills of fishes and the salt glands of reptiles and birds.
Mammalian kidneys are paired, bean-shaped structures, one located on each side against the dorsal inner surface of the lower back, outside the peritoneum. The kidneys receive a remarkably large blood flow (20-25% of the total cardiac output at rest) corresponding thus to the total blood volume every 4-5 minutes.
The outer functional layer, the cortex, is covered by a tough capsule of connective tissue. The inner functional layer, the medulla, sends papillae projecting into the renal pelvis that gives rise to the ureters, which empty into the urinary bladder.
Urine contains water and other by-products of metabolism, such as urea as well as other solutes, like NaCl, KCl, phosphates and others that are present at concentrations in excess of the body's requirement.
The functional unit of the mammalian kidney is the nephron, an intricate epithelial tube that is closed at its beginning but open at its distal end. Each kidney contains around one million nephrons (in human), which empty into collecting ducts. These ducts

combine to form papillary ducts, which eventually empty into renal pelvis. At the closed end, the nephron is expanded to form a cup-shaped Bowman's capsule. The lumen of the capsule is continuous with the narrow lumen that extends through the renal tubule. A tuft of capillaries forms the renal glomerulus inside Bowman's capsule. This remarkable structure is responsible for the first step in urine formation. An ultrafiltrate of the blood passes through the single-cell layer of the capillary walls, through a basement membrane, and finally through another single-cell layer of epithelium that forms the wall of Bowman's capsule. The ultrafiltrate accumulates in the lumen of the capsule to begin its trip through the various segments of the renal tubule, finally descending the collecting duct and eventually into the renal pelvis.

The wall of the renal tubule is one cell layer thick; this epithelium separates the lumen, which contains the ultrafiltrate, from the interstitial fluid. In some portions of the nephron, the epithelial cells are morphologically specialized for transport, bearing a dense pile of microvilli on their luminal, or apical, surfaces and deep infolding of their baso-lateral membrane. The epithelial cells of the proximal tubule are tied together by leaky tight junctions, which permit limited paracellular diffusion between the lumen and interstitial space surrounding the renal tubule.

The nephron can be divided into three main regions: the proximal nephron (Bowman's capsule and proximal tubule), the loop of Henle (with a descending limb and an ascending limb) and the distal nephron (after the ascending limb of the loop of Henle merges into the distal tubule). Distal tubules from many nephrons merge into a unique collecting duct.

The number of nephrons per kidney varies from several hundred in lower vertebrates to many thousands in small mammals, and a million or more in humans and other large species.

The loop of Henle, found only in the kidneys of birds and mammals, is considered to be of central importance in concentrating the urine. Vertebrates lacking the loop of Henle are incapable of producing urine that is hyperosmotic to the blood.

In mammals, the nephron is so oriented that the loop of Henle and the collecting duct lie parallel to each other. The glomeruli are found in the renal cortex, and the loops of Henle reach down into the papillae of the medulla; thus, the nephrons are arranged in a radiating fashion within the kidney.

Nephrons can be divided into two groups:

- juxtamedullary nephrons, which have their glomeruli in the inner part of the cortex and long loops of Henle that plunge deeply into the medulla;
- cortical nephrons, which have their glomeruli in the outer cortex and relatively short loops of Henle that extend only a short distance into the medulla.

The final urine composition is the result of three main processes:

- glomerular filtration of plasma to form an ultrafiltrate in the lumen of the Bowman's capsule;
- tubular reabsorption of approximately 99% of the water and most of the salts from the ultrafiltrate leaving behind and concentrating waste products such as urea;
- tubular secretion of a number of substances via active transport in nearly all instances.

3.2 The Proximal tubule

Based on its appearance at relatively low magnification, the proximal tubule can be divided into a convoluted part, the proximal convoluted tubule and a straight part, the proximal straight tubule. However, based on ultrastructure, the proximal tubule can alternatively be subdivided into three segments: S1, S2 and S3. The S1 segment starts at the glomerulus and includes the first portion of the proximal convoluted tubule. The S2 segment starts within the second half of the proximal convoluted tubule and continues into the first half of the proximal straight tubule. Finally, the S3 segment includes the distal half of the proximal straight tubule that extends into the medulla.

Both the apical (luminal) and the basolateral (peritubular) membranes of proximal-tubule cells are extensively amplified. Therefore, the apical membrane shows infolding in the form of a well-developed brush border system (Figure 3). This enlargement of the apical surface area correlates with the main function of this nephron segment, namely, the reabsorption of the bulk of the filtered fluid back into the circulation. From the S1 to the S3 segments, cell complexity progressively declines, correlating with a gradual decrease of reabsorptive rates along the tubule, thus, the cells exhibit a progressively less developed brush border system, diminished complexity of lateral cell interdigitations, a lower basolateral cell membrane area and a decrease in the number of mitochondria.

The basolateral membranes of adjacent proximal-tubule cells form numerous interdigitations, bringing abundant mitochondria in close contact with the plasma membrane. The interdigitations of the lateral membranes also form an extensive extracellular compartment bounded by the tight junctions at one end, and by the basement membrane of the epithelium at the other end. Proximal-tubule cells contain lysosomes, endocytic vacuoles, and a well-developed system of endoplasmic reticulum. Proximal-tubule cells are also characterized by a prominent Golgi apparatus, which is important for synthesizing many membrane components, sorting them and targeting them to specific surface sites.

3.3 Amino acid reabsorption

Amino acids released in the blood stream are reabsorbed by the proximal-tubule cells. Specific amino acid transporters, like in the small intestine, are localized in the brush border structure present at the apical site of these cells where they take up their substrates that are dissolved in the ultrafiltrate.

The amino acid transport machinery is not uniform along the proximal tubule; just after glomerular filtration occurs, the amino acid concentration in the ultrafiltrate is similar to that found in plasma, whereas at the end of the proximal tubule it is lower. Thus, while the first epithelial cells of the proximal tubule face a high solute concentration, more distal epithelial cells face decreasing substrate concentrations that can more effectively be reabsorbed by transporters with high affinity.

4. Amino acid transporters

4.1 General aspects

Amino acid transporters are macromolecules synthesized by all cell types in order to move such solutes across the cell membranes. They usually display a tertiary structure with membrane spanning segments that have important functions in the transport mechanism. These segments are mainly constituted by α-helices, which are particularly suitable to cross the lipid bilayer.

In kidney proximal tubule and small intestine, specialized amino acid transporters are localized to either one of the two specialized membranes, the apical (luminal) membrane or the basolateral one. Transporters at the apical membrane allow the passage of specific amino acids from the extracellular medium to the cell cytoplasm while the ones localized at the basolateral membrane are responsible for moving amino acids from the cell into the blood stream. This active transport process is referred as the transcellular pathway, which differs from the paracellular one where the substances do not cross the cell but pass between adjacent cells. In polarized epithelia, like the ones found in the small intestine and in the proximal tubule, the apico-basal polarity is important for the establishment of adhesive junctions and the formation of a paracellular diffusion barrier that prevents the movement of solutes across the epithelium (Gibson and Perrimon, 2003).

Once in the blood, amino acids are distributed throughout the body: they are taken up by tissues (particularly by the liver and the muscle) and they pass through the blood-brain barrier to enter the central nervous system (Smith, 2000; Stoll et al., 1993). In the placenta, amino acids pass through the placental barrier in both directions between the maternal and the foetus sides (Cariappa et al., 2003).

Amino acid transporters are also present in the membranes of some intracellular organelles, such as lysosomes and mitochondria (Boll et al., 2004; Porter, 2000).

4.2 Amino acid transport systems

The study of amino acid transport into animal cells actually began in 1914 with the observations of Van Slyke and Meyer who demonstrated tissue accumulation of amino acids against a concentration gradient. Description of individual transport activities began in the early 1960s with the pioneering work of Christensen ‘s laboratory (Oxender and Christensen, 1963). They described transport systems with different specificity for amino acids in mammalian cells (mainly erythrocytes, hepatocytes, and fibroblasts) (Christensen, 1990), and identified general properties of mammalian amino acid transporters: stereospecificity (transport selectivity for L-stereoisomers) and broad substrate specificity (several amino acids share a transport system). Since these initial studies, the main functional criteria used to define amino acid transporters have been

the type of amino acid transported (acidic, zwitterionic, or basic as well as other characteristics of the side chain), the precise substrate specificity, the kinetic properties, and the thermodynamic properties (equilibrative or uphill transport). This functional classification has been retained to date, since structural information on higher eukaryote amino acid transporters is incomplete (Broer, 2002; Palacin et al., 1998; Verrey et al., 2005). Another classification, involving all types of proteins (excluding pumps and channels) moving solutes from one side of a biological membrane to another (solute carriers, SLC), has been recently developed by the HUGO (the Human Genome Organization) Gene Nomenclature Committee. The new nomenclature has been introduced in order to uniform the names of proteins belonging to the SLC series (the complete list is available on the web site: http://www.gene.ucl.ac.uk/nomenclature/). There are 43 SLC families with overall more than 320 transporter genes (Wright M. W. et al., 2003). Out of these families, 9 are dedicated to or contain members that perform amino acid transport (Figure 4) (Boll et al., 2004; Chen et al., 2004; Gasnier, 2004; Halestrap and Meredith, 2004; Hediger et al., 2004; Kanai and Hediger, 2004; Mackenzie and Erickson, 2004; Palacin and Kanai, 2004; Verrey et al., 2004).

The original nomenclature introduced by Christensen was based on the first observations collected with functional studies in isolated cells and plasma membranes of perfused organs. Focus of these investigations was the substrate specificity, the kinetics, the driving forces and the different regulatory mechanisms which led to the identification of different transport systems for amino acids in mammalian plasma membranes (Christensen, 1985; Christensen, 1989). In most of the cases, the name of the transporter has one or more letters, which identify the specific amino acid transporter or the class of amino acids and, in general, a capital letter indicates Na^+ dependence, whereas a small letter Na^+ independence. This classification has been adopted previously for so called transport systems before the transporters had been molecularly identified.

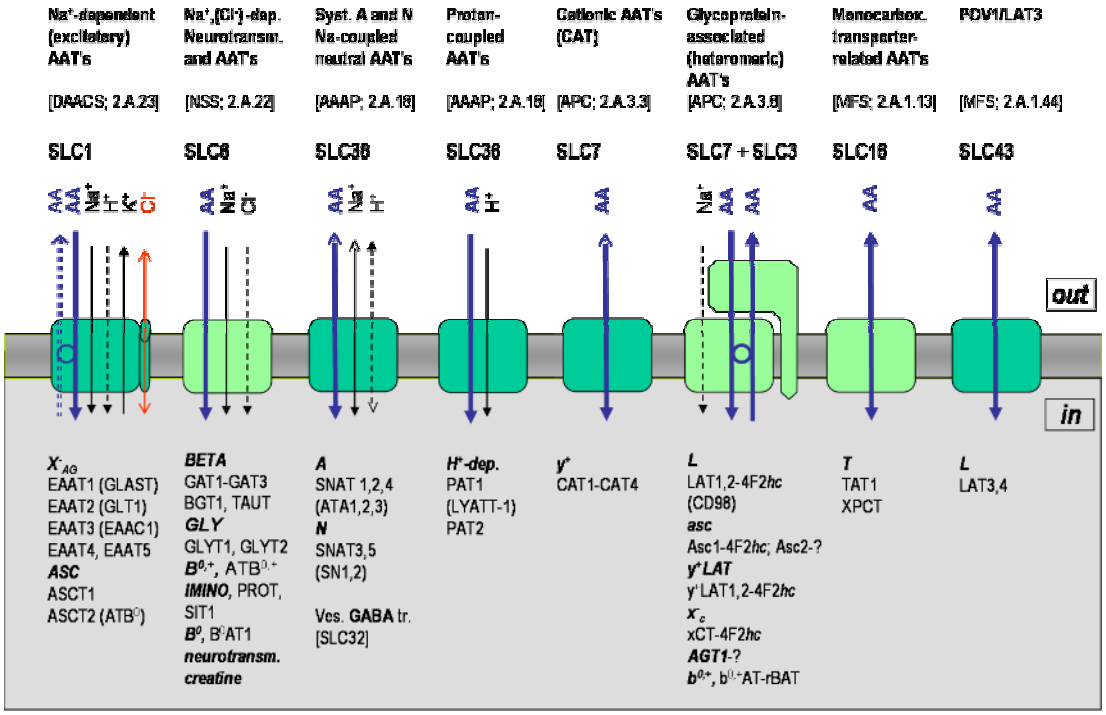

Figure 4. Mammalian amino acid transporter families. The arrows indicate the co-/counter-transport. Dashed arrows indicate that only some of the members of the family transport that substance. Slide courtesy of F. Verrey.

4.3 The SLC6 family

The SLC6 family comprises transporters that mediate solute translocation across cell plasma membranes by coupling solute transport to the cotransport of sodium down its electrochemical gradient. Some transporters cotransport chloride as well. The family includes transporters for the inhibitory neurotransmitters GABA and glycine, for the monoamine transmitters norepinephrine, serotonin, and dopamine, for the osmolytes betaine and taurine, the amino acid proline, and the metabolic compound creatine. In addition, this family includes a system B^{0+} cationic and neutral amino acid transporter, a B^0-system transporter, an IMINO-system transporter, and four transporters for which the solutes are unknown (Figure 5). In general, SLC6 transporters act to regulate the level of extracellular solute concentrations. In the central and the peripheral nervous system, the neurotransmitter reuptake transporters modulate signaling among neurons. They thus represent sites of action of various drugs and drugs of abuse. Furthermore, naturally occurring mutations in several of these proteins are associated with a variety of

neurological disorders. In kidney and small intestine, the amino acid transporters of this family mediate the luminal step of the (re)-absorption of diverse amino acids.

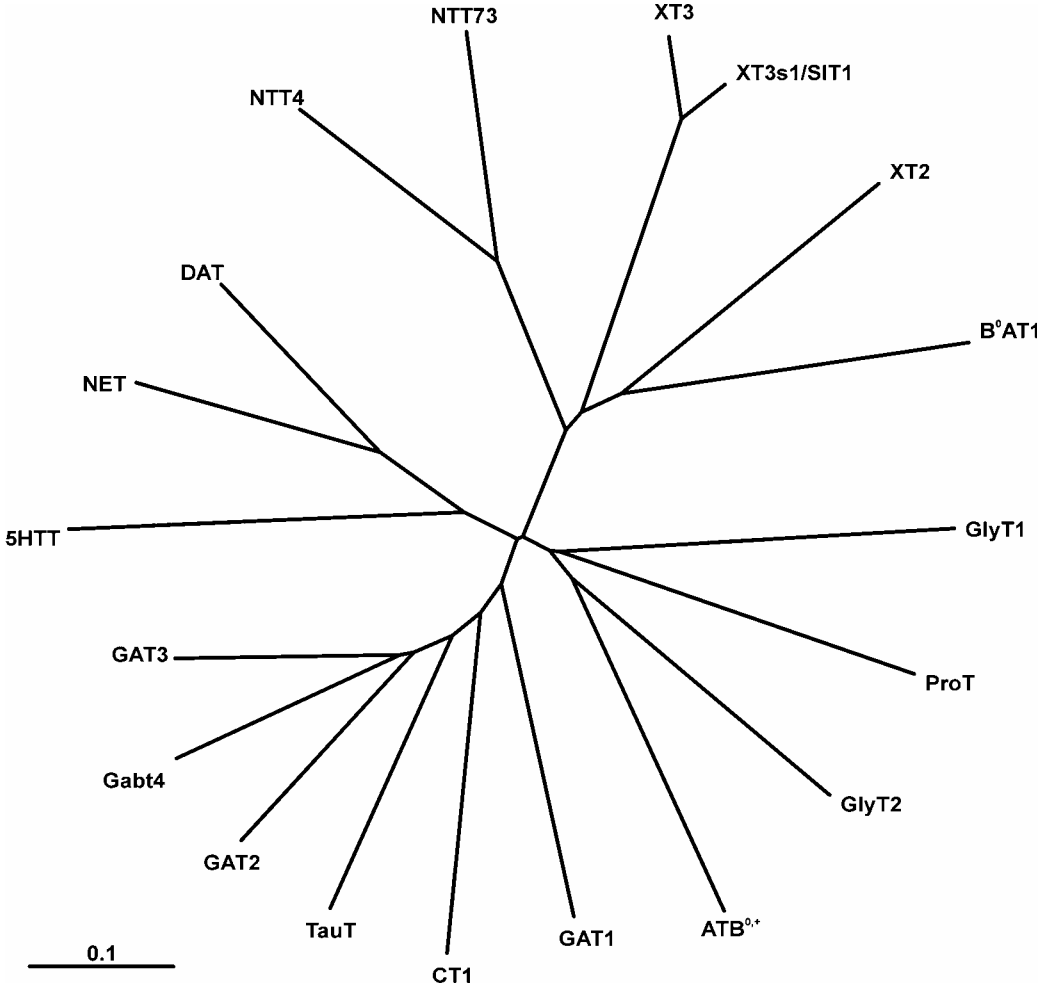

Figure 5. Phylogenetic tree of mouse Slc6 family. Protein sequences of the mouse Slc6 family members were aligned and a phylogenetic tree constucted. Accession numbers are: serotonin transporter (*5HTT*), Q60857; noradrenaline transporter, O55192; dopamine transporter, NP_034150 ; GABA transporter 1 (*GAT1*), NP_848818; creatine transporter (*CT1*), NP_598748; taurine transporter (*TauT*), NP_033346; GABA/betaine transporter (*GAT2*), P31651; GABA transporter 4 (*Gabt4*), P31650; GABA transporter 3 (*GAT3*), P31649; proline transporter (*ProT*), XP_140385; glycine transporter 1 (*GlyT1*) NP_032161; glycine transporter 2 (*GlyT2*) NP_683733; amino acid transporter $B^{0,+}$ (*$ATB^{0,+}$*), AAK43541; orphan transporter (*NTT73*), NP_780537; orphan transporter (*NTT4*), NP_758475; orphan transporter (*XT3*), NP_035861; amino acid transporter (*B^0AT1*), XP_127449; and orphan transporter (*XT2*, *isoformA12*), AAC27757; X transporter protein 3 similar 1 (*XT3s1/SIT1*), NP_631881.

The SLC6 transporters have an approximate length of 600 amino acids with 12 transmembrane segments and cytoplasmic NH_2- and COOH-terminal tails (Lill and

Nelson, 1998; Nelson, 1998; Yamashita et al., 2005). A large, extracellular loop, with glycosylation sites, is present between TM 3 and 4. Recent evidence suggests that at least some of these transporters function in homo-oligomeric form (Hastrup et al., 2001; Kilic and Rudnick, 2000; Schmid et al., 2001; Sorkina et al., 2003; Torres et al., 2003). The driving forces for the transport of substrates (neurotransmitter or amino acid) against their concentration gradient are provided by the electrochemical gradient for the cotransported Na^+. Cl^- is also co-transported by many members of this family. In addition, one member (the serotonin transporter SERT encoded by SLC6A4), requires the counter-transport of K^+ (Rudnick and Clark, 1993). The role of Cl^- in the transport process is not well understood. It is unlikely to provide an electrical driving force for transport since the resting membrane potential of many cells is near the Cl^- equilibrium potential; rather, it may play a role in enhancing Na^+ binding affinity and providing chemical driving force particularly necessary in excitable cells (Bossi et al., 2002; Loo et al., 2000). The domains that subserve substrate binding and the residues that form the permeation path are presently active areas of investigation. Some transporters show ion fluxes that exist in addition to stoichiometrically coupled uptake, while several show ion conductances in the absence of transmitter (Beckman and Quick, 1998).

A recent publication from Gouaux's group gives some insights on the possible structure of Na^+/Cl^- -dependent transporters and on the functional residues which could be involved in the binding of the substrate. They presented the crystal structure of a bacterial homologue of Na^+/Cl^- -dependent transporters ($LeuT_{Aa}$) from the bacterium *Aquifex aeolicus*, in complex with its substrate, leucine, and two sodium ions (Yamashita et al., 2005). This protein has 12 transmembrane helical regions (TM1 to TM12), together with numerous loops and helices on the intracellular and extracellular surfaces. It shows an unanticipated internal structural repeat in the first ten transmembrane helices, relating TM1–TM5 and TM6–TM10 by a pseudo-two-fold axis located in the plane of the membrane. The most striking feature is that TM1 and TM6 have breaks in their helical structure at positions approximately halfway across the membrane bilayer. Gouaux's group showed that in these regions the substrate (Leu) and the two Na^+ are bound during the transport cycle. Moreover, from the crystal structure data, there are other helical and loop segments on the solvent exposed surfaces of $LeuT_{Aa}$, which are

situated in regions that suggest a role in the transport mechanism (Yamashita et al., 2005).

4.3.1 System B^0

Most neutral amino acids are transported by system B^0, which was firstly described in the early '70s (Evers et al., 1976; Murer et al., 1976; Palacin et al., 1998; Sigrist-Nelson et al., 1975). In the last 30 years, system B^0 has been characterized in jejunal brush border vesicles (Munck and Munck, 1994; Stevens et al., 1982), bovine epithelial cells (Doyle and McGivan, 1992), and Caco-2 cells (Souba et al., 1992). These studies suggest that system B^0 is a Na^+-dependent, chloride-independent transporter that accepts a wide variety of neutral amino acids. Failures to reabsorb amino acids in the kidney and intestine underlie a number of inherited transporter diseases, with mutations in either rBAT or $b^{0,+}$AT causing cystinuria (Palacin et al., 2000), mutations of the IMINO system believed to cause iminoglycinuria (Chesney, 2001) and mutations of system B^0 thought to cause Hartnup disorder (Levy, 2001).

A phylogenetic analysis of mouse SLC6 family shows that four amino acid transporters, B^0AT1, XT2, XT3 and XT3s1/SIT1 form a separate cluster (Verrey et al., 2005) (Figure 5). They share high sequence similarity (Table 2) and they are all expressed in kidney and small intestine epithelia (See Results section).

Sequence A	Length (aa)	Sequence B (comparison)	Length (aa)	Sequence identity (%)
B^0AT1 (Slc6a19)	634	XT3 (Xtrp3)	635	43
B^0AT1 (Slc6a19)	634	XT2 (Slc6a18)	615	52
B^0AT1 (Slc6a19)	634	XT3s1/SIT1 (Slc6a20)	592	46
XT3 (Xtrp3)	635	XT2 (Slc6a18)	615	45
XT3 (Xtrp3)	635	XT3s1/SIT1 (Slc6a20)	592	90
XT2 (Slc6a18)	615	XT3s1/SIT1 (Slc6a20)	592	46

Table 2. Amino acid sequence comparison. The four mouse Slc6 proteins have been compared using ClustalW multiple sequence alignment program (http://www.ebi.ac.uk/clustalw/).

4.3.1.1 B^0AT1 (Slc6a19)

Unlike other transporters that were molecularly identified several years ago, no transporter corresponding to system B^0 was identified before 2004, when Broer and colleagues cloned and functionally characterized the first mouse B^0-type transporter (Broer et al., 2004). This transporter was named B^0AT1 (Slc6a19).

Heterologous expression of B^0AT1 cDNA in *Xenopus laevis* oocytes induced a Na^+-dependent, Cl^--independent uptake of neutral amino acids with an apparent affinity for L-leucine uptake in the order of magnitude previously measured in other systems (Bohmer et al., 2005; Broer et al., 2004; Camargo et al., 2005; Camargo SMR et al., 2005; Samarzija and Fromter, 1982; Stevens et al., 1982).

Mutations of system B^0 were long thought to cause Hartnup disorder (MIM 234500 OMIM), an autosomal recessive disorder resulting from impaired neutral amino acid transport, largely limited to the kidneys and the small intestine. Its diagnostic hallmark is a striking neutral hyperaminoaciduria (Baron et al., 1956; Levy, 2001). A number of additional symptoms have been reported in Hartnup disorder patients, including photosensitive skin rash, ataxia, and psychotic behaviour (Baron et al., 1956; Levy, 2001). Nevertheless, many of those affected remain asymptomatic despite the hyperaminoaciduria. This variation in manifestations of Hartnup disorder may be a consequence of compensation for the reduced amino acid transport by increased peptide transport in the intestine or the presence of genetic or environmental modifiers, such as dietary variations. Despite its apparently mild phenotype, Hartnup disorder has been a model disease, because it illustrates the principles of amino acid reabsorption in epithelial cells. Homozygosity mapping in consanguineous families has recently localized the disorder to chromosome 5p15 (Nozaki et al., 2001).

The hypothesis that homozygote mutations of the corresponding gene leads to Hartnup disorder was verified in a large fraction of the tested cases, including in the original Hartnup family (Broer et al., 2005; Kleta et al., 2004; Seow et al., 2004). The question remains as to whether the cases of Hartnup disorder that do not map to SLC6A19 are from mutations in other transporters or from defects in another gene product necessary for the correct expression and/or function of B^0AT1 (Kleta et al., 2004).

4.3.1.2 XT2 (Slc6a18)

The first report about XT2 (Slc6a18) and XT3 (Xtrp3) is from Nash and colleagues (Nash et al., 1998). The cDNAs of mouse XT2 they obtained showed the existence of six splice variants. Among these, the A12 isoform is the closest to human XT2 (SLC6A18) and to the orthologue in rat, ROSIT (Obermuller et al., 1997; Wasserman et al., 1994). The chromosomal location of the gene for XT2 in the mouse was shown to be on chromosome 13, within a large linkage group conserved with human chromosome 5 (Justice and Stephenson, 1994).

The expression of these isoforms in heterologous systems in transfected cells and oocyte expression systems failed to determine conclusive substrate specificity (Nash et al., 1998; Quan et al., 2004).

Wasserman's group reported in 1994 that ROSIT (renal osmotic stress induced Na^+,Cl^--organic solute cotransporter) mRNA is expressed in the renal cortex and outer medulla (Wasserman et al., 1994). It was also shown that hypernatremia caused a large increase in the expression of ROSIT mRNA in renal cortex, outer medulla, and possibly small intestine, suggesting that the substrate that is transported may serve as an organic osmolyte or osmolyte precursor for the body. The distribution of ROSIT mRNA is unique and is different from that of taurine and betaine and Na^+/myoinositol transporters. Uptake studies using *Xenopus laevis* oocytes expressing ROSIT were all negative, suggesting that ROSIT is not involved in the transport of neurotransmitters, amino acids, or the major organic osmolytes (Wasserman et al., 1994). Very recently, the group of Tomita examined the intranephron localization and regulation of ROSIT mRNA expression using microdissected nephron segments from control and dehydrated rats (Baba et al., 2004). The results showed that ROSIT mRNA expression was stimulated in whole nephron segments by dehydration. ROSIT mRNA expression in kidney proximal tubule was stimulated by hypertonicity, but not urea. The failure of urea with the same osmolarity to stimulating ROSIT mRNA expression could be explained by a low osmotic effect of urea due to its high permeability or by the inhibitory effect of urea on metabolic pathways. This report suggested that ROSIT might participate in the transport of amino acids in the control conditions and that of organics osmolytes in dehydration.

Finally, a study in post-ischemic rat kidney showed that renal osmotic stress-induced cotransporter mRNA levels were already decreased eight hours post-ischemia. At seven days post-ischemia, ROSIT mRNA reappeared in a mosaic pattern in the regenerating S3 segment, being fully expressed three weeks after the insult except for focal areas (Obermuller et al., 1997).

Recently, Caron's group generated a XT2-knockout mouse. In screening urine from XT2-knockout mice by high-pressure liquid chromatography and mass spectrometry, they found a significantly elevated concentration of glycine. To study glycine handling, $XT2^{+/+}$ and $XT2^{-/-}$ mice were injected with radiolabeled glycine, and urine samples were collected to monitor glycine excretion. After 2 h, $XT2^{-/-}$ mice were found to excrete almost twice as much glycine as the $XT2^{+/+}$ controls ($P = 0.03$). To determine whether the absence of the XT2 transporter affected sodium and fluid homeostasis, they measured systolic blood pressure by computerized tail-cuff manometry. Systolic blood pressure was significantly higher in $XT2^{-/-}$ mice (127 ± 3 mmHg) than in wild-type controls (114 ± 2 mmHg; $P < 0.001$). This difference in systolic blood pressure was maintained on high and low salt feeding. To examine whether the alteration in blood pressure and the defect in glycine handling were related, systolic blood pressure was measured in the $XT2^{-/-}$ mice during dietary glycine supplementation. Glycine loading caused systolic blood pressure to fall in the $XT2^{-/-}$ mice from 127 ± 3 to 115 ± 3 mmHg ($P < 0.001$), a level virtually identical to that of the wild-type controls. These data suggest that the XT2 orphan transporter is involved in glycine reabsorption and that the absence of this transporter is sufficient to cause hypertension (Quan et al., 2004).

4.3.1.3 XT3 (Xtrp3)

XT3 gene in human is localized on chromosome 3. Kiss and co-workers, characterizing this mRNA in 2001, discovered a differently spliced form of the mRNA in brain, designated XT3a. Primers used for the amplification of XT3 from the brain cDNA library produced two bands observed on the agarose gel. The sequence of the shorter band indicated that exon 5 is alternatively spliced and is not present in the XT3a splice form (Kiss et al., 2001). The brain-specific isoform is predicted to lack one of the 12 putative transmembrane domains, whereas the isoform expressed in kidney has an overall

domain structure similar to B^0AT1 (Kiss et al., 2001). The longer splice form is 592 amino acids long while the shorter one (XT3a) has only 555 amino acids.

In mouse, two separate genes exist adjacent one another on chromosome 9, XT3 and XT3s1, 635 and 592 amino acids long, respectively. They are 90% identical and XT3s1 shows higher similarity to the human XT3 and to the rat rB21A compared with the mouse XT3. Therefore, it has been suggested that the mouse XT3s1 gene is the orthologue of the human XT3, whereas mouse XT3 is a new product of XT3s1 duplication (Kiss et al., 2002).

Mouse XT3s1 and human XT3 have recently been functionally characterized and renamed SIT1 (Sodium/Imino-acid Transporter 1) (see next paragraph) (Kowalczuk et al., 2005; Takanaga et al., 2005). The function of mouse XT3 remains unknown.

Screening experiments to identify the substrate(s) of mouse XT3 failed to identify specific uptake with any of the tested compounds (all 20 amino acids, osmolytes and neurotransmitters); however, immunofluorescence microscopy demonstrated that epitope-tagged variants of the protein products of the XT3 cDNAs were present on the plasma membrane of transfected cells (Nash et al., 1998).

Our group also tried to characterize the function of mouse XT3 but without success. Immunofluorescence analysis of *Xenopus laevis* oocytes injected with mXT3 cRNA showed no surface expression. Similar results were obtained when mXT3 was transfected in Madin-Darby canine kidney (MDCK), Murine Principal Kidney Cortical Collecting Duct (mpkCCD) or Human Embryonic Kidney 293 (HEK293) cell lines (Ristic, unpublished results). Apical staining was observed only when mXT3 was transfected in Opossum kidney (OK) cells but no specific function could be detected upon radiolabelled amino acids exposure (Ristic and Romeo, unpublished data).

4.3.2 System IMINO

The transport of proline has been studied extensively in epithelial cells from kidney and intestine (Munck and Munck, 1995; Silbernagl et al., 1975; Stevens et al., 1984).The amino acid is completely reabsorbed in the proximal tubule of the kidney and also efficiently absorbed in the intestine. Several routes have been described for the epithelial transport of proline: first a specific Na^+-dependent transporter for proline and hydroxyproline, called the IMINO system (Stevens and Wright, 1985; Stevens and

Wright, 1987), secondly a transporter shared by proline and glycine and some other amino acids, such as GABA (γ-aminobutyric acid) and β-alanine, which has been termed the 'imino acid carrier' (Munck et al., 1994; Roigaard-Petersen et al., 1987), and, thirdly, the Na^+-dependent neutral-amino-acid-transport system, B^0 (Ganapathy et al., 1983). Depending on the tissue and species, either the IMINO system or the imino acid carrier may carry the main load of proline transport in epithelia (Munck and Munck, 1994). The molecular correlate of the imino acid carrier is the proton/amino acid transporter PAT1 (Anderson et al., 2004). System B^0 is encoded by B^0AT1 gene (Broer et al., 2004), but the molecular identity of the IMINO system has remained elusive until very recently (Takanaga et al., 2005).

The IMINO system has been characterized in some detail in vesicles from rabbit jejunum (Munck and Munck, 1994; Stevens and Wright, 1985; Stevens and Wright, 1985; Stevens and Wright, 1987). These studies indicate that proline is co-transported with Na^+ and Cl^- ions with a stoichiometry of 1:2:1. Na^+ ions are thought to bind to the transporter before the substrate does. At physiological Na^+ concentrations, the K_m for proline is about 0.3 mM. Proline is the only proteinogenic amino acid accepted by the IMINO system. Additional substrates are L-pipecolate, hydroxyproline, proline methyl ester, betaine and MeAIB (N-methylaminoisobutyric acid). The transporter is stereoselective, preferring L-proline over D-proline (Stevens and Wright, 1985).

4.3.2.1 XT3s1/SIT1 (Slc6a20)

As mentioned previously, very recently two independent groups cloned and characterized XT3s1/SIT1 from mouse, human and rat and showed that it corresponds to system IMINO (Kowalczuk et al., 2005; Takanaga et al., 2005), renaming it SIT1. Takanaga and colleagues showed that rat SIT1 expressed in *Xenopus laevis* mediates the uptake of imino acids such as proline and pipecolate, as well as N-methylated amino acids (e.g. MeAIB, sarcosine). SIT1-mediated proline transport was shown to be pH-independent and insensitive to inhibition by alanine or lysine. Proline transport was Na^+-dependent, Cl^--stimulated, and voltage-dependent. Li^+, but not H^+, could substitute for Na^+. Human SIT1 also functioned as a Na^+-dependent proline transporter. Rat SIT1 mRNA was expressed in epithelial cells of duodenum, jejunum, ileum, stomach, caecum, colon, and kidney proximal tubule S3 segment. SIT1 mRNA was also

expressed in the choroid plexus, microglia, and meninges of the brain and in the ovary (Takanaga et al., 2005). Kowalczuk and colleagues took into consideration both mouse gene products, mXT3 and mXT3s1/SIT1. They demonstrated that expression of mouse XT3s1, but not XT3, in *Xenopus laevis* oocytes induced an electrogenic Na^+-and-Cl^--dependent transport for proline, hydroxyproline, betaine, N-methylaminoisobutyric acid and pipecolic acid. Expression of XT3s1 was found in brain, kidney, small intestine, thymus, spleen and lung, whereas XT3 prevailed in kidney and lung. They also proposed that the two homologues could be termed 'XT3s1 IMINO(B)' and 'XT3 IMINO(K)' to indicate their tissue expression (Kowalczuk et al., 2005).

5. *In vivo* and *in vitro* models for amino acid transporter studies

5.1 *In vivo* models: knockout mice

Renal transport of amino acids was originally investigated in intact animals by measuring their urinary excretion and with microperfusion experiments using tracer flux measurements, as well as electrophysiological recordings (Evers et al., 1976; Fass et al., 1977; Sigrist-Nelson et al., 1975).

The possibility to easily produce genetically modified mice, precisely targeting the gene of interest, allows the investigation of the resulting phenotype using methods as those mentioned above. Knockout mice exist for many transport proteins. For example, the analysis of GlyT knockout mice has revealed distinct functions of individual GlyT subtypes in synaptic transmission and provided animal models for two hereditary human diseases, glycine encephalopathy and hyperekplexia. These studies suggested that selective GlyT inhibitors could be of therapeutic value in cognitive disorders, schizophrenia and pain (Eulenburg et al., 2005).

Another example is the Slc7a9 knockout mouse providing a model to investigate in vivo the role of $b^{0,+}$AT in cystinuria. Expression of $b^{0,+}$AT protein is completely abolished in the kidney of $Slc7a9^{-/-}$ mice which present a dramatic hyperexcretion of cystine and dibasic amino acids, while $Slc7a9^{+/-}$ mice show moderate but significant hyperexcretion of these amino acids (phenotype non-I). Forty-two per cent of the knockout mice develop cystine calculi in the urinary system. Histopathology in kidney reveals typical changes for urolithiasis (tubular and pelvic dilatation, tubular necrosis, tubular hyaline droplets and

chronic interstitial nephritis). Thus, Slc7a9 knockout mice provide a valid model of cystinuria which can be used in the study of genetic, pharmacological and environmental factors involved in cystine urolithiasis (Feliubadalo et al., 2003).
Another model is the Slc6a18 (XT2) knockout mouse described previously (Quan et al., 2004).
Thanks to the high homology with humans, mice are good models for investigation of human diseases. In this sense, the major advantage is the possibility to analyse the phenotype of mutant organisms. This involves the major technical and conceptual difficulty represented by the expression of different transport systems with overlapping substrate specificity.

5.2 Studies on differentiated cells in culture

Other studies of amino acid transport have been performed on cultured epithelial cells (primary cultures and immortalized cell lines). Epithelial cells, as those from the renal proximal tubule and the small intestinal villus, are characterized by the fact that they have distinct plasma membrane domains: an apical and a basolateral one. The ability of epithelial cells to mediate vectorial transport of ions and solutes against their concentration gradients depends on the asymmetrical distribution of transporters at the cellular surface.
Established cell lines of renal origin are frequently used for analyzing renal transport function. One disadvantage of every study with an established cell line, however, is the relative dedifferentiation compared to te cells of origin and the fact that the initial genetic homogeneity could be lost at higher passage numbers due to spontaneous mutations. Several cultured epithelial cell lines of renal origin are known to express amino acid uptake across the apical and/or basolateral membrane: $LLCPK_1$ (ATCC CRL 1392) (Rabito and Karish, 1982; Rabito and Karish, 1983), MDCK (Boerner and Saier, 1985), HEK-293 (ATCC CRL 1573), OK (ATCC CRL 1840) cells etc. The cell line that has been extensively used as a model for proximal tubule transport to date is the OK cell line. The proximal tubule derived opossum kidney, OK cell line expresses a quite complete set of amino acid transporters known to be involved in the vectorial trans-epithelial flux of amino acids. For instance, OK cells express rBAT-associated system $b^{0,+}$ exchange

activity in the apical pole (Mora et al., 1996), the basolateral system L isoform LAT2/4F2*hc* and the basolateral system y^+L (most probably y^+LAT/4F2*hc* transporter) (Fernandez et al., 2003). Recently, in our laboratories, some studies on XT3 were carried out in OK cells using antisense RNA or siRNA to "knock down" the specific transporter allowing to demonstrate the contribution of opossum XT3 in the cell system (Ristic et al., 2005).

5.3 *In vitro* expression models : *Xenopus laevis* oocytes

With the identification of cDNAs encoding specific amino acid transporters, their expression in heterologous systems has become possible. To date, the most common *in vitro* model system being employed for the expression and investigation of amino acid transporters is the *Xenopus laevis* oocyte system.

The oocytes of the South African clawed frog *Xenopus laevis* are widely used for the expression of heterologous proteins. *Xenopus laevis* is easily kept and bred in captivity and oocytes are easily prepared. They represent an accessible laboratory tool that presents different practical advantages. Since the *Xenopus laevis* oocytes are cells specialized for the production and storage of proteins for later use during embryogenesis, they represent a good system to translate efficiently exogenous mRNA into proteins. Furthermore, since mature oocytes are fully equipped with all substrates needed for growth, they do not need to take up nutrients from the outside and therefore do not express high levels of endogenous transport systems at the plasma membrane.

In the context of mammalian amino acid transporters, oocytes could be largely used as expression model, despite the presence of several distinct endogenous transport systems. The Na^+-dependent systems $B^{0,+}$ for neutral and cationic amino acids (Taylor et al., 1989), ASC for small neutral amino acids (Campa and Kilberg, 1989) and x^-_{ag} for anionic amino acids (Steffgen et al., 1991) and the Na^+-independent systems asc, L, y^+, $b^{0,+}$ and x^-_c (Ishii et al., 1991) have been detected in oocytes, but at a rather low level.

As any heterologous expression system, the *Xenopus laevis* oocyte presents some disadvantages too. Some studies indicate that the *Xenopus laevis* oocytes may be limited in their capacity to translate selected mRNAs or to modify their protein products correctly (Snutch, 1988). Oocytes may also have different signaling pathways than

genuine tissue, therefore regulation studies of the expressed proteins should be performed in other more appropriate expression systems.

6. Contribution of this PhD to epithelial transport studies

The amino acid transporters I was focusing on during my PhD work were referred as orphan transporters when I joined the laboratory of Prof. Verrey three years ago. The function of XT2, XT3, B^0AT1 (at that time called simXT2) and XT3s1 was unknown. Many attempts to functionally characterize XT2 and XT3 had been already tried not only by our group but also by others (Nash et al., 1998). Initially, we tried to express them in heterologous systems, like *Xenopus laevis* oocytes, and in mammalian cell lines, such as MDCK and LLCPK, but the proteins could not be expressed at the cell surface, preventing all kind of functional studies with radiolabelled amino acids. Only a cell line was found to be able to express mXT2 and mXT3 at the cell surface: the OK cells. Focusing on XT3, all 20 amino acids and many other substances, like neurotransmitters and osmolytes, were offered to mXT3-expressing cells in presence and absence of Na^+ in order to define the substrate specificity but no uptake in addition to that mediated by the endogenous transporters was measured for these compounds. In the mean time, polyclonal antibodies were raised in rabbits against all four orphan transporters and the first localization study was performed on mouse kidney for mXT2 and mXT3 by J. Loffing (formerly at the Institute of Anatomy, University of Zurich) and then also on mB^0AT1 and mXT3s1 (Romeo et al., 2005). Our interest in XT3 led us to start a project aimed at producing a knockout mouse for this protein. I was working on the production of the targeting vector amplifing the genomic sequence from C57BL/6J ES cells but I encountered technical problems for the cloning of the so called long arm (see Materials and Methods section) and after repetitive attempts the project was discontinued. Few months later, Broer's group cloned and functionally characterized the first B^0-system transporter, mB^0AT1 (Broer et al., 2004). A link between B^0-system transport and Hartnup disorder had for long been hypothesised but the proof came from two independent studies, one from Broer's group and another in which we collaborated (Broer et al., 2005; Kleta et al., 2004; Seow et al., 2004). Accurate genetic analysis of several Hartnup families revealed that many different point mutations in the gene were responsible for the disorder.

Very recently, mXT3s1 has also been functionally characterized by two independent studies showing that this protein is an IMINO-transport system and renamed SIT1 (Kowalczuk et al., 2005; Takanaga et al., 2005).

Additional studies have been performed in our laboratories to further characterize mB^0AT1 and mXT3s1/SIT1 using two-electrode voltage clamp techniques and radiolabelled amino acid uptake (Camargo SMR et al., 2005; Ristic et al., 2005).

The physiological role of XT2 and XT3 remains unclear. The study on XT2 knockout mice showed a mild glycinuria with increased systolic pressure in animals lacking the transporter in comparison with wild type mice (Quan et al., 2004). After reading the publication, we found at least three points that require clarification. The first is related to the fact that the animals used for the analysis came from the first and second generation, having still a mixed genetic background 129/Sv and C57BL/6J as the mouse XT2 gene was isolated from a 129/Sv genomic library and the targeting vector was electroporated in RW4 embryonic stem cells (Quan et al., 2004). The second concerns the method used for the measurement of the blood pressure, namely the tail-cuff technique. These types of measurements require extensive handling of the animals, possibly leading to artefacts and gives only a punctual view of blood pressure. The third point is the fact that the urine amino acid measurements were not performed optimally to evaluate the potential decrease in amino acid reabsorption other than of glycine. For these reasons and in order to further characterize the phenotype of $XT2^{-/-}$ mice, we obtained from Prof. Caron few heterozygous $XT2^{+/-}$ males that we used for starting a backcross in C57BL/6J. After completing this process, the mice will be firstly screened for aminoaciduria and for elevated blood pressure using an implanted blood pressure telemeter. In addition, mice will be challenged with different protein content diets to assess the ability of the kidney to respond to such extreme conditions in absence of a potential amino acid transporter.

MATERIALS AND METHODS

1. Cell culture

1.1 Opossum kidney cells

Opossum kidney (OK) cells were cultured at 37°C and 5% CO2 in Dulbecco's Modified Eagle Medium (DMEM) (Gibco, Basel, Switzerland) and Ham's F12 Nutrition mixture (Gibco, Basel, Switzerland) 1:1 in presence of 5×10^4 units penicillin/liter (Sigma Aldrich, Switzerland), 50 mg streptomycin/liter (Sigma Aldrich, Switzerland), 2 mM L-glutamine (Sigma Aldrich, Switzerland), 40 mM HEPES (Sigma Aldrich, Switzerland) and 10% fetal calf serum (Sigma Aldrich, Switzerland).
At confluency cells were subcultured with 0.25% trypsin in 0.53 mM EDTA solution, after removal of the culture medium and extensive washing with PBS (phosphate buffered saline pH 7.4). The subcultivation ratio was 1:10 for maintenance of the cells in culture and plated on 100 mm plastic culture dishes (Corning, Fisher Scientific AG, Wohlen, Switzerland).

1.2 mXT3 stably transfected OK cell line

Cells for transient transfection were subcultivated 1:15 and plated on 35 mm or 60 mm plastic culture dishes (Corning, Fisher Scientific AG, Wohlen, Switzerland). Transfection was performed the day after the subcultivation using FuGene 6® transfection reagent (Roche Diagnostics Schweiz AG, Rotkreuz, Switzerland). 1 μg of mXT3-pIRES-CD8 (pIRES-CD8 vector was constructed based on pIRES-neo, BD Biosciences Clonetech, with the addition of the sequence encoding for the CD8; kindly given by Michel Fink) (Fig. 1) plasmid DNA was pre-mixed with 3 μl of FuGene 6® and incubated for 15 minutes at room temperature before applying the mixture to the cells. Cells undergoing transfection received a medium change just before the application of the transfection mixture: the recommended medium was as the normal culture medium but without antibiotics and without fetal calf serum (minimal medium). Transfected cells were kept in

the minimal medium for 4 hours, then a same volume of complete culture medium was added.

Cells were incubated at 37°C and 5% CO2 for 36-48 hours before selection was performed.

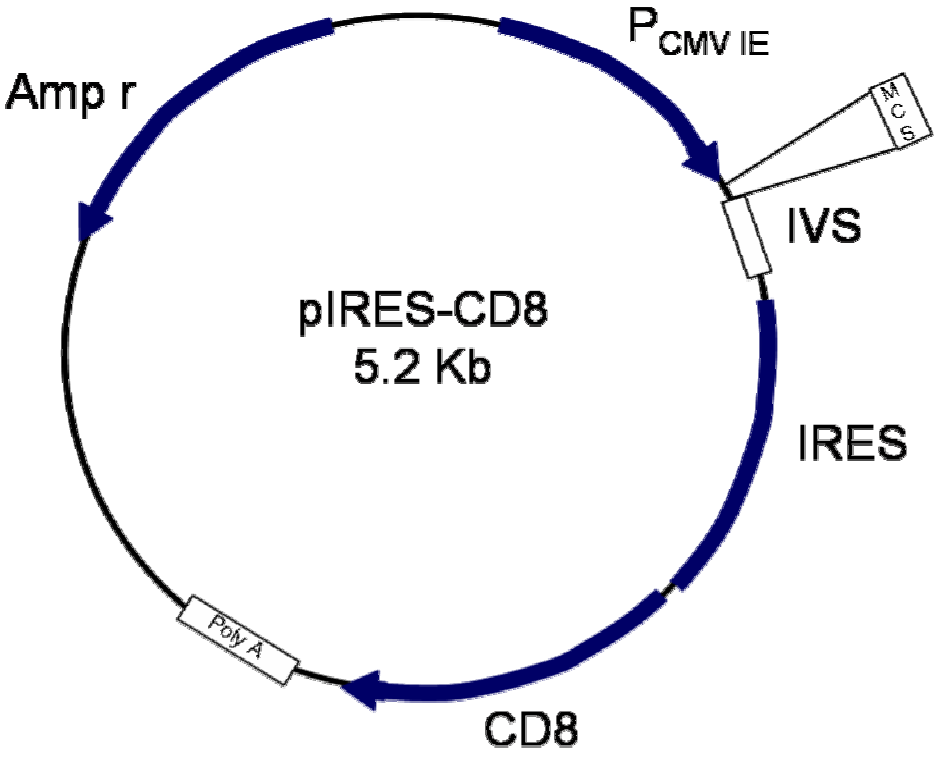

Figure 1. pIRES-CD8 vector. The vector was constructed based on pIRES-neo (BD Biosciences Clonetech) with the addition of the sequence coding for CD8. mXT3 was inserted in the multiple cloning site (MCS) using the restriction site for Eco RI.
Amp r: ampicillin resistance gene; PCMV IE: promoter for the encephalomyocarditis virus; IVS: Synthetic intron; IRES: Internal ribosome entry site; CD8: sequence coding for the CD8 receptor; Poly A: polyadenilation site.

Selection was performed using anti-CD8 coated metallic beads (Dynal biotech, Invitrogen Corporation, Oslo, Norway) which were incubated with the cells for 5 minutes at room temperature and rocked on a bench shaker. Cells were then trypsinized as described above and collected in a 15 ml Greiner tube (CellStar, E&K Scientific Products, California, USA). By using a 10 cm long, 3 cm wide magnet cells with beads interacting with the CD8 (possibly expressing also mXT3) were separated from all the

others. Cells with beads were then plated in 35 mm dishes and kept in culture till confluence was reached.
A further selection was performed after 1 week with the same procedure. Cells still expressing the CD8 were collected, diluted 100 times and plated in 96-well culture plate in order to have ideally one cell/well.
Cells in the 96-well plate were grown till confluence, trypsinized and plated on 35 mm dishes, half of them having a glass coverslip for further immunofluorescence procedure.
Cells on glass coverslip at confluence were fixed in 4% paraformaldeyde-PBS solution (pH 7.4) and stained with anti-mXT3 affinity purified antibody (see below).

2. Animal model: mice

2.1 Housing and handling

Male C57BL/6J mice were used for different experiments further described in this section. The approximate age of the animals ranged from 6 to 12 weeks. Mice were housed in the Animal facility of the Institute of Physiology, University of Zurich, under the supervision of qualified personnel from the Institut für Labortierkunde (LTK) of the University of Zurich.
Mice were housed in groups of 3 to 5 in the Tecniplast Sealsafe™ Individually Ventilated Cages (IVC) (dimensions 365 x 207 x 140 mm 1284L Eurostandard Type II L, Techniplast) or in groups of maximum 3 animals in smaller filter top cages (dimensions 267 x 207 x 140 mm; 1264C Eurostandard Type II, Techniplast).
In IVCs filtered air is delivered to the cage top level through a self-closing valve when docked in position on a Sealsafe rack. Exhaust air exits the cage through an independent self-closing valve, to avoid commixture of air.
Animal handling was according to the Swiss Animal Welfare laws and approved by the Kantonales Veterinäramt Zürich. All the people involved in the animal handling received at least the basic one-week animal handling course (Module 1 LTK) from the Institut für Labortierkunde (LTK) of the University of Zurich (see certificate of attendance in the CV section).

Specific procedures used for the below mentioned experiments are explained in detail in the next sections.

2.2 Tissue preparation for immunohistochemistry, protein extraction and total RNA extraction

2.2.1 For immunohistochemistry

Male C57BL/6J mice (10-12 weeks old) were anesthetized with ketamine and xylazine i.p. and perfused through the left ventricle with PBS followed by a buffered paraformaldehyde solution (4%, pH 7). Kidneys and small intestine were removed, flushed with fixative solution, cut and embedded in Tissue-Tek® O.C.T™ Compound (Sakura Finetek Europe B.V., The Netherlands) just before freezing in liquid nitrogen.

2.2.2 For protein extraction

Male C57BL/6J mice (10-12 weeks old) were anesthetized with ketamine and xylazine i.p. followed by cervical dislocation and organs were rapidly harvested. The segment from duodenum to ileum was harvested, rinsed several times with ice-cold PBS (phosphate buffered saline pH 7.4) and the mucosa cell layers were scraped off on ice and transferred into ice-cold homogenization buffer (300 mM mannitol, 5 mM EGTA, 12 mM Tris HCl, pH 7.1) with protease inhibitor cocktail (Sigma-Aldrich, Switzerland), containing 4-(2-aminoethyl)benzenesulfonyl fluoride (AEBSF), pepstatinA, E-64, bestatin, leupeptin, and aprotinin. Kidneys were harvested too. The samples were homogenized with a tip sonicator, 10 mM $MgCl_2$ was added and samples kept on ice for 30 min. Samples were then centrifuged 15 min at 900 g. The supernatant was then centrifuged at 12000 g for 30 min at 4 °C and the pellet resuspended in membrane buffer (300 mM mannitol, 20 mM Hepes Tris pH 7.4) containing protease inhibitor cocktail.

2.2.3 For total RNA extraction

Male C57BL/6J mice approximately 12 weeks old were sacrificed by i.p. injection of ketamine/xylazine and subsequent cervical dislocation; tissues were collected and rapidly frozen until further use. Stomach, duodenum, jejunum, ileum and colon were harvested, rinsed several times with ice-cold PBS (phosphate buffered saline pH 7.4) and the mucosa cell layers were scraped off on ice and rapidly frozen. The duodenum was identified as proximal of the ligament of Treitz (first 2 cm), the jejunum as the upper part (upper 2/5) of the small intestine distal of the ligament of Treitz and the ileum as the lower part (lower 2/5) of the small intestine ending before the caecum. Between duodenum and jejunum, 5 cm of tissue were removed as a safety margin as well as 10 cm between jejunum and ileum. Total colon was used for mucosa isolation.

2.3 Treatments of WT C57BL/6J mice with modified food/water

2.3.1 High and low sodium diets

Three groups of six male C57BL/6J mice each, approximately 10 weeks old, were housed in three independent IVCs and received for 48 hours one of the following diet regimes:

- control animal group: 0.3% NaCl pellet food and tap water *ad libidum*;
- low sodium animal group: sodium free pellet food and tap water *ad libidum*;
- high sodium animal group: 0.3% NaCl pellet food and 2% sucrose /3% NaCl in the drinking water *ad libidum*.

2.3.2 Induction of metabolic acidosis/alkalosis

Three groups of five male C57BL/6J mice each, approximately 8-10 weeks old, were housed in three independent IVCs and received for 7 days one of the following diet regimes:

- Control animal group: regular pellet food and tap water *ad libidum*;

- Acidosis animal group: regular pellet food and 2% sucrose/0.28 M NH_4Cl in the drinking water *ad libidum*;
- Alkalosis animal group: regular pellet food and 2% sucrose/0.28 M $NaHCO_3$ in the drinking water *ad libidum*.

2.4 XT2 heterozygous mice

2.4.1 Generation of XT2 KO mice (by Dr. Hui Quan, Prof. Marc Caron's group, Duke University Medical Center, Durham, NC, USA)

The mouse XT2 gene was isolated from a 129/Sv genomic library. A targeting vector was constructed by using an 8-kb genomic DNA fragment containing exon 1 and intron 1. A DNA fragment containing the whole exon 1 and part of intron 1 was replaced by a 3.5-kb loxP-flanked Neo-TK selection cassette (Fig. 2), and a PGK-DT cassette was inserted upstream for negative selection. The vector was linearized at a unique NotI site and electroporated into RW4 embryonic stem (ES) cells. Homologous recombinants were screened from the G418-resistant colonies by PCR and confirmed by Southern blot analysis. Male chimeras produced by injection of targeted ES cells into C57BL/6J blastocysts were bred with C57BL/6J females. Germ line transmission of the targeted mutation was screened by PCR and verified by Southern blot analysis of tail DNA. Heterozygotes were then mated with transgenic C57BL/6J mice carrying a CMV-Cre transgene (a gift from Yuan Zhuang at Duke University). Constitutively expressed Cre recombinase excises the loxP-flanked Neo-TK cassette, which renders heterozygous animals without the Neo-TK selection cassette ($XT2^{+/-}$) (Quan et al., 2004).

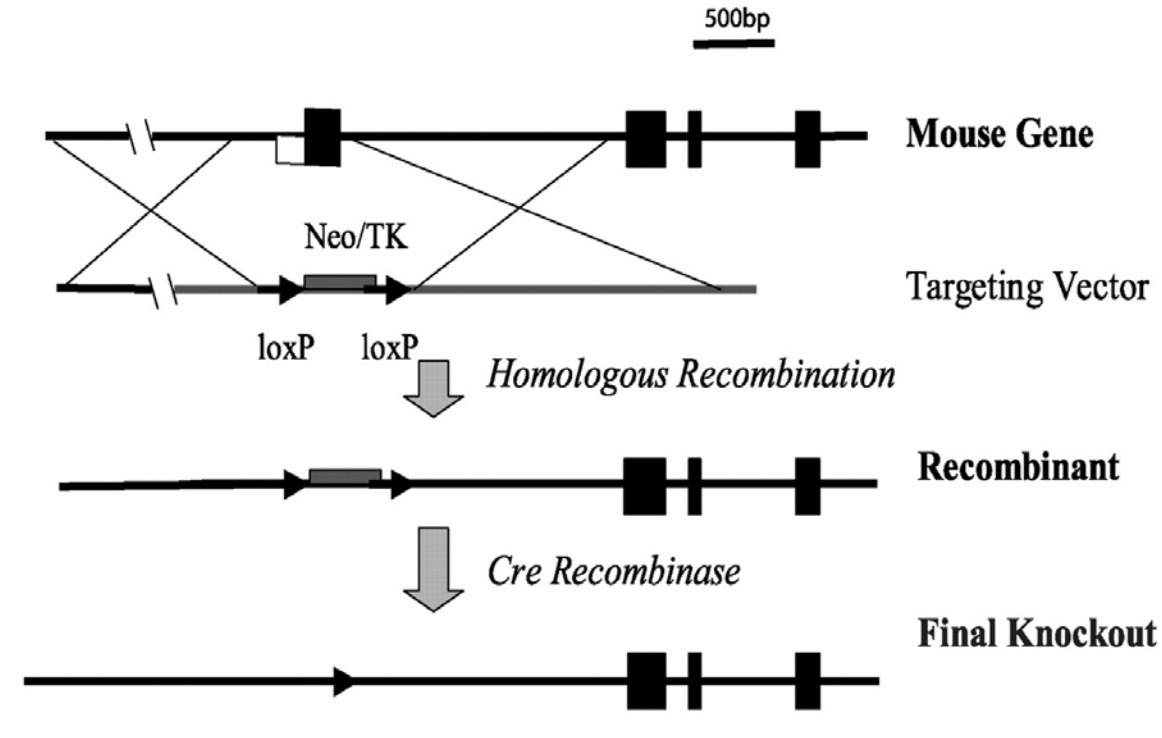

Figure 2. Generation of XT2-null mutant mice. Targeting strategy for disruption of the XT2 gene.

2.4.2 Backcrossing of XT2 heterozygous mice with C57BL/6J mice and genotyping

Heterozygous male mice, approximately 8 weeks old, were kindly given to us by Prof. Marc Caron (Duke University Medical Center, Durham, NC, USA). After one week recovery in the Animal Facility of the Institute of Physiology (University of Zurich) mice were paired 1:1 with C57BL/6J wild type female mice, approximately 8 weeks old. At each generation tail biopsies were collected from 4 weeks old pups, digested overnight at 55 °C in 400 μl of lysis buffer containing 100 mM Tris HCl pH 8.5, 5 mM EDTA, 0.2% SDS, 200 mM NaCl and 200 μg/ml Proteinase K (Sigma-Aldrich, Buchs, Switzerland). After heat inactivation of the enzyme for 10 minutes at 95 °C, 100 μl of 5 M NaCl and DNA was extracted by adding 500 μl of Chloroform-Isoamylalcool (49:1) (Sigma-Aldrich, Buchs, Switzerland). Samples were vortexed and centrifuged 5 minutes at 14000 rpm in a bench-top centrifuge (Vaudaux-Eppendorf AG, Basel, Switzerland). The aqueous supernatant phase was transferred to a fresh tube and DNA was precipitated by adding 1 volume of 2-Propanol (Sigma-Aldrich, Buchs, Switzerland). To allow the DNA

precipitation the samples were kept a -20 °C for at least 30 minutes before centrifuging them for 5 minutes at 14000 rpm in a bench-top centrifuge. The pellet was then washed with 70% Ethanol solution and centrifuged again. Pellet was dried at least 30 minutes at room temperature and then resuspended in DNase-free water. Concentration of the samples was measured with UV/VIS spectrophotometer (Biorad, Hercules CA, USA).

100 μg of DNA was further used for PCR. PCR reaction was performed in presence of 16.6 mM ammonium sulfate, 6.7 mM MgCl2, 67 mM Tris HCl pH 8.8, 5 mM β-mercaptoethanol, 6.7 μM EDTA, 1 mM each dNTPs, 10% DMSO, 0.32 mM sense primer, 0.5 mM antisense primer and 1.25 unit of EurobioTaq® DNA polymerase (Eurobio Laboratories, France). The reaction were run in a bench-top PCR cycler: initial denaturation 1 minute and 30 seconds at 93 °C, 40 cycles 93 °C 30 seconds, 57 °C 30 seconds, 72 °C 3 minutes, final elongation 72 °C for 5 minutes. Half of the reaction was loaded on a 1% agarose gel containing 0.5 μg/ml ethidium bromide. In Figure 3 a representative gel showing the genotype of several screened mice.

Two to three heterozygous males were chosen for further backcrossing with WT C57BL/6J females. At the forth generation genomic DNA from six heterozygous males was further analysed for 96 C57BL/J6 markers using GenoMouse Kit (Elchrom Scientific, Cham, Switzerland). Every DNA is tested for 96 specific C57BL/J6 genetic markers spread on all the 19 autosomes by PCR. The reaction is also performed on a C57BL/6J WT mouse as reference. Results are then compared and heterozygous mice carrying the highest number of C57BL/6J markers are selected for furher backcrossing.

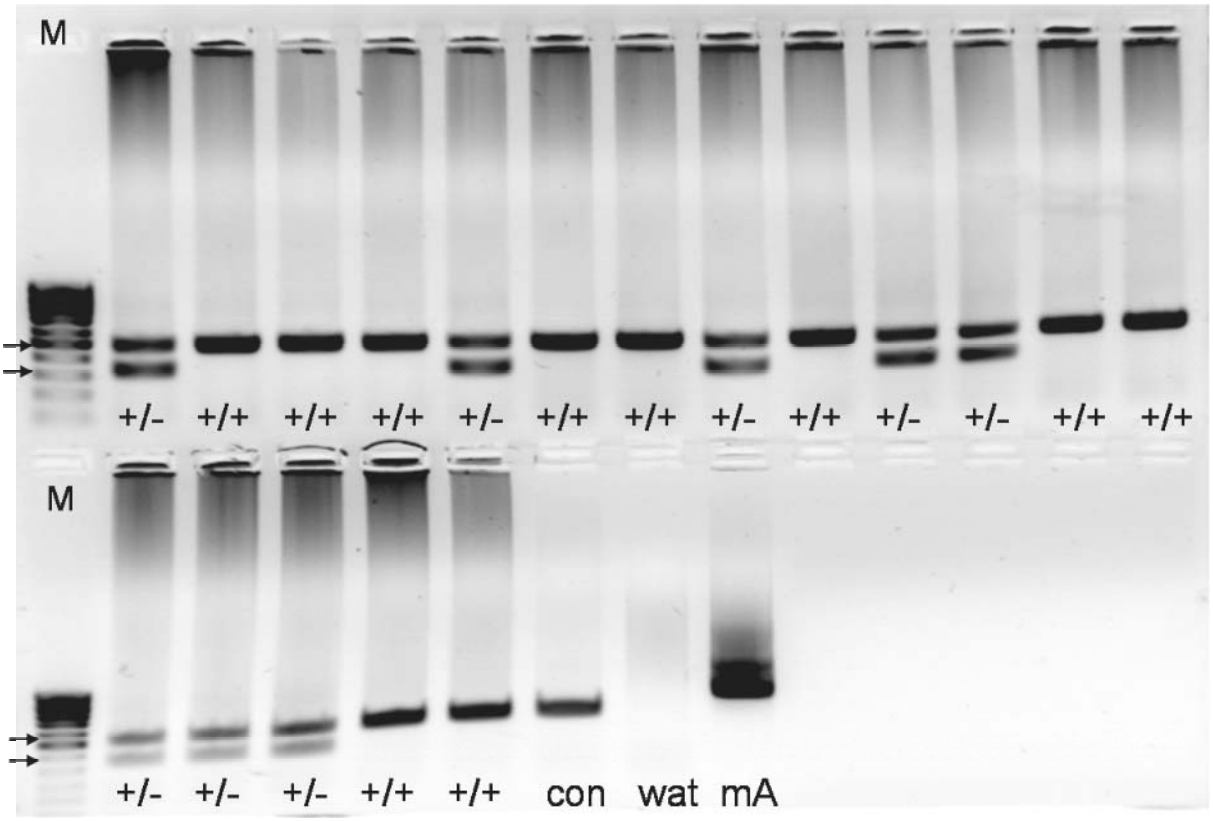

Figure 3. Genotyping results. Analysis of mouse XT2 genomic PCR product in a 1.0% agarose gel stained with ethidium bromide. A PCR product of 526 bp is seen in wild-type (+/+) and heterozygous mutants (+/-) together with a 421-bp fragment which would be the only fragment present in homozygous mice (not shown). Con: control PCR with WT genomic DNA; wat: reaction with no template present; mA: mβ-actin internal PCR control (size of the fragment 756 bp); M: molecular weight marker. The two arrows indicate the sizes of the specific bands.

2.4.3 Telemetry Probe Implantation Procedure

A system for telemetric measurements using the DSI radiotelemetry system (Data Sciences International, St. Paul, MN) with the TA11PA-C10 pressure and activity implant (Data Sciences International, St. Paul, MN) was set up at the Institute of Physiology.

For data collection and analysis a Dataquest ART Data Exchange Matrix and a Dataquest Acquisition and Analysis System ART (Data Sciences International, St. Paul, MN) were purchased.

2.4.3.1 Pressure-sensing catheter implantation

Male and female C57BL6/J XT2 wild type ($XT2^{+/+}$), heterozygous ($XT2^{+/-}$) and homozygous ($XT2^{-/-}$) mice were anesthetized with ketamine (65 mg/kg ip), xylazine (13 mg/kg ip) and ace promazine (2 mg/kg ip), and the neck was shaved and disinfected. Animals were placed on their backs on a heated surgical surface with forelimbs secured using tape and the head held parallel to the body by a small piece of tubing looped around the upper incisors and anchored to the surface. This allows easier access to the region to be dissected. A ventral midline skin incision was made from the lower mandible posteriorly to the sternum (~3 cm), and the submaxillary glands were gently separated using sterile cotton swabs. The left common carotid artery was isolated using fine forceps, with care being taken to avoid disturbing nerve fibers running parallel to the artery. The left carotid is preferable, since the right brachiocephalic artery branches off from the right carotid artery, potentially compromising blood flow to this region. Two silk ligatures (7–0, Braintree) were passed under the vessel and used for both ligation and retraction. The anterior silk suture, placed just caudal to the bifurcation of the interior and exterior carotid arteries, was used to ligate the artery. The posterior suture, placed loosely about 0.5 cm from the anterior tie, was used for temporary occlusion of the artery during catheter insertion. Gentle tension was applied to both ligatures to slightly retract and lift the vessel before making a tiny incision in the carotid artery just posterior to *suture a* using Vannas spring micro-scissors (Fine Science Tools, catalog no. 15610-08). After carefully removing the protective cover from the tip of the catheter, the catheter was gently grasped using vessel cannulation forceps (Fine Science Tools, catalog no. 00608-11) and inserted into the carotid artery with the aid of fine forceps used to hold the vessel incision open. The occlusive posterior ligature was released, and the catheter was advanced to the point where the small notch on the tubing (the transition between the thin-walled tubing and remaining outer tubing, 10 mm from the tip) resided at the vessel opening. Inserting the catheter up to this landmark notch assures the critical placement of the pressure-sensing tip just inside of the thoracic aorta. The notch also serves as a useful tool for anchoring the catheter into the vessel; the loose ends of anterior ligature were tied securely around the catheter at the notch. The loose ends of the occlusive posterior ligature were also brought up and tied securely around

the vessel/catheter. A single microdrop of Nexaband veterinary adhesive was applied to the site of catheter insertion into the vessel. It should be emphasized that that only a very small amount of adhesive is required, and that care should be taken to avoid undue application of adhesive to surrounding tissues and nerve fibers.

2.4.3.2 Implantation of transmitter subcutaneously along the right flank

Through the same ventral neck incision, a subcutaneous pouch was formed for placement of the transmitter body along the animal's right flank. Using a pair of blunt dissecting scissors (Fine Science Tools, catalogue no. 14018-14), the skin was gently dissected free from underlying tissue starting at the right neck region and proceeding posteriorly to form a "pocket" along the right flank. It is important that the pocket be made sufficiently large to house the transmitter without unduly stretching the skin, because pressure necrosis could result. The transmitter was slipped under the skin and down into the pocket along the flank as close to the right hindlimb as possible. A small drop of Nexaband was placed on the catheter in the right neck region to further secure the device. The neck incision was closed using 6–0 silk and further sealed with tissue adhesive. Mice were kept warm on a heating pad and monitored closely until fully recovered from anaesthesia.

3. Immunohistochemistry

3.1 Immunolabelling procedure

Frozen tissues were stored at –80°C. Serial sections of 5 μm were cut on a cryostat and collected on polylysine-coated slides (Kindler, Freiburg, Germany). Sections were incubated 5 min in SDS 0.1%, washed 3 times with PBS and then incubated with the primary antibodies (diluted in PBS, TritonX-100 0.04%) 1 hour at room temperature. Sections were then washed 3 times and incubated with the secondary antibody (diluted in PBS, TritonX-100 0.04%) for 1 hour at room temperature. After washing 5 times the sections were mounted using DAKO Mounting medium (DakoCytomation Denmark A/S, Denmark). Sections were viewed on Leica SP1 UV CLSM confocal microscope (Leica

Microsystems Inc., Buffalo New York, USA). Images were further processed (merged) using Photoshop 7.

3.2 Antibodies

Rabbit-anti-mB^{0}AT1 antibody (NH_2-terminal; antigen peptide NH_2-MVR LVL PNP GLE ERIC- $CONH_2$ (16aa); affinity purified antibody, dilution 1:200), rabbit-anti-mXT2 (NH_2-terminal; antigen peptide NH_2- MAQ ASG MDP LVD IED ERC -$CONH_2$ (18 AA); affinity purified, dilution 1:200), rabbit-anti-mXT3 (NH_2-terminal; antigen peptide NH_2- MES PSA HAV SLP EDE ELC -$CONH_2$ (18 AA); affinity purified, dilution 1:200), rabbit-anti-mXT3s1 (COOH-terminal; antigen peptide NH_2-CIRN RLK RGG SAP VA -COOH (15 AA); affinity purified antibody, dilution 1:200) and goat-anti-m4F2hc (Santa Cruz Biotech, Santa Cruz CA,USA, 1:400). Secondary antibodies were Alexa Fluor® 594 donkey anti-rabbit IgG (1:1000; Molecular Probes, Portland, Oregon, USA) and Alexa Fluor® 488 donkey-anti-goat IgG (1:500; Molecular Probes, Portland, Oregon, USA). The secondary antibodies alone as well as antibodies pre-incubated with the specific peptides (1 hour at room temperature) did not produce any significant staining in all tissues tested.

4. Western blotting

4.1 General procedure

After measurement of the total protein concentration (BioRad protein kit, Biorad, Hercules CA, USA), 20 μg of BBMVs (brush-border membrane vesicles) were used for the deglycosylation reaction as described below. Samples were solubilized in Laemmli sample buffer, and separated on a 10% polyacrylamide gel. For immunoblotting, proteins were transferred electrophoretically from unstained gels to PVDF-membranes (Immobilon-P, Millipore, Bedford, MA, USA). After blocking with 2% Top BLOCK™ powder (Juro, Lucerne, Switzerland) in Tris-buffered saline/0.1% Triton X-100 for 60 min at room temperature or overnight at 4° C, the blots were incubated with the primary antibodies for 3 hours at room temperature or overnight at 4 °C. The primary antibodies were the same affinity purified rabbit antibodies as described in the previous paragraph

and all were used at a 1:1000 dilution. After washing and subsequent blocking for 1 hour at room temperature, blots were incubated with secondary antibody goat anti-rabbit conjugated with Horseradish Peroxidase (1:10,000; BD Transduction Laboratories, Lexington, KY, USA) for 1 h at room temperature. Antibody binding was detected with the SuperSignal® West Pico Substrate (Pierce Socochim, Lausanne, Switzerland). Chemiluminescence was detected with a DIANA III camera (Raytest Schweiz, Dietikon, Switzerland). The specificity of the antibodies used was tested using preincubation (1 h at room temperature) with the immunizing peptides (final concentration peptide: 200 μg/ml XT2 and 400 μg/ml B^0AT1, XT3 and XT3s1).

4.2 Endo-beta-N-acetylglucosaminidase F (PNGase F) assay

Hydrolysis of Asn-oligosaccharides was carried out using endo-beta-N-acetylglucosaminidase F enzyme (New England Biolabs, USA). 20 μg of kidney or small intestine brush-border membrane vesicles (BBMVs) from adult (10-14 weeks old) C57BL/6J and NRMI mice were the substrate for the enzyme. The samples were first heated at 65 °C for 15 minutes in the provided buffer containing β-mercaptoethanol and SDS. The reaction mix was then incubated 1 hour at 37 °C in the reaction buffer and 1% NP-40 in the presence or absence of the enzyme. The reaction mixture was run on a 10% SDS-polyacrylamide gel and the Western blotting performed as described previously.

5. RT-real time PCR

5.1 RNA extraction and reverse transcription (RT) reaction

Total RNA was extracted from the different tissues using the RNeasy Mini Kit (Qiagen AG, Basel, Switzerland). For RNA extraction, tissues were thawed in RLT buffer (Qiagen) containing 10 μl/ml of β-Mercaptoethanol (Sigma-Aldrich, Buchs, Switzerland) and homogenized on ice. RNA was bound to columns and treated with DNase for 15 minutes at 25°C to reduce genomic DNA contamination. Quantity and quality of total eluted RNA were assessed by spectrometry and agarose gel electrophoresis. Each RNA

was diluted to 100 ng/μl and 1 μl was used as template for reverse transcription with TaqMan® Reverse Transcription Kit (Applied Biosystems, Foster City, CA, USA) in presence of 2.5 μM of Random Hexamers primers (Applied Biosystems).

5.2 Real time PCR

Real-time PCR was performed using as template 1 μl of cDNA synthetized by reverse transcription. The reaction was set up following the Applied Biosystems recommendations in the TaqMan® Universal PCR master mix (Applied Biosystems). Primers and probes were designed using Primer Express software from Applied Biosystems. Primers were chosen to result in amplicons of 70-100 bp that span the intron-exon boundaries, to avoid the effects of potentially contaminating genomic DNA. The specificity of the primers was first tested on cDNA derived from several tissues and resulted in a single product of the expected size (data not shown). Probes were labelled with reporter dye FAM at the 5' end and the quencher dye TAMRA at the 3' end (Microsynth, Balgach, Switzerland). Reactions were run in 96-well optical reaction plates using a Prism 7700 cycler (Applied Biosystems). Thermal cycles were set at 95°C (10 minutes) and the 40 cycles at 95°C (15 seconds) and 60°C (1 minute) with auto ramp time. To analyze the data, the threshold was set to 0.06 (value in the linear range of amplification curves). All the reactions were run in duplicates. The abundance of the target mRNAs was calculated relative to a reference mRNA (mGAPDH). Assuming an efficiency value of 2 (fold-increase in input mRNA required to decrease the cycle number by 1), relative expression ratios were calculated as $R = 2^{(Ct(GAPDH) - Ct(test))}$, where Ct is the cycle number at the threshold and test stands for the tested mRNAs (Dave et al., 2004).

6. Targeting vector preparation for knocking out XT3 gene in mouse

XT3 gene is located on chromosome 9. The whole gene of about 40 kb is constituted by 11 exons and 10 introns. In the intronic sequence between the first and the second exon there are three gaps of unknown sequence. Therefore, this region has not been considered for the design of the knockout vector. (Figure 5A)

The targeting vector (kindly provided by Rainer Waldmann, Sophia Antipolis, France, to Prof. Warth, formerly at our Institute) contains two negative selection markers, thymidine kinase (TK) and diphtheria toxin (DT) together with a positive selection marker, neo (neomycin resistance gene). Three loxP sites flank the neomycin resistance gene and can be used for the generation of conditional knockout constructs. (Figure 4)

The final vector configuration is shown in Figure 5B.

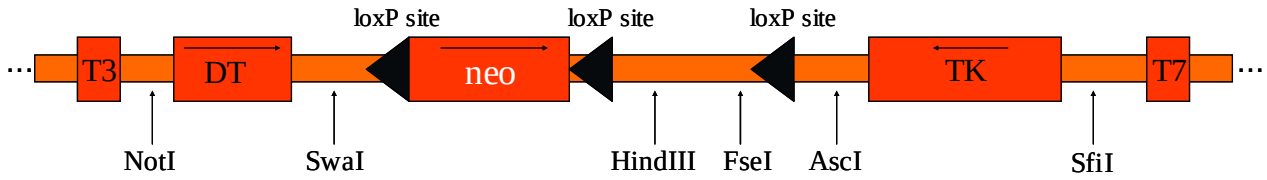

Figure 4. Targeting vector. The unique restriction sites are indicated with arrows. DT: diphtheria toxin; TK: thymidine kinase; neo: neomycin resistance gene; T3 and T7: bacterial RNA polymerase promoters.

Oligonucleotides have been designed on exon 3 (sense primer 5'-GGCCTCTGTGTACTTCAATG-3') and on exon 5 (antisense primer 5'-TGTGAACATGTATGCCAGG-3') for the PCR amplification of a 2.8 kb fragment, so called short arm of the targeting vector. Another couple of oligonucleotides were placed on exon 6 (sense primer 5'-TGGGCTTAGGGTGTGGTG-3') and exon 8 (antisense primer 5'-GGATGGCCGTTCCTGTC-3') to produce a fragment 6.4 kb long, so called long arm.

The template used in the PCR reaction is the genomic DNA extracted from C57BL6 ES cells (kindly provided by Prof. B. Ledermann, Institute für Labortierkunde, University of Zürich). All PCR reaction were performed using Pfu Turbo DNA Polymerase (Stratagene, La Jolla, CA) using the buffer supplied by the company and following the protocol optimized by the company, in presence of 0.5 μM each primers (oligonucleotides) and 0.2 mM each dNTPs.

Oligonucleotides (Microsynth, Balgach, Switzerland) for the amplification of the short arm produced a 2.8 kb-fragment that was purified over a 0.7% agarose gel using QIAquick Gel Extraction Kit (Qiagen AG, Basel, Switzerland). At the same time, the targeting vector was digested with 10 units/μg of DNA with SwaI restriction enzyme

(New England Biolabs, USA) in order to obtain blunt ended extremities, which would be compatible for ligation with the blunt ended fragment generated by Pfu Turbo DNA polymerase. The digested vector was then dephosphorylated with Calf Intestinal Alkaline Phosphatase (CIAP) (Promega, Catalys AG, Wallisellen, Switzerland). Ligation followed the dephosphorylation reaction: the PCR fragment and the dephosphorylated vector were mixed in presence of T4 DNA ligase (Promega, Catalys AG, Wallisellen, Switzerland) and incubated overnight at 16 °C. XL-1 Blue Supercompetent cells (Stratagene, La Jolla, CA) were chemically transformed using 10% of the ligation reaction. Clones were screened by gel electrophoresis after specific endonuclease digestion to confirm the presence of the insert in the vector and to check its correct orientation.

As it was not possible to obtain the long fragment from a single PCR reaction, a unique restriction site (AflII) in the intronic sequence between exon 7 and 8 was selected to be further used to join two halves of the long arm. PCR was performed with two new sets of oligonucleotides designed one on exon 6 just before the FseI restriction site (sense 5'-ATAACTGGCCGGCCTCATTGTGTCTGTCATC-3') and intron between exons 7 and 8 after AflII restriction site (antisense primer 5'-GAAAAGGTGGGTCAAAATAATG-3') and the other set on the intron spanning exons 7 and 8 before the AflII restriction site (sense primer 5'-GGCCTGTGATTCTGGTTGC-3') and the intron between exons 8 and 9 soon after the AscI restriction site (antisense primer 5'-GTAGATGGCGCGCCGTTCCTGTCCCC-3'). PCR fragment were separated on 0.7% agarose gel and purified as described above. The two fragments were then ligated in pBluescript II SK(-) (Stratagene, La Jolla, CA) previously digested with EcoRV endonuclease (Promega, Catalys AG, Wallisellen, Switzerland) to allow blunt end ligation as described previously. After bacterial transformation, clones were screened. Correct clones were further digested with FseI-AflII endonucleases (New England Biolabs, USA) for the fragment obtained with the first set of primers and with AflII-AscI (New England Biolabs, USA) for the fragment obtained with the second set of primers. Excised fragments were gel purified and ligation was performed by mixing the two halves of the long fragment with the targeting vector previously digested with FseI and AscI (New England Biolabs, USA). The junction of the two parts was not successful.

Therefore, other trials to obtain the full length long arm were made, using the original oligonucleotide pair placed on exon 6 (sense primer 5'-TGGGCTTAGGGTGTGGTG-3') and exon 8 (antisense primer 5'-GGATGGCCGTTCCTGTC-3'). Finally, the expected size band was obtained, purified using QIAquick Gel Extraction Kit (Qiagen AG, Basel, Switzerland), digested with FseI and AscI endonucleases and ligated in the vector previously digested with the same pair of restriction enzymes. Also in this case the reaction was not successful and the project was temporarily discontinued.

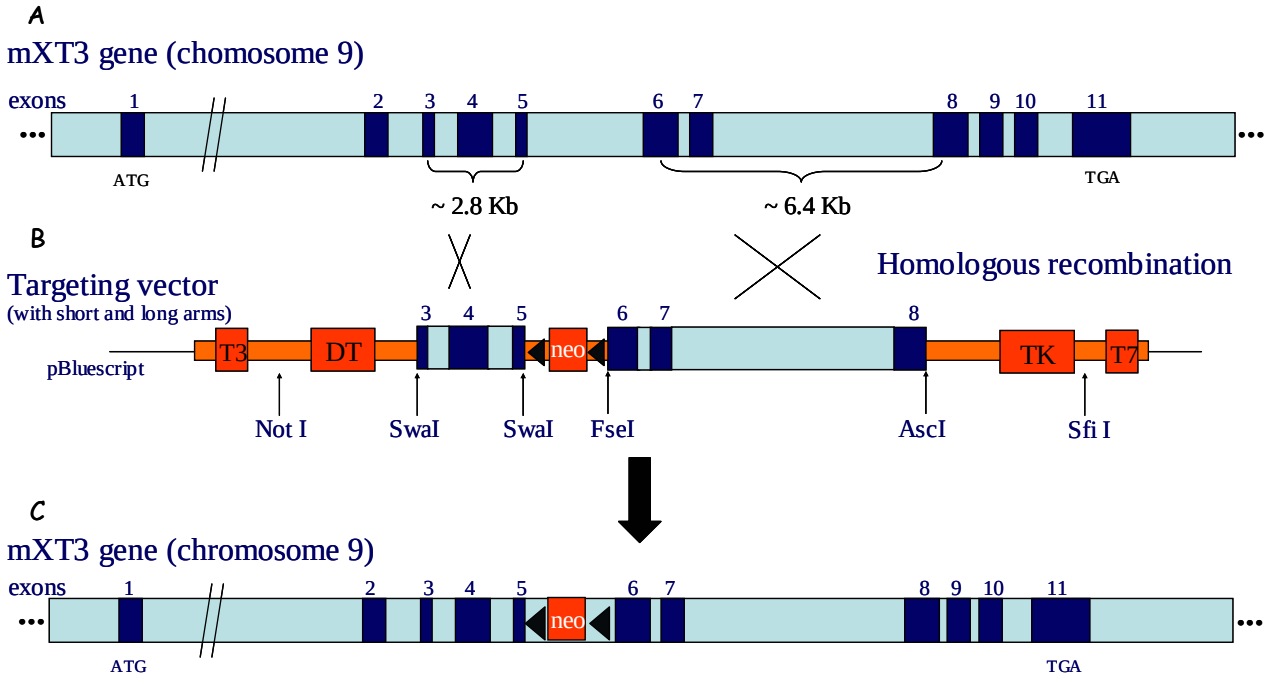

Figure 5. Models of the XT3 gene on mouse chromosome 9 (A), of the targeting vector containing the short (inserted in the SwaI restriction site) and the long (inserted between FseI and AscI restriction sites) arms (B) and of the modified XT3 gene after homologous recombination in transfected ES cells (C).

RESULTS

1. mXT3 stably transfected OK cells

The expression of B^0-cluster transporters in epithelial cell lines has been initiated in the laboratory of Prof. Verrey first with XT2 and XT3 several years ago. Several attempts by a former PhD student using the kidney epithelial cell lines mpkCCD, MDCK and HEK-293 did not elicit any amino acid transport and using polyclonal antibodies raised in rabbits in was shown in all these cell lines that the transporters remained intracellular (Ristic, unpublished results).

Encouraging results were obtained when I expressed mXT2 and mXT3 cDNAs in the Opossum Kidney (OK) cell line. These cells were chosen for two main reasons: first OK cells express many proximal tubule cell-like properties *in vitro* and second, they are easy to transfect.

Particular emphasis was given to the expression and subcellular localization of mXT3. The first results of immunolocalization of transiently transfected OK cells with cDNA coding for XT3 showed mostly an apical “patchy” pattern of fluorescence which represents the OK cells microvilli with XT3 transporter. A similar pattern had been shown before for sodium-phosphate (Na-Pi) type IIa cotransporters in OK cells (Hernando et al., 2000). We need to mention that the efficiency of transient transfection of OK cells 24 h after addition of XT3 cDNA was ~ 10-20%. The immunohistochemistry was performed when the culture reached confluence (after 72 h) and at this stage the number of transfected cells was low.

For this reason, we produced a stably transfected OK cells using cDNA coding for mouse orphan transporter XT3 and CD8. Cells were selected using anti-CD8 metallic beads as described in details in the “Materials and Methods” section. Expression of XT3 transporter was analyzed by immunofluorescence, showing that stably expressed XT3 is localized at the apical membrane of OK cells (Figure 1). The observed different sorting behaviour of the same transporter in different cell lines confirmed the hypothesis that not only molecular determinants on the transporter are decisive for an apical sorting, but that also the cellular context is of importance.

Several attempts were made to differentiate the transport due to exogenous XT3 from the endogenous one and from the other transport systems in the OK cells but without success. One reason for this failure might be that the activity of the exogenous transporter was masked by the one of the endogenous XT3 and probably by other amino acid transporter systems of these cells.

We therefore decided to take another approach focusing on the characterization of OK cell endogenous transporters (Ristic et al., 2005).

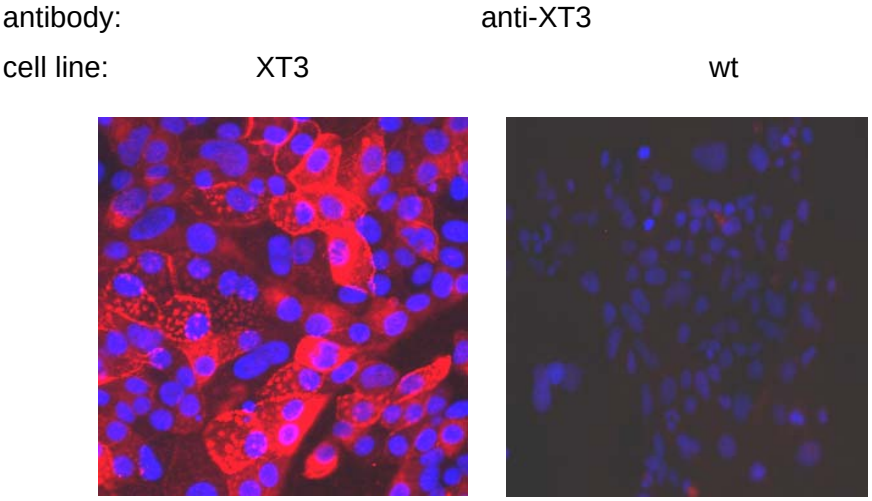

Figure 1. Immunofluorescence of OK cells. The stable XT3-transfected protein is expressed at the apical membrane of OK cells within microvilli. XT3-transfected and untransfected OK cells were grown to confluence on glass coverslips and further processed for immunofluorescence. Double staining of nuclei in blue and XT3 protein in red.

2. Localization of SLC6 transporters of B^0AT-cluster

2.1 Tissue mRNA distribution of B^0AT-cluster transporters

The results presented in the next 6 pages have been published on The American Journal of Physiology (Romeo et al., 2005).

The relative abundance of mRNAs encoding the four related transporters B^0AT1, XT2, XT3 and XT3s1/SIT1 was measured in several organs/tissues by Taq Man® real-time RT PCR using GAPDH as internal standard. Figure 2 shows the relative abundances of these transcripts. A high expression level of all four mRNAs was found in kidney, relative

to GAPDH approximately 10% for B^0AT1, XT2 and XT3 and 1% for XT3s1. In small intestine mucosa, the level of B^0AT1 mRNA was similar to that found in kidney and XT3s1/SIT1 mRNA was abundant as well. In contrast, XT2 and XT3 mRNAs were 100- to 1000-fold less abundant and displayed an axial gradient towards the ileum. In all tested tissues but muscle (and very low in heart) the transcript of at least one of these transporters was detected. Interestingly, the spleen that is not considered as an epithelial organ does express all four mRNAs to some extent. In the brain, XT3s1/SIT1 showed the strongest expression while no XT2 mRNA was detected. In contrast to some of our negative data obtained by TaqMan® real time RT-PCR on tissues of two C57BL/6J mice, a recent publication showed qualitatively the expression of XT3 mRNA in mouse lung and of XT3s1/SIT1 mRNA in mouse muscle and hearth (Kowalczuk et al., 2005). We have no explanation for this difference that could be of technical nature or due to the use of another mouse strain.

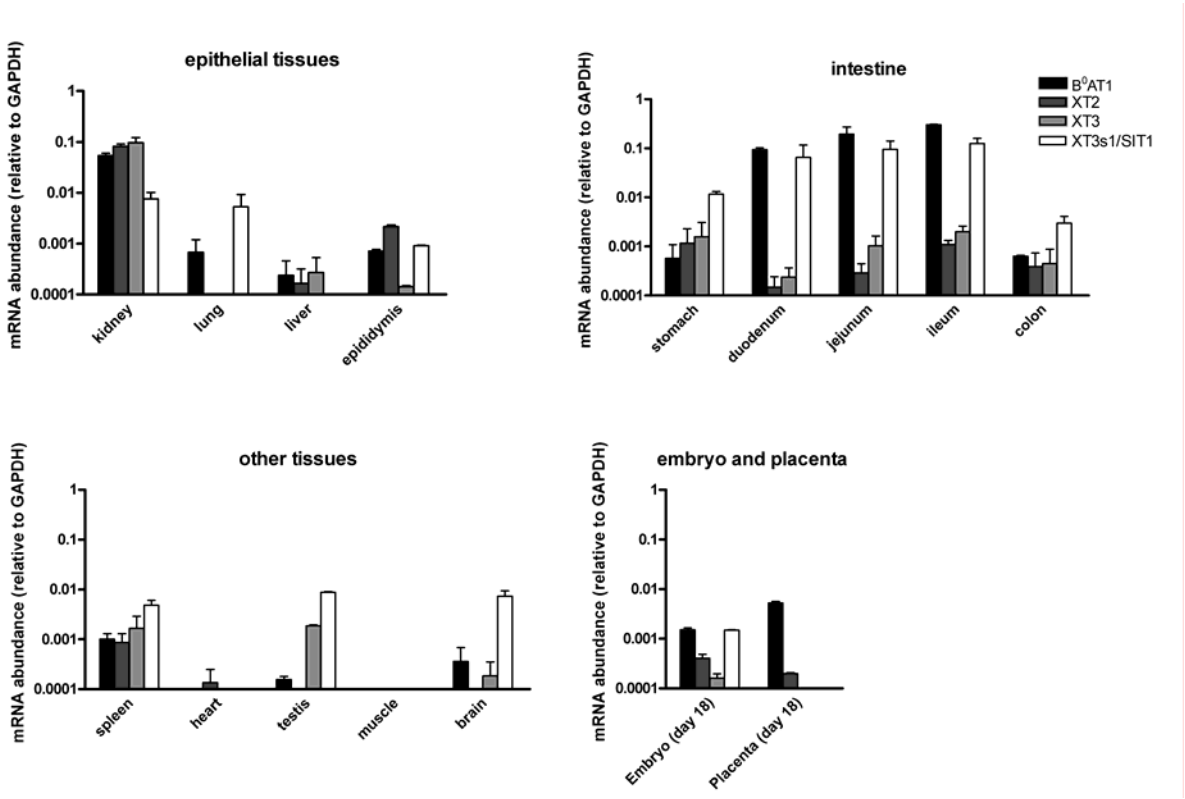

Figure 2. Relative mRNA abundance of mB^0AT1, mXT2, mXT3 and mXT3s1/SIT1. The abundance of mRNAs was measured by real time RT-PCR (see Material and Methods) and the level of the tested transporter mRNAs relative to that of GAPDH is indicated for each tissue. A relative abundance of 1 corresponds to the copy number of GAPDH mRNA the expression of which was relatively homogenous within RNA of epithelial tissues (cycle number to reach threshold (Ct): from 23.23 for kidney to 26.59

for colon) and other tissues (Ct 22.74 for heart to 28.81 for spleen). Significant expression of all four B^0AT-cluster mRNAs was found in kidney and small intestine where B^0AT1 and XT3s1/SIT1 mRNAs were the highest. XT3s1/SIT1 mRNA is also abundant in brain, testis, spleen, stomach and lung. The mean relative mRNA abundance tested independently in two mice is shown. Values are expressed as mean ± S.E.M.

2.2 Glycosylation of B^0AT1 and related transporters

B^0AT1 displays five or six N-glycosylation consensus sites within its putative extracellular loops that are distant enough from the closest transmembrane segment to be potentially glycosylated (http://www.cbs.dtu.dk/services/NetOGlyc/). In contrast, the three transporters XT2, XT3 and XT3s1/SIT1 display only two to three such potentially glycosylated consensus sites (Bennett and Kanner, 1997; Chen et al., 1998; Mingarro et al., 2000). Figure 3 shows the effect of the treatment of small intestine and kidney brush border vesicle proteins with endo-beta-N-acetylglucosaminidase F (PNGase F), an enzyme that cleaves off high-mannose and terminally glycosylated N-glycans (Elder and Alexander, 1982).

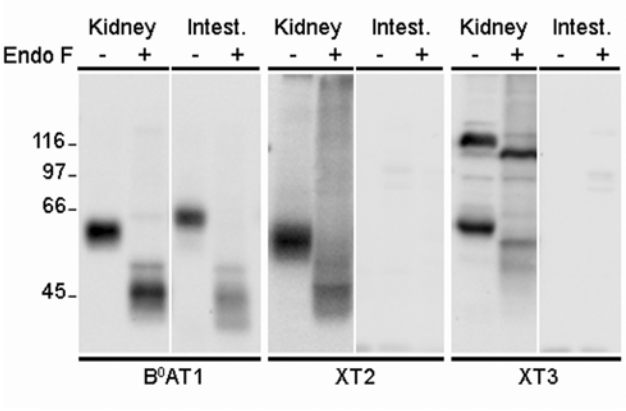

Figure 3. **Endoglycosidase assay on kidney and small intestine BBMVs.** 20 μg of kidney and total intestine BBMVs were separated on a 10% polyacrylamide gel after treatment with (+) or without (-) PNGase F enzyme and submitted to Western blotting. XT2 and XT3 were not detected in intestine whereas the anti-XT3s1/SIT1 antibody does not function in Western blotting. As expected from N-glycosylation site predictions, a shift of the specific band towards lower molecular weights was observed for B^0AT1, XT2 and XT3.
The particular migration of deglycosylated XT3 in comparison with deglycosylated B^0AT1 and XT2 could be due to differential post-translational modifications not investigated in this study.

The unique strong band corresponding to B^0AT1 migrates at the level of approximately 70 kD and deglycosylation shifts this band to approximately 48 kD. This fast migration for a protein with a calculated molecular weight of 71 kD could be due to its very hydrophobic nature. The shift in the relative migration induced by deglycosylation is compatible with the cleavage of four to six complex N-glycans. In the case of XT2, the fully glycosylated form migrates around 57 kD and the deglycosylated one around 48 kD (calculated MW 69 kD) as that of B^0AT1. Again, the apparent MW of the deglycosylated form is compatible with the highly hydrophobic nature of the polypeptide and that of the glycosylated form suggests, as expected, the presence of two or three complex N-glycans. The migration pattern of XT3 is more complex. There are two major bands, one migrating at approximately 62 kD and another, of variable intensity between experiments, around 120 kD. We do not know why deglycosylated XT3 migrates slower than B^0AT1 and XT3s1/SIT1 (apparent MW of 62 versus 48 kD) and forms apparently also a dimer. A potential explanation for the slightly slower migration of XT3 could be a differential post-translational modification other than N-type glycosylation. Concerning the higher MW band, the most likely hypothesis is that it corresponds to a homodimer that resists denaturation and reduction. Endo F treatment produced a shift of both bands indicating the presence of N-glycans. In the case of XT3s1/SIT1 no such information could be obtained since the antibody failed to recognize any specific band in Western blot (data not shown).

2.3 Axial and subcellular localization of B^0AT-cluster transporters in kidney

Immunohistochemistry showed that B^0AT1, XT2, XT3 and XT3s1/SIT1 localize to the apical brush border membrane of proximal tubule cells. No specific staining was observed in other nephron segments or structures. The axial distribution of the four proteins along the proximal tubule differs, as shown in Fig. 4. The heavy chain of the heterodimeric amino acid transporters 4F2hc (CD98) is shown in green as basolateral marker (Dave et al., 2004; Rossier et al., 1999). B^0AT1 is expressed mainly in the early proximal tubules (S1 segment) starting at the glomerulus. The distribution of XT2 along the proximal tubule is essentially restricted to the later segments S2 and S3 and thus quite complementary to that of B^0AT1. XT3 and XT3s1/SIT1 were detected in the brush

border membrane all along the proximal tubule, their levels decreasing slightly towards the end (Fig. 4g). The axial distribution of the transporters (red) is clearly visible in the low magnification pictures of consecutive mouse kidney sections (Fig. 4a-d) while the characteristic brush-border membrane staining is appreciable in the high magnification pictures (Fig. 4e-h).

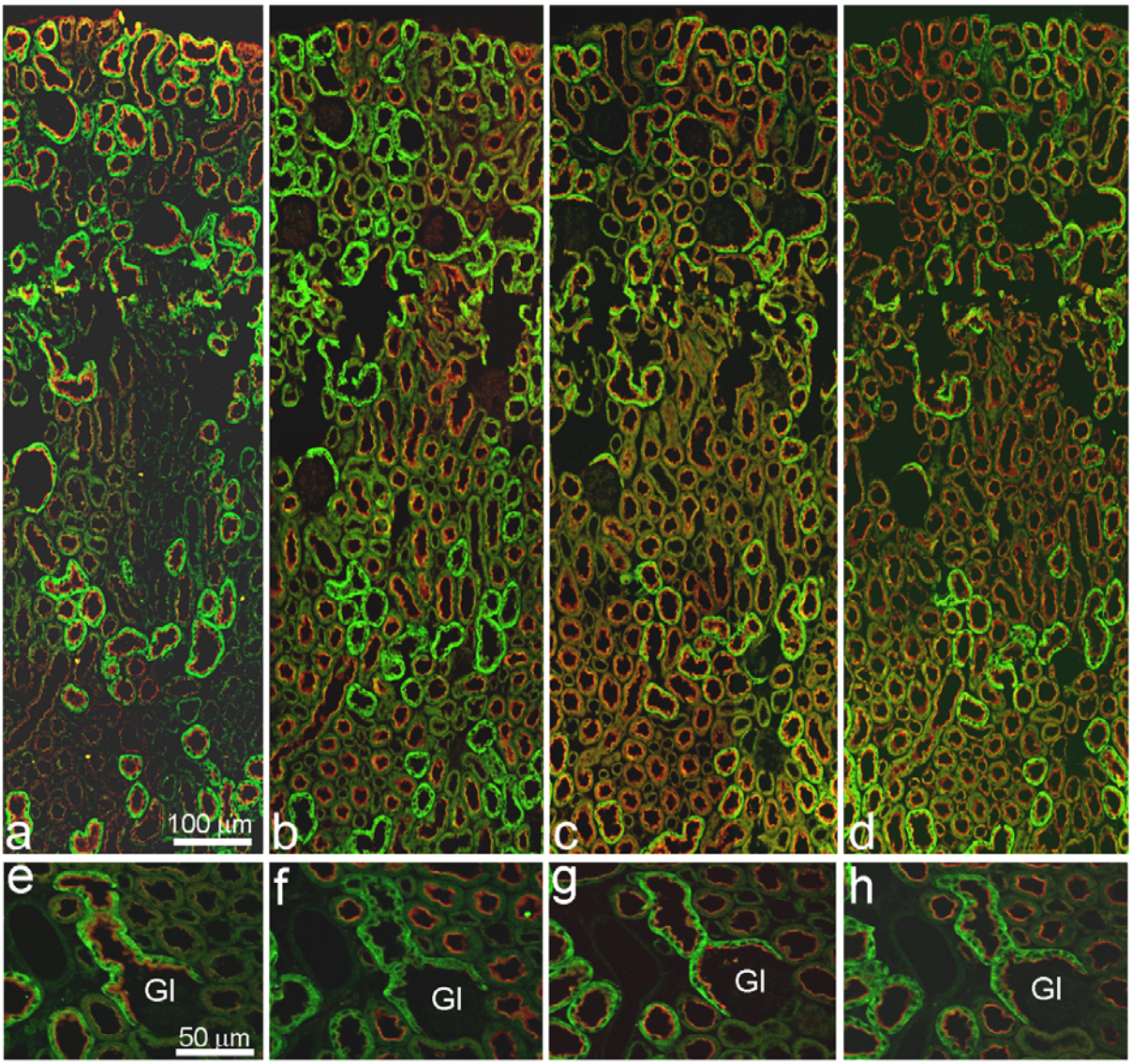

Figure 4. Localization of B^0AT1, XT2, XT3 and XT3s1/SIT1 in kidney. Immunohistochemistry localized each of the four proteins to the brush-border membrane of kidney proximal tubules (red) while 4F2hc (CD98) was used as basolateral marker (green). The upper row shows consecutive overview sections of kidney cortex while the lower row shows higher magnifications. a and e, B^0AT1; b and f, XT2; c and g, XT3s1/SIT1; d and h, XT3. The bars are in the upper row 100 µm and 50 µm in the lower row. Gl, glomerulus.

2.4 Segmental and subcellular localization of B^0AT-cluster transporters in small intestine

All along the mouse small intestine (duodenum, jejunum and ileum), the affinity purified anti-B^0AT1, anti-XT2 and anti-XT3s1/SIT1 antibodies showed a strong apical staining of the enterocytes lining the intestinal villi whereas no signal was detected with the anti-XT3 antibody. The staining is shown in Fig. 5 for jejunum with the four B^0-cluster transporter antibodies (red channel) and anti-4F2hc (green channel) as basolateral marker (Dave et al., 2004; Rossier et al., 1999). Mucus-secreting goblet cells did not show any basolateral or apical staining, indicating that these transporters are expressed only by the transporting enterocytes.

The fact that staining was observed for XT2 whereas no specific staining was seen with the anti-XT3 antibody is probably antibody-specific. Indeed, the mRNA of these two gene products was of similar low abundance in small intestine and for both proteins we did not obtain any signal on Western blots of small intestine brush-border membrane, unlike with kidney brush border membranes where both were detected. As expected for proteins involved in the function of differentiated enterocytes, the signal showed a clear gradient along the villi, being low in the crypts and stronger towards the tips.

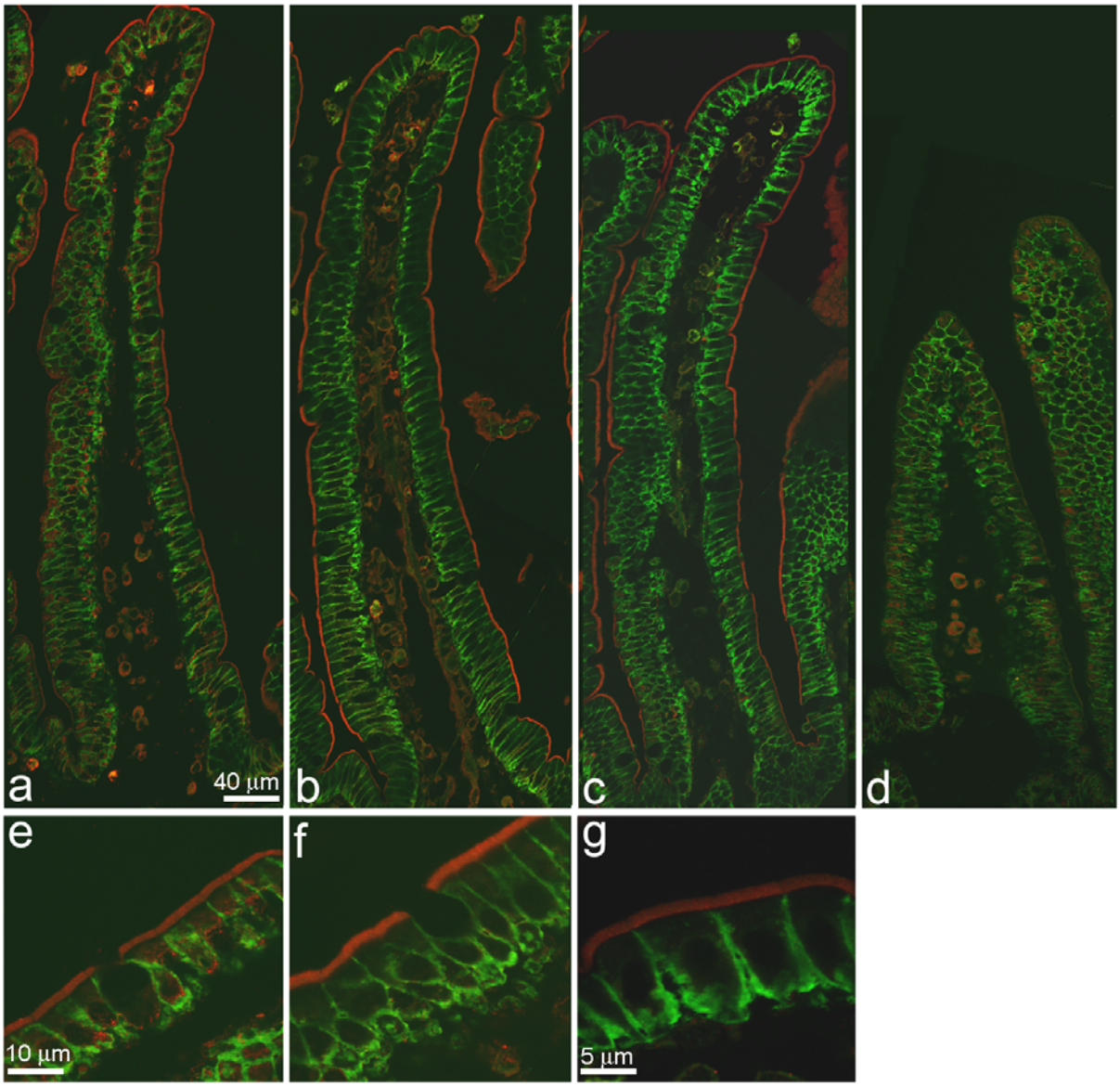

Figure 5. Localization of B^0AT1, XT2, XT3 and XT3s1/SIT1 in small intestine. Immunohistochemistry localized three out of four transporters (B^0AT1, XT2 and XT3s1/SIT1, red) to the brush-border membrane of intestinal villi with an axial gradient toward the tip. XT3 staining was not clearly visible. Anti-4F2hc antibody labels the basolateral membrane of intestinal epithelial cells (green) . Unlabelled spaces between enterocytes correspond to goblet cells. The upper row shows low and the lower row high magnification images. a and e, B^0AT1; b and f, XT2; c and g, XT3s1/SIT1; d, XT3. The bars are in the upper row 40 µm and 10 µm in the lower row (e and f) and 5 µm (g).

3. Regulation studies on mice challenged with modified diets

3.1 High and low sodium diet treatment

In 1994 Wasserman and colleagues molecularly characterized the rat homologue of XT2, calling it ROSIT for Renal Osmotic Stress-Induced Na^+/Cl^- -dependent organic Transproter (Wasserman et al., 1994). It was shown, by Norhtern blot analysis, that rats made hypernatremic by gavage display a marked increase in ROSIT/XT2 mRNA levels in renal cortex, renal outer medulla and possibly in intestine. Following studies by Obermuller and colleagues, showed by in situ hybridization high levels of ROSIT/XT2 mRNA in late proximal kidney tubule (S3 segment) and investigated the alteration of ROSIT/XT2 transcript in response to ischemic acute tubular necrosis, as the S3 segment is the major site of damage in the post-ischemic kidney. The study showed that ROSIT/XT2 mRNA levels were decreased in response to the damage (within 7 days) and that they were back to the normal level three weeks after ischemia (Obermuller et al., 1997). In 2004 Baba and colleagues investigated the localization and regulation of the renal osmotic-stress-induced Na-Cl organic solute cotransporter (ROSIT/XT2) mRNA expression by RT-PCR using microdissected nephron segments from control and dehydrated rats. They showed that ROSIT/XT2 mRNA was expressed predominantly in PST and to a lesser extent in cortical thick ascending limbs and cortical collecting ducts in control rats, and dehydration caused an increase in the expression in all nephron segments (Baba et al., 2004).

Based on these results we decided to investigate the regulation of the expression of the mouse ROSIT orthologue, mXT2, and also of the other three related genes, mB^0AT1, mXT3 and mXT3/SIT1 by real-time RT-PCR and Western blot. As described in the Materials and Methods section, 18 male C57BL/6J mice were divided into three groups and received diets with different Na^+ contents. After two days, mice were sacrificed and kidneys harvested. Real-time RT-PCR was performed for the four B^0-cluster transporter and both mGAPDH and mβ-actin were used for relative quantification. At first we evaluated the effect of Na^+ on the two housekeeping genes, mGAPDH and mβ-actin, to make sure that no regulation would occur under these conditions (Figure 6). The

analysis revealed that there is no effect on these two transcripts in the different conditions.

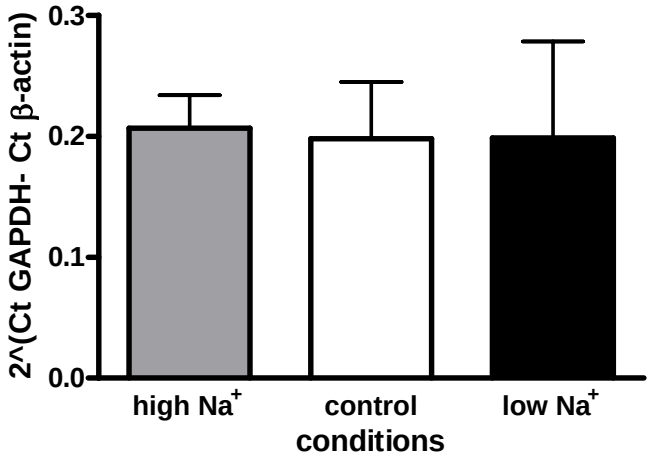

Figure 6. Real-time RT-PCR on mGAPDH and mβ-actin. The effect of different Na^+ content diets was evaluated on two housekeeping gene, mGAPDH and mβ-actin. The graph shows that there is no effect due to the different treatments. Statistical analysis was performed with ONE-WAY ANOVA test with Dunnett's multiple comparison test.

The effectiveness of the short-term treatment was evaluated performing real-time RT-PCR on the same kidney cDNAs probing mGAT2. mGAT2 (slc6a12) is the orthologue of rat and human BGT1 (SLC6A12). In renal epithelial cells, BGT1 is localized to the basolateral membrane and mediates betaine uptake and accumulation (Yamauchi et al., 1991). The mRNA is most abundant in the medullary thick ascending limb and the inner medullary collecting duct (Miyai et al., 1996) and is regulated by the hydration state *in vivo* (Moeckel et al., 1997), being induced by hypertonicity. Similar observations were obtained from *in vitro* studies: BGT1 transport activity is low in renal MDCK cells maintained in isotonic medium but is strongly induced in response to prolonged (24h) hypertonic stress (Kempson, 1998; Yamauchi et al., 1991; Yamauchi et al., 1992).
The two-days treatment of the mice was effective as shown in Figure 7. mGAT2 mRNA levels were indeed significantly increased ($p < 0.01$) in the "high Na^+" condition and unchanged in the "low Na^+" condition, compared with the "control".

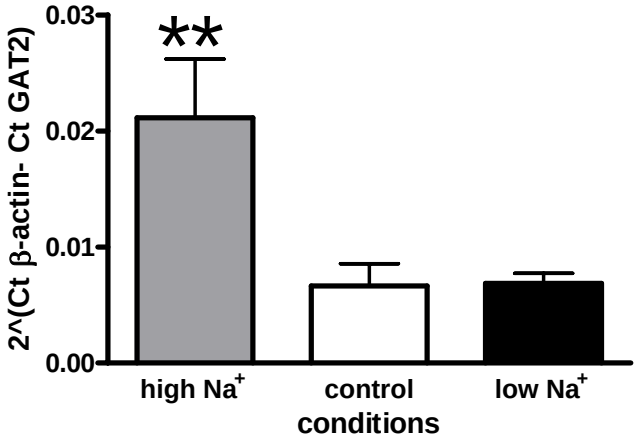

Figure 7. Real-time RT-PCR on mGAT2. The regulation of mGAT2 was evaluated in the three different conditions and the relative quantification of the transcript was calculated using mβ-actin as reference gene. Statistical analysis was performed with ONE-WAY ANOVA test with Dunnett's multiple comparison test. Stars indicate significant difference versus control ($P < 0.01$).

Figure 8 shows the result of the real-time RT-PCR performed on kidney mRNA of three mice from each group. A significant upregulation of mB^0AT1 transcript induced by the high Na^+ diet was observed while the same treatment led to a significant downregulation of mXT3 mRNA. The effect of the low sodium diet was to increase significantly mXT3 and mXT3s1/SIT1 transcripts. No other significant variations could be observed, in particular no change in XT2 (ROSIT orthologue) mRNA level.

The protein expression levels were analysed on kidney BBMVs (See Materials and Methods). For Western blotting, 20 μg of BBMVs proteins were separated on polyacrilamide gels and blotted on PVDF membranes. Membranes were then probed with mB^0AT1, mXT2, mXT3 and mβ-actin antibodies. Figure 9 shows the quantification of each of the tested transporters relative to mβ-actin signal. Differently from what was observed by real-time RT-PCR at the mRNA level, no significant regulation was detectable at the protein level. Finally, as mentioned above, in the case of XT3s1/SIT1 no information could be obtained since the antibody failed to recognize any specific band in Western blot.

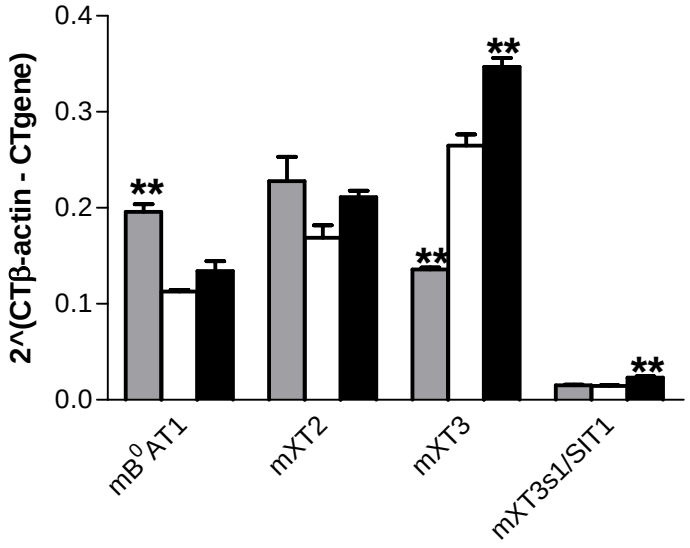

Figure 8. Relative mRNA abundance of mB^{0}AT1, mXT2, mXT3 and mXT3s1/SIT1. The abundance of mRNAs was measured by Taq Man® real time RT-PCR and the level of the tested transporter mRNAs relative to that of mβ-actin is indicated for each condition. Significant upregulation of the mB^{0}AT1 transcript was found in response to high sodium content diet treatment while a downregulation was observed for the mXT3 transcript in the same condition. The low sodium content diet resulted in significant upregulation of the mXT3 and the mXT3s1/SIT1 transcripts.
The color code is the same as in Figure 6 and 7.
ONE-WAY ANOVA test with Dunnett's multiple comparison test. Stars indicate significant difference versus control ($P < 0.01$).

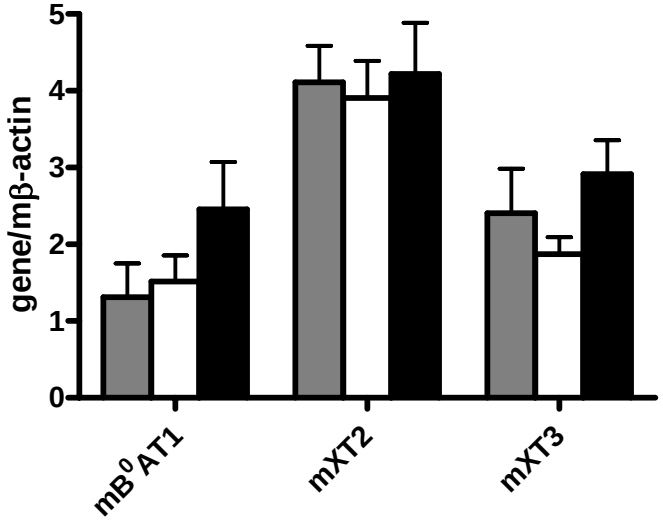

Figure 9. Relative protein abundance of mB^{0}AT1, mXT2 and mXT3. The abundance of the transporter proteins was estimated by Western blotting relative to the mβ-actin signal. No significant regulation was detected for the different conditions for any

transporter. mXT3s1/SIT1 could not be quantitated due to the lack of reactivity of the antibody on Western blots. Statistical analysis was performed with ONE-WAY ANOVA and using Dunnett's multiple comparison test.

The different results obtained with the two techniques are probably due to intrinsic characteristics of quantifying mRNA levels versus protein. Real-time RT-PCR is extremely precise and reliable when compared to manual quantification of Western blot. In addition, there is no constant relationship between mRNA levels, protein production and protein pool and furthermore BBMVs proteins represent only a part of the cellular protein content whereas the mRNA was from total kidney. Thus it appears that the changes in some transporter mRNA levels induced by different salt diets do not translate into changes in protein luminal cell surface expression.

3.2 Induction of metabolic acidosis and alkalosis

The mammalian proximal tubule reabsorbs 75-90% of the filtered HCO_3^-. This reabsorptive process involves luminal and basolateral transport, both of which may require Na ions. Na^+-dependent acid-base transporters include 1) a luminal Na^+-H^+ exchanger that is inhibited by amiloride (NHE-3 in kidney) and 2) a basolateral electrogenic Na^+/HCO_3^- cotransporter (NBC) that is sensitive to the blocking action of disulfonic stilbene derivatives (Geibel et al., 1989). The electrogenic Na^+/HCO_3^- cotransporter (symporter) is the major HCO_3^- transporter of the renal proximal tubule and also plays a noteworthy role in Na^+ reabsorption (Boron et al., 1997).

During chronic metabolic acidosis (CMA), the plasma levels of glutamine are increased and so is glutamine metabolism in the kidney tubule cells. Degradation of glutamine results in the formation of ammonium (NH_4^+) and bicarbonate (HCO_3^-) ions, which are excreted into the pre-urine and transported to the peritubular blood, respectively. This process contributes to counteract acidosis and to restore normal pH.

Glutamine transport plays and important role both for the generation of ammonia that is used for protein excretion and for that of bicarbonate. Edwards' group molecularly identified a protein, SN1 (SNAT3, SLC38A3), corresponding to the neutral amino acid transport system N (Chaudhry et al., 1999; Palacin et al., 1998) and thus mediates Na^+-dependent glutamine transport. SNAT3 is localized in astrocytes in the brain and retina,

liver, kidney and adipose tissue (Mackenzie and Erickson, 2004). It has recently been shown to be expressed basolaterally in proximal kidney tubule and to be strongly induced in acidosis (Solbu et al., 2005) (Moret et al., in preparation).

Glutamine is also one of the favourite B^0AT1 substrates (Bohmer et al., 2005; Camargo et al., 2005). To investigate the possible contribution of B^0AT1 and related transporters in amino acid and in particular glutamine cellular import during metabolic acidosis and alkalosis, we submitted mice to acidosis and alkalosis by supplying 0.28 M NH_4Cl and 0.28 M $NaHCO_3$ in the drinking water, respectively, for 7 days. Then mice were sacrificed and kidney harvested to analyze the mRNA and protein content. Figure 10 shows the expected upregulation of mSNAT3 transcript by real-time RT-PCR in mice having metabolic acidosis, a result that validates our treatment. The increase is about 6-fold compared to control mice while there is no effect of metabolic alkalosis on mRNA levels of treated mice.

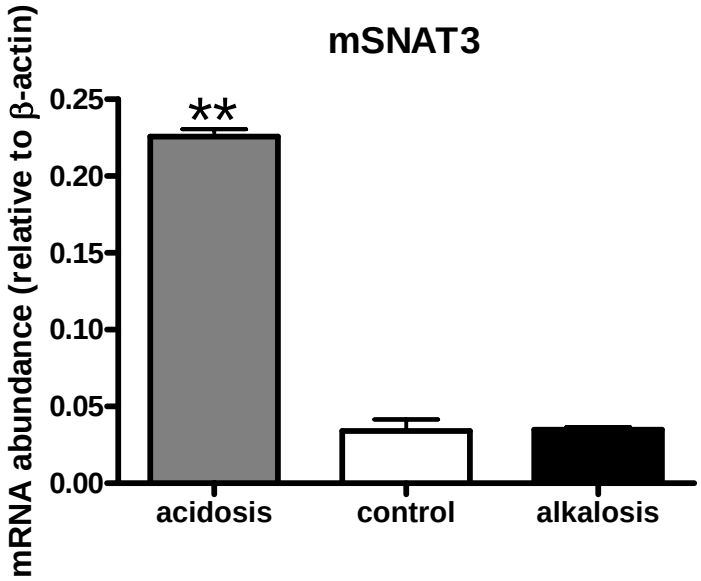

Figure 10. Real-time RT-PCR of mSNAT3 mRNA. The regulation of mSNAT3 mRNA was evaluated in the three different conditions and the relative quantification of the transcript was calculated using mβ-actin as reference gene. A 6-fold increase in the mSNAT3 transcript was observed. Statistical analysis was performed with ONE-WAY ANOVA test with Dunnett's multiple comparison test. Stars indicate the statistical significance of the difference relative to the control ($P < 0.01$).

The mRNA abundance of mB^0AT1 and related transporters is shown in Figure 11. A statistically significant downregulation of B^0AT1 mRNA was observed in animals

receiving NH_4Cl in the drinking water. A small decrease in the transcript levels of mXT2 and mXT3s1/SIT1 was observed in mice that developed metabolic alkalosis and an increase in mXT3s1/SIT1 mRNA in acidotic mice. No significant effect was observed for the mXT3 transcript in either condition.

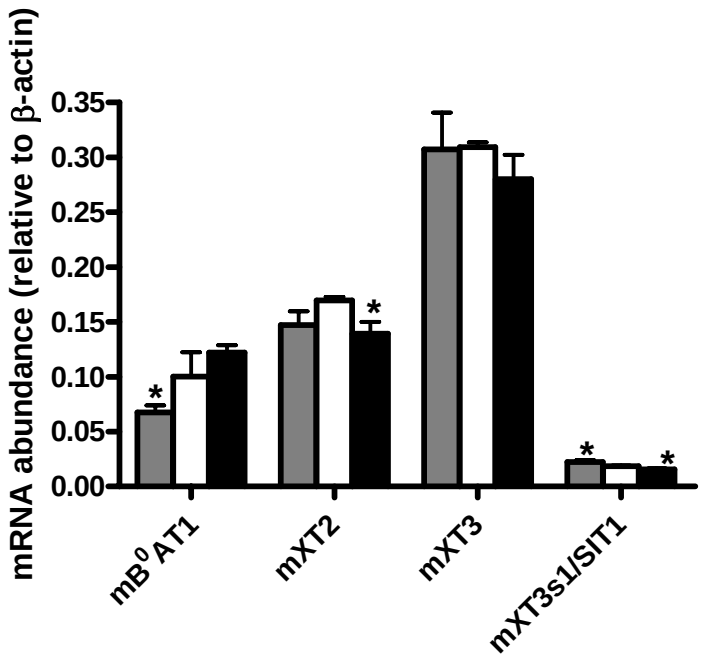

Figure 11. Relative mRNA abundance of mB^{0}AT1, mXT2, mXT3 and mXT3s1/SIT1. The abundance of mRNAs was measured by real time RT-PCR and the level of the tested transporter mRNAs relative to that of mβ-actin is indicated for each condition. A statistically significant downregulation of the mB^{0}AT1 and the mXT3s1/SIT1 transcripts was found in response to metabolic acidosis and for the mXT2 and the mXT3s1/SIT1 transcripts during metabolic alkalosis. No significant variations were observed for mXT3 in both conditions. Statistical analysis was performed with ONE-WAY ANOVA test with Dunnett's multiple comparison test. Stars indicate a statistically significant change versus control ($P < 0.05$).
The colour code is the same as in Figure 10.

The relative abundance of the transporter protein expressed in the luminal brush border was also evaluated and the results are shown in Figure 12. To perform Western blotting 20 μg of kidney BBMVs were separated on SDS-PAGE and transferred onto PVDF membranes that were then incubated with antibodies directed against mB^{0}AT1, mXT2 and mXT3. Anti-mβ-actin antibody was used as reference to evaluate the relative

abundance of these B^0-cluster transporters. As in the case of the Western blot shown in Figure 9, no significant differences were observed for the different transporters in treated and non-treated mice. As in the case of the different Na^+ diets the reason could be the different sensitivity of the two techniques as well as the material used.

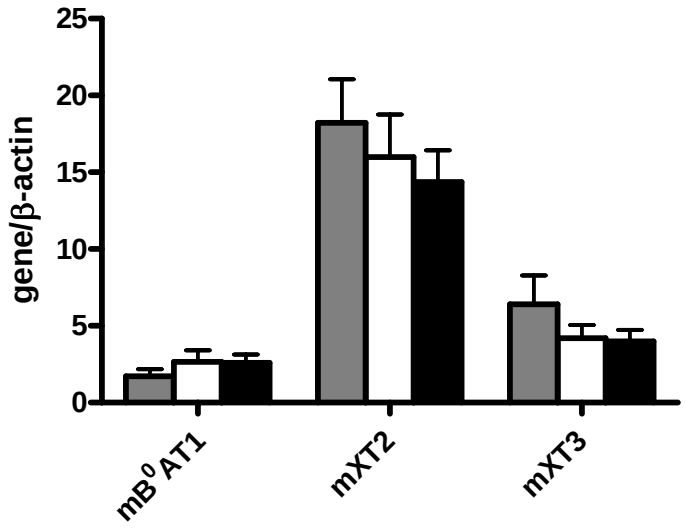

Figure 12. Relative protein abundance of mB^0AT1, mXT2 and mXT3. The abundance of proteins was measured by Western blotting relative to mβ-actin signal. No significant regulation was detected for the different conditions and transporters. It was not possible to make the evaluation for mXT3s1/SIT1 due to lack of reactivity of the antibody in Western blotting. Statistical analysis was performed with ONE-WAY ANOVA test with Dunnett's multiple comparison test.

4. XT3 knockout mice generation

Functional investigations of the XTs were initially pursued with different i*n vitro* models, such as mammalian cells and *Xenopus laevis* oocytes. Focusing on mXT2 and mXT3 these studies failed to elucidate their function. Therefore, we tought to use a different approach, creating a knockout mouse for XT3.

The mouse XT3 gene is located on chromosome 9, extends over about 40 kb and it is constituted by 11 exons and 10 introns. Analyzing the gene sequence of mXT3 available three years ago, we immediately had to exclude from the targeting vector plans the use of the intronic sequence between the first and the second exon due to long stretches of unknown sequence. The strategy that we then followed for the construction of the

targeting vector to be used for the transfection of the embryonic stem cells has been already described in the Materials and Methods section.

As mentioned, the PCR amplification of the long sequence located between exons 6 and 8 first required much technical adaptation and then the fragment resisted multiple attempts of cloning into the targeting vector. Therefore and also because this first member of the SLC6 cluster of interest SLC6A19, was identified and characterized as B^0 transporter (Broer et al., 2004), we decided to provisionally discontinue this project. We then focused on a XT2 knockout mouse obtained from M. Caron that is being currently backcrossed and characterized by D. Singer, a new PhD student of our lab.

DISCUSSION

1. Expression of mXT3 in Opossum Kidney cells

Functional characterization of the B^0-cluster transporters mXT3 and mXT2 was first attempted in mammalian cell lines and *Xenopus laevis* oocytes. Their expression in oocytes and in several mammalian cell lines resulted in no induced amino acid transport due to lack of surface expression. The only cell line showing apical surface expression for mXT2 and mXT3 was the Opossum kidney (OK) cell line, from which we later cloned the ortholog genes for XT3, XT2 and B^0AT1 (Ristic et al., 2005). Focusing on XT3, we produced a stably transfected cell line, hypothesising that the presence of the transporter at the apical surface would allow its functional characterization. Despite the apical localization of mXT3, stably transfected OK cells were not a useful tool for the investigation of the transport characteristics of mXT3, as the transport measured in cells expressing the exogenous transporter was not significantly different from the transport expressed endogenously in wild type cells. The difficulty of differentiating mXT3-induced transport from the overall transport measured in these cells could be due to several reasons. For instance the complexity of an intact cell system with its pool of amino acid transporters possibly having overlapping substrates with the transporter of interest. Moreover, the expression level of the exogenous transporter might be not enough to be distinguished from the total transport measured and/or might be masked by the endogenous XT3 transporter.

Hypothesising that mXT3 could be a B^0-type transporter, we decided to first investigate the B^0-type neutral amino acid uptake in wild type OK cells. Using this approach we could demonstrate that OK cell monolayers display a B^0-type Na^+- dependent neutral amino acid transport which is suggested to be mediated by more than one B^0-like transporter. Moreover, hybrid depletion and RNA silencing experiments showed that the opossum orthologue of human and mouse SIT1, oSIT1, plays a major role for the Na^+-dependent apical uptake of neutral amino acids in OK cells (Ristic et al., 2005).

2. B^0-cluster transporter in kidney and small intestine

2.1 B^0AT-related transporters in human and in mice

As described in the Introduction section (4.3), the majority of the members in the SLC6 family mediate the translocation of neurotransmitters across the cell membrane and fewer are involved in amino acid uptake, such as B^0AT1 and its related transporters, which form a separate cluster. In human, the cluster has three members while in mouse there is an additional one.

XT2 and B^0AT1 genes are organized in tandem on chromosome 5p15 in human, the locus where the Hartnup disorder has been mapped (Kleta et al., 2004; Seow et al., 2004). In mouse, these genes are located on chromosome 13 in a region, which is synthenic to human 5p15. The two mouse proteins have a degree of identity of about 50%.

In human, there is a single XT3 gene (SLC6A20) located on chromosome 3p21.3 for which two splice variants have been detected. Surprisingly, the brain-specific isoform is predicted to lack one of the 12 putative transmembrane domains, whereas the isoform expressed in kidney has an overall domain structure similar to B^0AT1 (Kiss et al., 2001). In mouse and in rat, there are two corresponding genes organized in tandem on chromosome 9, XT3 and XT3s1, the latter encoding XT3s1/SIT1 (Takanaga et al., 2005). The identity between XT3 and XT3s1/SIT1 proteins is 90%, with complete identity over long stretches and large differences only in the NH2- and COOH- termini. XT3s1/SIT1 shares a higher degree of identity (91%) with human XT3 compared with mouse XT3 that is only 86% identical. It appears thus that the mouse XT3 gene is the product of a relatively recent duplication and that mouse XT3s1/SIT1 more closely resembles human XT3 (Kiss et al., 2002).

Our localization data suggest that mouse XT3s1/SIT1 has a broader expression pattern than mouse XT3. Similarly, EST databases reveal that rat SIT1 is also widely-distributed, as pointed out in the publication on rat SIT1 (Takanaga et al., 2005). This rat gene, previously referred to as XT3 or rB21a, is in reality the orthologue of mouse XT3s1/SIT1 (Takanaga et al., 2005). In situ hybridization in mouse and in rat did not

distinguish between the two gene products and revealed their localization in brain, kidney and small intestine (Kowalczuk et al., 2005; Takanaga et al., 2005).

2.2 Tissue localization of the B^0AT-cluster transporters

The B^0AT-cluster transporters are mainly expressed in tissues that contain epithelia. They are all abundantly expressed in kidney and they are also present in small intestine where B^0AT1 and XT3s1/SIT1 mRNAs are 100- to 1000-fold more abundant than those of XT2 and XT3. Immunofluorescence experiments in kidney and small intestine show that all four transporters localize to the brush border membrane of epithelial cells, a localization that is compatible with a role in apical uptake of solutes, for instance amino acids in the case of B^0AT1 and imino acids in the case of XT3s1/SIT1. This localization agrees with the known function of B^0AT1 that is defective in Hartnup disorder (Broer et al., 2004; Kleta et al., 2004; Seow et al., 2004) and with that of XT3s1/SIT1 that was shown in *Xenopus laevis* oocytes to mediate a transport corresponding to that of brush border imino system (Kowalczuk et al., 2005; Takanaga et al., 2005). It is noteworthy that the two other luminal transporters did not produce, in the same expression conditions, any reproducible amino acid transport. Interestingly, these transporters (XT2 and XT3) appeared on immunofluorescence images not to localize to the surface of *Xenopus laevis* oocytes (data not shown). From their high level of similarity with B^0AT1 and XT3s1/SIT1 respectively, one can suggest the hypothesis that XT2 and XT3 might exert similar but complementary functions.

2.3 Differential localization of the B^0AT-cluster transporters along the kidney proximal tubule and in small intestine

B^0AT1 localizes to the early part of the proximal tubule (S1 and S2 segments), very similarly to $b^{0,+}$AT1, the catalytic subunit of the apical cystinuria transporter, and to the basolateral heterodimeric transporters y^+LAT1- and LAT2-4F2hc that are known to play an important role in the basolateral export of amino acids (Bauch et al., 2003; Borsani et al., 1999; Dave et al., 2004; Fernandez et al., 2002; Pfeiffer et al., 1999; Torrents et al., 1999; Verrey et al., 2004). The common S1-S2 localization of these transporters

suggests that they are part of high capacity amino acid transport machinery. In contrast, XT2, the "tandem" transporter of B^0AT1, localizes also to the brush border membrane of the proximal tubule, but with a complementary axial distribution, namely mainly in S3, the late segment of the proximal tubule. This differential and complementary axial localization of related transporters along the proximal tubule resembles that of the two sodium-glucose co-transporters (SGLT1 and -2) and of the two proton-driven peptide transporters (PEPT1 and -2) where in both cases the low affinity form localizes to the early part and the high affinity form to the late part of the proximal tubule (Kanai et al., 1994; Leibach and Ganapathy, 1996; Liang et al., 1995; Pajor et al., 1992; Poppe et al., 1997; Shen et al., 1999; You et al., 1995). As in these cases, B^0AT1 that localizes to the early part of the proximal tubule displays a relatively low apparent affinity with a $K_{0.5}$ of around 1 mM for its best amino acid substrates (Camargo et al., 2005). However, the function of its potentially “complementary” transporter XT2 is not yet clear, although it has been suggested based on the characterization of a knock out mouse that it is a high affinity glycine transporter (Quan et al., 2004). Interestingly, from these two transporters, it is the low affinity B^0AT1 that is more abundant in small intestine, similar to the situation of PEPT1 (Leibach and Ganapathy, 1996).

In contrast, the axial distribution of the ”tandem” transporters XT3s1/SIT1 and XT3 overlaps entirely along the kidney proximal tubule whereas in small intestine, only XT3s1/SIT1 is strongly expressed, both at the mRNA and protein levels. The localization the of XT3s1/SIT1 mRNA in the pia mater and plexus choroideus suggests that this transporter is also involved in L-proline transport in and out of the brain (Kowalczuk et al., 2005).

3. Dietary regulation of B^0-cluster transporters

3.1 Lack of major regulation of B^0-cluster transporters by Na^+ load or deprivation

In vivo studies on rats showed that ROSIT/XT2 is regulated by changes in sodium intake as a function of changes in the body fluid osmolarity (Baba et al., 2004; Obermuller et al., 1997).

Based on these observations, we hypothesised that the expression of ROSIT/XT2 mouse ortholog, mXT2 (SLc6a18), could be also affected in response to sodium load. In addition, we decided to extend our investigation to the other B^0-related genes, B^0AT1, XT3 and XT3s1/SIT1 and to treat mice with a sodium free diet. Mice treated with two different sodium content diets resulted in small mRNA variations of the four transporters but no change could be detected by Western blot analysis of the luminal cell surface proteins. The effectiveness of our treatment was confirmed by the analysis of the GAT2 (Slc6a12) mRNA level which was significantly upregulated in response to high salt diet, as expected.

Taken together these data show only a mild regulation of B^0-cluster transporters at the mRNA level by these treatments. Moreover, we could show that mXT2, in contrast to the results published for rat ROSIT/XT2, is apparently not osmotic-stress inducible, at least not by the high salt treatment that significantly upregulated GAT2 transporter mRNA. In drawing our conclusions, we need to consider that the gavage treatment for making the rats hypernatremic and our diet with high salt content given to mice are not identical and that this difference could explain the lack of mXT2 regulation in our study.

3.2 Lack of major regulatory effect of metabolic acidosis and alkalosis on B^0AT-related transporters

During metabolic acidosis, the Na^+-dependent glutamine transporter (SNAT3) is upregulated to increase the glutamine metabolism, leading to the production of more ammonium and bicarbonate (HCO_3^-). Bicarbonate transport to the peritubular blood counteracts acidosis and thereby helps maintaining the physiologically slightly alkaline blood pH (7.4).

Several transport systems can transport glutamine across plasma membranes. However, many of these systems either are not expressed in the kidney or are obligatory exchangers and thus unable to perform net translocation of amino acids across the plasma membrane (Chaudhry et al., 2002; Palacin et al., 1998). From the B^0-cluster transporters, B^0AT1 is known to transport glutamine (Bohmer et al., 2005; Camargo et al., 2005). Therefore we asked whether it was upregulated by acidosis similarly to SN1, that was shown in rats submitted to chronic metabolic acidosis to be increased five- to

six-fold in cortical tubule in parallel with the phosphate-activated glutaminase, a mitochondrial enzyme involved in ammoniagenesis (Solbu et al., 2005).

Our study in mice shows that induction of metabolic acidosis results in more than 4-fold increase in SNAT3 mRNA but has no major effects on the B^0AT-related transporter mRNAs, except for a slight downregulation of B^0AT1 and a mild upregulation of the mXT3s1/SIT1 transcript. Similarly, no regulation was observed during metabolic alkalosis.

Western blot analysis on the luminal cell surface proteins did not show any effect in both conditions.

Taken together our data suggest that B^0-cluster transporters are not sensitive to changes in the acid-base state, being expressed at similar levels in the different conditions tested.

4. Conclusions

The transporters B^0AT1, XT2, XT3 and XT3s1/SIT1 form a phylogenetic cluster within the SLC6 family. Besides their protein sequence similarity, they share brush-border localization in the proximal kidney tubule and are, as shown for B^0AT1 and XT3s1/SIT1, Na^+-dependent transporters of amino/imino acids. From this group of transporters, the two functionally characterized members are also the ones highly expressed in small intestine. All tissues expressing B^0AT-cluster members, with the exception of spleen, serve trans-epithelial/endothelial transport functions. Thus, the localization and the structural similarity of the pairs B^0AT-XT2 and XT3s1/SIT1-XT3 together suggest that the orphan transporters XT2 and mouse XT3 possibly exert epithelial amino- and imino(amino) acid transports which could be complementary to the function of B^0AT1 and XT3s1/SIT1, respectively.

Moreover, *in vivo* studies demonstrated that B^0AT-related transporters are only very mildly regulated by treatments that alter body fluid osmolarity and acid-base balance suggesting that they are constitutive elements of the proximal tubule reabsorption machinery and thus not involved primarily in providing substrates for metabolic tasks of these epithelial cells.

5. Future perspectives

The results presented in this PhD thesis contribute to the understanding of tissue localization and *in vivo* regulation of four mouse proteins belonging to the Slc6 family. Up to date only two of them, B^0AT1 and SIT1, have been functionally characterized while for XT2 a knock-out mouse is available and currently being investigated in our laboratory.

This characterization of the phenotype of the XT2 knock-out mouse that will include analysis of the amino acid levels in urine and blood could shed light on the function of this transporter in kidney. Moreover, using telemetric blood pressure measurements, we will investigate the functional role for XT2 in blood pressure control. Indeed, such an effect has been suggested by Caron's study in which XT2 knock out mice were shown to have an elevated blood pressure (Quan et al., 2004). Because XT2 knock out mice had shown in this study only a mild renal phenotype, this will be further analyzed by challenging them with high and low protein diets that might reveal more clearly transport defects. Additionally, since the mildness of the phenotype could be the result of compensatory mechanisms as for instance an increased expression of one or more other B^0-cluster transporters also localized in the late proximal tubule, real-time RT PCR and Western blot analysis could be used to test their expression levels in XT2 knock out mice compared to wild type animals.

As proposed for XT2, also the function of XT3 could be discovered using a knock out mouse. The finalization of the targeting vector I partially constructed could be the first step for the production of such a mouse model lacking XT3. The resulting phenotype could then be analysed using similar methods as described for the XT2 knock out mouse.

Finally, elucidating the function of XT2 and XT3 will clarify the role of these transport proteins for the reabsorption of amino acids in the kidney proximal tubule and will help to understand the differential localization of these proteins along the tubule that was observed by immunohistochemistry.

ADDENDUM

Project: Physiological role of 2-P-domain K^+ channels: Phenotypic analysis of the TASK2 knockout mouse.

Supervisor: Prof. Dr. Richard Warth, University of Regensburg, Germany

1. INTRODUCTION

1.1 The potassium channel family

Potassium channels are protein complexes that form K^+-selective pores in biological membranes, allowing the passive transport of K^+ through membranes. They play a major role in the control of K^+ homeostasis and cell volume but also in physiological functions that are associated with modifications of the electrical membrane potential such as neurotransmitters and hormone secretion and neuronal and muscular excitability. A wide variety of K^+ currents have been recorded in native tissues that can be distinguished according to their functional and pharmacological properties. In the last 15 years many K^+ channels have been cloned and characterized in expression systems. Since 1998 the structures of five different prokaryotic K^+ channels have been determined by x-ray crystallography, including KcsA (Doyle et al., 1998; Zhou et al., 2001), MthK (Jiang et al., 2003) (a Ca^{2+}-gated K^+ channel), KirBac (Kuo et al., 2003) (an inward-rectifier K^+ channel), KvAP (Jiang et al., 2003) (a voltage-dependent K^+ channel) and Kv1.2 K^+ (a voltage-dependent K^+ channel with its ß2 subunit) (Long et al., 2005; Long et al., 2005). They are multimers of hydrophobic subunits that form the ionic pore itself, often associated with accessory subunits (for review, see Refs. (Coetzee et al., 1999; Jan and Jan, 1997)). More than 60 pore-forming subunits have now been cloned in mammals. They are classified into three groups according to their membrane topology (Figure 1) (Buckingham et al., 2005). The largest group comprises subunits that contain a hydrophobic core with six transmembrane segments (6TMS) and one pore (1P) domain (figure 1c). This domain is directly involved in the formation of the selectivity filter that provides the specificity for K^+ transport. The second family is formed by pore-forming subunits having only 2TMS and 1P domain (Figure 1a). The extensive characterization of these two types of cloned subunits both *in vitro* and *in vivo*, as well as the isolation of associated regulatory subunits, has allowed the reconstitution of many different types of K^+ channels such as voltage-gated K^+ channels, Ca^{2+}-dependent K^+ channels, ATP-sensitive K^+ channels, G protein-coupled K^+ channels, and inward rectifiers.

The last group of K^+-selective pore-forming subunits corresponds to proteins with 4TMS and 2P domains, instead of one as for the other K^+ channel families (Figure 1b). This unique feature is at the origin of their name, 2P domain K^+ channels or K_{2P} channels.

1.2 Two-pore-domains channels

The first mammalian member of the two-pore-domains channel family was identified in 1996 and named TWIK1 (Tandem of P-domains in a weak inwardly rectifying K^+ channel) (Lesage et al., 1996). Fourteen other family members are now identified and subclassified based on their sensitivity to fatty acids, stretch, or protons (Lesage, 2003). According to the classification proposed by Buckingham the two-pore-domain channels can be subdivided into five functionally distinct groups: TWIK-like channels, stretch-activated TREK-like channels (TWIK-related K^+ Channel), TRAAK-like channels (TWIK-related arachidonic acid stimulated K^+ channel) activated by polyunsaturated fatty acids, acid-sensitive TASK1-like channels (TWIK-related acid-sensitive K^+ channels), and TRESK (TWIK-related spinal cord K^+ channel) (Buckingham et al., 2005; Lesage et al., 1996; Lesage and Lazdunski, 2000; Sano et al., 2003).

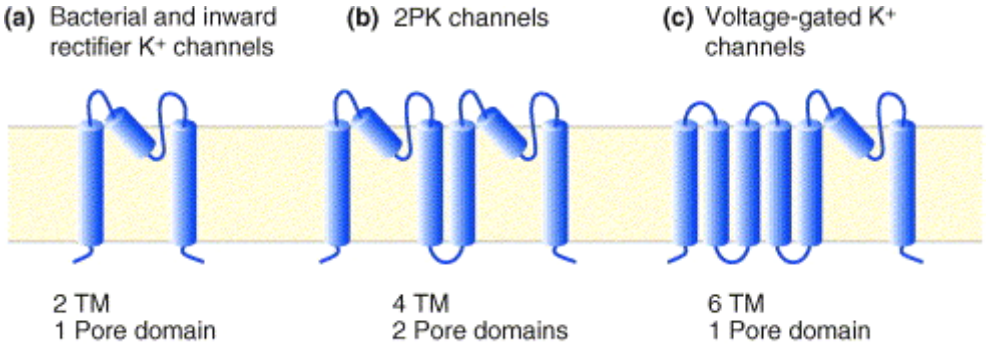

Figure 1. The topology of the transmembrane (TM) and pore-forming (P) domains of the three main classes of K^+ channels in animals: **(a)** inward rectifier channels, which contain two TM domains and one P domain; **(b)** two-pore-domain channels, which contain four TM domains and two P domains; and **(c)** SHAKER-like, voltage-gated K^+ channels, which contain six TM domains and one P domain. From (Buckingham et al., 2005)

1.2.1 TASK-2

TASK-2 was isolated from human kidney and its gene was mapped to chromosome 6p21 (Reyes et al., 1998). It is expressed in various epithelial tissues including the pancreas, placenta, lung, small intestine, colon, and at highest levels in kidney (Reyes et al., 1998; Warth et al., 2004). This is in contrast to TASK-1 and TASK-3 channels, which are mainly expressed in the CNS (Reyes et al., 1998). Moreover, immunolabeling for TASK-2 was observed in rat carotid bodies, peripheral chemoreceptive organs, which express also other 2P K^+ channels (Kummer and Yamamoto, 2002; Yamamoto et al., 2002).

TASK channels are sensitive to extracellular pH, the channel currents are maximal at alkaline pH and progressively inhibited as pH decreases: e.g. TASK-2 displays 90% of its maximal current at pH 8.8 but only 10% at pH 6.5 (Reyes et al., 1998). Moreover, TASK-2 currents are sensitive to anaesthetics, being inhibited by lidocaine and bupivacaine and activated by halothane and chloroform (Reyes et al., 1998).

My experiments contributed to the characterization of a TASK-2 knockout mouse model that has been created by K. Mitchell via disruption of the TASK-2 gene by a vector containing the genes for lacZ/neo and placental alkaline phosphatase (PLAP) (Mitchell et al., 2001). In particular, the respiratory and the renal phenotypes have been investigated using the following Materials and Methods.

2. MATERIALS AND METHODS

2.1 Genotyping

Tail biopsies were digested and treated as described in the Material and Method section of the main doctoral thesis. To localize the precise site of insertion of the secretory-trap vector into the TASK-2 gene I designed several primer pairs including the gene region of intron 1. PCR has been performed using different DNA polymerases: Advantage-GC Genomic Polymerase (BD Bioscience, Belgium), Advantage HF Polymerase (BD Bioscience, Belgium), EurobioTaq polymerase (Eurobio, France) and Pfu Turbo DNA Polymerase (Stratagene, La Jolla, CA, USA), using the buffers supplied and following

the protocol optimized by the company (including cycler conditions), in presence of 0.5 μM each primers (oligonucleotides) and 0.2 mM each dNTPs. Therefore, a real time PCR strategy to genotype TASK2 mice has been designed. Real time PCR has been performed with the same procedures described in the Material and Method section of the main doctoral thesis. The sequences of primers and probe used are: sense primer 5'- CCATTCGACCACCAAGCG-3'; antisense primer 5'- AAGACCGGCTTCCATCCG-3'; internal probe 5'- AACATCGCATCGAGCGAGCACGTA-3' labelled with reporter dye FAM at the 5' end and the quencher dye TAMRA at the 3' end (Microsynth, Balgach, Switzerland).

The primers used for the PCR to exclude the insertion in the intron 2-3 are: sense primer on exon 2 5'-CACAGTCATCACCACCATCG-3'; antisense primer on exon 3 5'-TAGAAGACACAGAAGAGGCGC-3'.

2.2 X-Gal Staining

Anesthetized mice were perfused via the left ventricle with 10 ml of heparinized 0.9% NaCl solution at 37°C and subsequently 50 ml of 3% paraformaldehyde solution at 37°C and pH 7.4. Cryosections of kidneys (10 and 20 μm) were stained overnight at 37°C in the following mixture: 0.1 M phosphate buffer, X-gal (5-Bromo-4-chloro-3-indolyl β-D-Galactoside)1 mg/ml, 5 mM potassium ferricyanide, 5 mM potassium ferrocyanide, and 2 mM $MgCl_2$.

The targeting vector produced by Mitchell and colleagues encodes a β-galactosidase/neomycin-resistance fusion protein (β-geo) with a membrane-spanning domain. Both enzymatic activities of the fusion protein (resistance to neomycin and β-galactosidase activity) are only achieved when the transgene inserts within a gene that provides a secretory signal. In our case, the β-galactosidase (β-gal) is inserted in the TASK-2 gene and therefore is under its promoter. In TASK-2 knockout mice β-gal cleaves the X-gal glycosidic linkage in cells where TASK-2 promoter is active, such as proximal tubule cells, producing a soluble, colourless indoxyl monomer. Subsequently, two of the liberated indoxyl moieties form a dimer, which is non-enzymatically oxidized.

The resultant halogenated indigo is a very stable and insoluble blue compound. The ferricyanide and ferrocyanide form a blue precipitate (Prussian blue) upon reaction with free ferric ion which is soluble only in organic solvents and does not diffuse during the staining procedure. Wild type tissue is also stained in parallel to set the background due to the endogenous lysozomal β-gal present in all tissues. Its pH optimum is very low, and thus it is not very active in the pH 7.5-7.6 of the buffer used for the staining.

2.3 Plethysmographic measurements

Respiratory function was studied using whole body plethysmography on TASK-2 knockout mice (EMKA Technologies, France) (Figure 2). In contrast to "true" plethysmography, ventilation parameters are not measured as gas volumes by this setup but calculated from pressure changes after a calibration procedure. The important advantage of the device is the possibility of measuring respiratory parameters in non-anesthetized, unrestrained mice. Several respiratory parameters could be recorded from wild-type and knockout mice using iox software (EMKA Technologies, France).

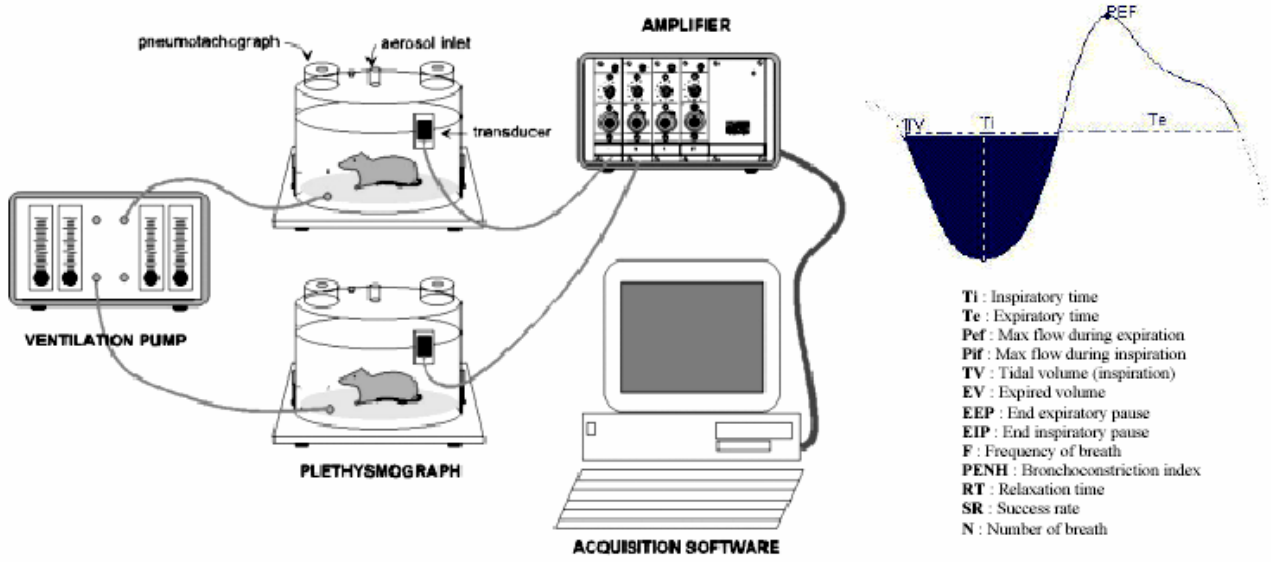

Figure 2. Whole body plethysmography. Four mice can be tested in parallel. On the right-hand side the respiratory parameters recorded by the software are depicted.

3. RESULTS

3.1 Genotyping of TASK-2 mice

The generation of TASK-$2^{-/-}$ mice was performed using a modified gene-trapping strategy that allows the isolation of insertional mutations specifically in secreted and membrane-spanning protein (Mitchell et al., 2001). By this technique the precise site of insertion of the secretory-trap vector into the target gene is not known. For that reason, such knockout mice have to be genotyped by neomycin-specific dot-blot. In principle, this technique works also for TASK-2-mice, but often it is difficult to distinguish between heterozygous and homozygous mice. Thus, this part of my project was aimed at establishing a PCR-based genotyping protocol which allows to clearly distinguishing heterozygous from homozygous mice. Dr. Mitchell suggested that the point of vector insertion is located in intron 2. Therefore, I tested several primer pairs in order to find a strategy for PCR-based genotyping of TASK2 mice using forward primers on exon 2. Unfortunately, I could not find such primers and, in addition, I could rule out an insertion of the targeting vector into intron 2 (Figure 3b). My data clearly indicate that the point of insertion is in the intron 1 which comprises around 30 kb and several CG-rich and repeats-containing regions (Figure 3a). Unfortunately, I could not precisely localize the point of insertion of the vector probably because of the large size of intron 1 and its “PCR-resistant” sequences. Therefore, I have established real-time PCR to genotype newborn mice by assessing the amount of a neomycin-specific amplicon.

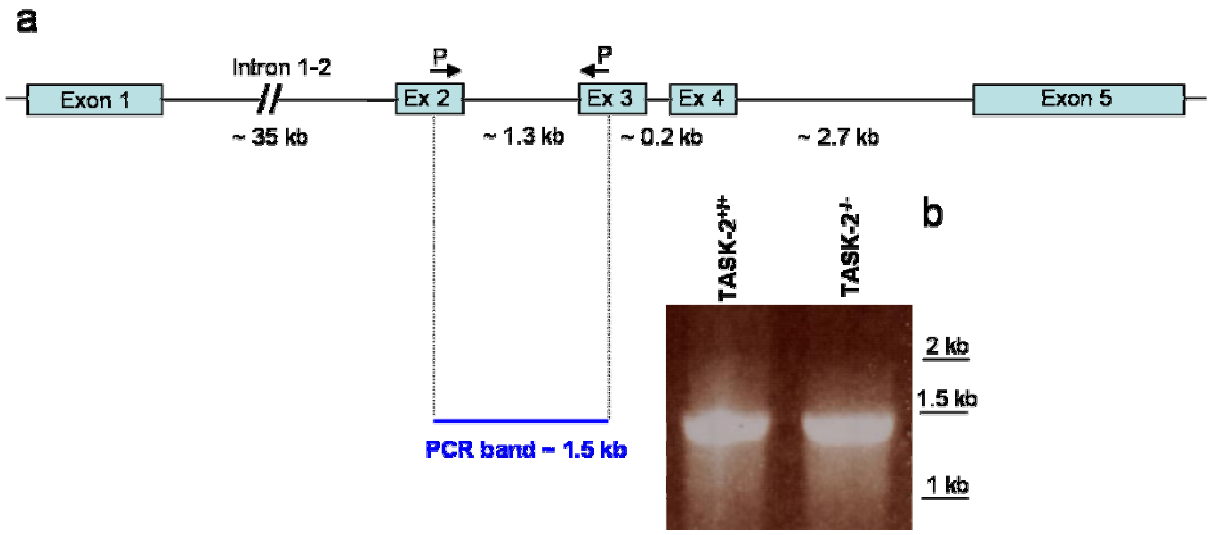

Figure 3. PCR-based genotyping of TASK-2 knockout mice. a. drawing of the TASK-2 gene on Chromosome 14 showing the arrangement of exons and introns. Intron sizes are indicated. P, primers. b. PCR product of the two primers depicted in the drawing on exons 2 and 3 using as template TASK-$2^{+/+}$ and TASK-$2^{-/-}$ genomic DNA. The identical band in both reactions demonstrate that the targeting vector is not inserted in the intron 2-3.

3.2 Localization of TASK-2

Expression analysis of TASK-2 by Northern blot and PCR indicated a very strong expression of this channel in the kidney, however, the precise distribution along the nephron was not clear (Reyes et al., 1998). I used the lacZ gene insertion by the knockout vector to visualize cells with an activated TASK-2 promotor via X-gal coloration. In kidney kryo-sections of TASK-2 $^{+/-}$ a strong X-gal staining was found in proximal tubules (Figure 4) and in papillary collecting ducts. Sections from wild-type animals did not show such a staining.

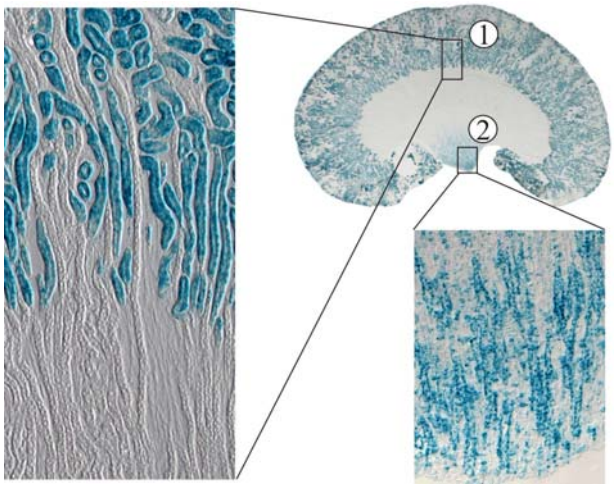

Figure 4. TASK-2 localization along the nephron. X-gal staining was performed on a 20 μm thick whole kidney section of a TASK-2 $^{+/-}$ mouse. Strong staining was found in convoluted and straight proximal tubules (1) and in papillary collecting ducts (2). Higher magnification pictures of respective areas are shown in inserts (Warth et al., 2004).

3.3 Plethysmographic measurements

In order to investigate the physiological role of TASK-2 in the regulation of ventilation, we used TASK-2 knockout mice for whole body plethysmographic measurements. Several respiratory parameters were recorded from wild-type and knockout mice.

In plethysmographic experiments, we found significant differences in the respiration pattern of TASK-2 knockout mice in comparison with wild-type animals. Hypoxic conditions were generated into the chambers by reducing the percentage of oxygen from 21 to 6, replacing the oxygen with nitrogen. The mice were kept in this condition for 15 minutes and the respiratory parameters were registered.

The knockouts were not able to cope with the oxygen reduction. This suggests a role of TASK-2 in the regulation of the respiration (Figure 5).

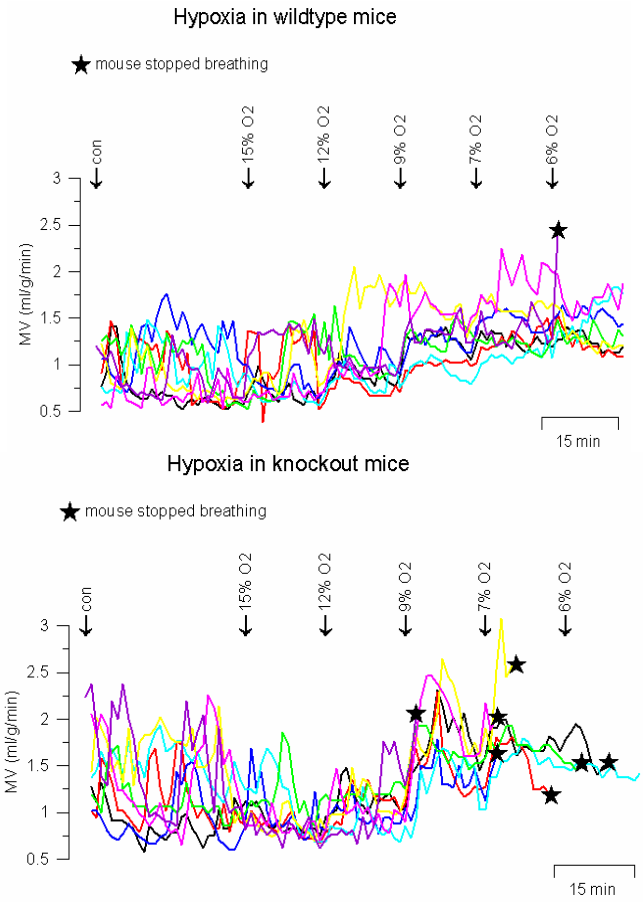

Figure 5. Plethysmography on TASK-2$^{+/+}$ and TASK-2$^{-/-}$ mice. Minute volume recording from different mice (for every mouse a different color) during hypoxia experiments. Wild-type mice are shown in the upper panel, TASK-2 knockouts in the lower one. The stars indicate the points where animals stopped breathing.

4. DISCUSSION

4.1 TASK2 targeting vector is inserted in intron 1

The secretory-trap vector produced by Mitchell and colleagues allows the access to all classes of proteins targeted to the secretory pathway and the insertions in these genes can be efficiently transmitted to the germ line (Mitchell et al., 2001). The genotyping strategy used by Mitchell and colleagues was based on dot-blot hybridization of tail biopsies (Brennan and Skarnes, 1999; Mitchell et al., 2001). We decided to use a different approach, designing specific primers for the PCR-based genotyping analysis. Firstly, we needed to identify the exact targeting vector insertion site. After excluding the

insertion in the intron 2-3 (Figure 3) we focused on the intron between exons 1 and 2 where the vector could have been inserted. The technical difficulties due to this intronic sequence lead us to modify our genotyping strategy quantifying by real time PCR the relative amount of the neomycin-resistance gene. This approach led to the successful screening of TASK-2 knockout mice.

4.2 TASK-2 localizes to proximal tubules and collecting ducts in mouse kidney

Reyes and colleagues showed by Northern blot and RT-PCR analyses that the TASK-2 message is poorly expressed or absent in the nervous and muscular systems but it is present in epithelial tissues, such as lung, colon, intestine, stomach, liver, and particularly in the kidney (Reyes et al., 1998; Warth et al., 2004). The distribution of TASK-2 within kidney cortex was examined by *in situ* hybridization, suggesting that the expression of TASK-2 is restricted to the cortical distal tubules and the collecting ducts (Reyes et al., 1998). In these structures, K^+-selective currents have been postulated to play a major role in the volume regulation and in the control of the negative potential of tubule cells, in the K^+ recycling across the basolateral membranes in conjunction with the Na-K-ATPase, and in the K^+ secretion into the tubular lumen in concert with Na^+ influx through amiloride-sensitive Na^+ channels (for reviews, see (Giebisch, 1998; Wang et al., 1997).

In contrast to the observations of Reyes and colleagues, our localization study on kidney sections from TASK-$2^{+/-}$ mice showed that the task-2 promoter-driven X-gal staining is present all along the proximal tubule and in papillary collecting ducts but not in cortical distal tubules or cortical collecting ducts (Warth et al., 2004). Together with our French collaborators, we have investigated the functional role of TASK-2 in the kidney. Patch-clamp experiments (performed by P. Poujeol) on proximal tubular cells isolated from wild-type and TASK-$2^{-/-}$ knockout mice showed that TASK-2-mediated K^+-conductance is activated during the basolateral transport of $NaHCO_3$ because extracellular HCO_3^- stimulated pH-sensitive TASK-2. By this mechanism, TASK-2 channels hyperpolarize the basolateral membrane thereby supporting further electrogenic $NaHCO_3$ export. To test the physiological significance of these in vitro data, we performed a series of *in vivo* experiments using the TASK-2 knockout mouse. TASK-2-/- mice when challenged with

high $NaHCO_3$ load displayed impaired Na^+ and water handling due to defects in proximal tubular $NaHCO_3$ reabsorption. Moreover, under control conditions TASK-2 knockout mice had higher urinary pH and HCO_3^- excretion leading to slight metabolic acidosis. In conclusion, these results demonstrate the importance of the functional coupling of TASK2 activity and proximal $NaHCO_3$ transport via basolateral, extracellular alkalinization. In addition, TASK-2 might be another candidate gene for genetic defects of proximal tubular bicarbonate reabsorption which lead to the syndrome o “proximal renal tubular acidosis” (OMIM 603493) (Warth et al., 2004).

4.2 Respiration of TASK-2$^{-/-}$ is affected during hypoxic conditions

The ability to maintain an adequate supply of oxygen is essential for survival. In many mammalian species, the major peripheral sensory organs for monitoring arterial oxygen level are the carotid bodies. The carotid body contains chemoreceptors that respond to hypoxia, hypercapnia and changes in hydrogen ion concentration (Gonzalez et al., 1994). Hypoxia activates the arterial oxygen receptors in the carotid bodies, which in turn stimulates the brainstem respiratory centre (via the carotid sinus nerve) and leads to a reflex increase in respiratory rate. The carotid body comprises clusters of ovoid type I (glomus) cells which are surrounded by glial-like type II (sustentacular) cells (for a review see (Gonzalez et al., 1994; Gronblad, 1983). It is generally accepted that type I cells are the initial sites of oxygen sensing. Hypoxia inhibits oxygen-sensitive K^+ channels in type I cells, which in turn leads to depolarization and Ca^{2+} entry via voltage-gated Ca^{2+} channels. The rise in intracellular [Ca^{2+}] ([$Ca^{2+}]_i$) in turn triggers the release of multiple neurotransmitters from type I cells (Gonzalez et al., 1994; Prabhakar, 2000).
Depolarization of type I cell during hypoxia has been suggested to involve the inhibition of several oxygen sensitive K^+ currents, including TASK-like K^+ channels. It has been shown that several types of voltage insensitive channel, TASK-1, TASK-2, TASK-3 and TRAAK, are expressed in type I cells of the rat carotid body. The so-called background leak K^+ current is inhibited by hypoxia in the rat isolated glomus cells thereby initiating the signal transduction cascade for hypoxia sensing (Yamamoto et al., 2002). During my thesis work, I have performed a pilot study to elucidate the potential role of TASK-2 in

oxygen sensing. We observed a larger scattering of the minute volumes of TASK-2 knockout mice under normoxic and hypoxic conditions. Moreover, lowering of oxygen (less than 9%) in the plethysmography chamber led several TASK-$2^{-/-}$ mice to stop breathing although respiratory depression could not been detected in those animals before. These observations suggest an impairment of the respiratory response upon hypoxia in TASK-2 knockout mice; however, other reasons to stop respiration (e.g. overall reduced performance and health) have still to be ruled out. The presumable localization of TASK-2 in oxygen-sensing cells in the carotyd bodies (Yamamoto et al., 2002) suggests that intact TASK-2 channels are required for the physiological cellular response to hypoxia. Based on the data presented here, a following-up study has now been started in Regensburg to examine TASK-2 expression in carotid bodies and central respiratory centres and the regulation of respiration in TASK-2 knockout mice in more detail.

BIBLIOGRAPHY

Achler, C., Filmer, D., Merte, C. and Drenckhahn, D. (1989) Role of microtubules in polarized delivery of apical membrane proteins to the brush border of the intestinal epithelium. *J Cell Biol*, **109**, 179-189.

Anderson, C.M., Grenade, D.S., Boll, M., Foltz, M., Wake, K.A., Kennedy, D.J., Munck, L.K., Miyauchi, S., Taylor, P.M., Campbell, F.C., Munck, B.G., Daniel, H., Ganapathy, V. and Thwaites, D.T. (2004) H+/amino acid transporter 1 (PAT1) is the imino acid carrier: An intestinal nutrient/drug transporter in human and rat. *Gastroenterology*, **127**, 1410-1422.

Avissar, N.E., Ryan, C.K., Ganapathy, V. and Sax, H.C. (2001) Na(+)-dependent neutral amino acid transporter ATB(0) is a rabbit epithelial cell brush-border protein. *Am J Physiol Cell Physiol*, **281**, C963-971.

Baba, T., Nonoguchi, H., Itoh, K., Nakayama, Y., Kohda, Y., Inoue, T. and Tomita, K. (2004) Gene regulation of renal-osmotic stress-induced Na-CL organic solute cotransporter. *Nephron Exp Nephrol*, **96**, e89-96.

Baron, D.N., Dent, C.E., Harris, H., Hart, E.W. and Jepson, J.B. (1956) Hereditary pellagra-like skin rash with temporary cerebellar ataxia, constant renal amino-aciduria, and other bizarre biochemical features. *Lancet*, **271**, 421-428.

Bauch, C., Forster, N., Loffing-Cueni, D., Summa, V. and Verrey, F. (2003) Functional cooperation of epithelial heteromeric amino acid transporters expressed in madin-darby canine kidney cells. *J Biol Chem*, **278**, 1316-1322.

Beckman, M.L. and Quick, M.W. (1998) Neurotransmitter transporters: regulators of function and functional regulation. *J Membr Biol*, **164**, 1-10.

Bennett, E.R. and Kanner, B.I. (1997) The membrane topology of GAT-1, a (Na+ + Cl-)-coupled gamma-aminobutyric acid transporter from rat brain. *J Biol Chem*, **272**, 1203-1210.

Boerner, P. and Saier, M.H., Jr. (1985) Hormonal regulation of the System A amino acid transport adaptive response mechanism in a kidney epithelial cell line (MDCK). *J Cell Physiol*, **122**, 316-322.

Bohmer, C., Broer, A., Munzinger, M., Kowalczuk, S., Rasko, J.E., Lang, F. and Broer, S. (2005) Characterization of mouse amino acid transporter B0AT1 (slc6a19). *Biochem J*, **389**, 745-751.

Boll, M., Daniel, H. and Gasnier, B. (2004) The SLC36 family: proton-coupled transporters for the absorption of selected amino acids from extracellular and intracellular proteolysis. *Pflugers Arch*, **447**, 776-779.

Boron, W.F., Fong, P., Hediger, M.A., Boulpaep, E.L. and Romero, M.F. (1997) The electrogenic Na/HCO3 cotransporter. *Wien Klin Wochenschr*, **109**, 445-456.

Borsani, G., Bassi, M.T., Sperandeo, M.P., De Grandi, A., Buoninconti, A., Riboni, M., Manzoni, M., Incerti, B., Pepe, A., Andria, G., Ballabio, A. and Sebastio, G. (1999) SLC7A7, encoding a putative permease-related protein, is mutated in patients with lysinuric protein intolerance. *Nat Genet*, **21**, 297-301.

Bossi, E., Giovannardi, S., Binda, F., Forlani, G. and Peres, A. (2002) Role of anion-cation interactions on the pre-steady-state currents of the rat Na(+)-Cl(-)-dependent GABA cotransporter rGAT1. *J Physiol*, **541**, 343-350.

Brennan, J. and Skarnes, W.C. (1999) Gene trapping in mouse embryonic stem cells. *Methods Mol Biol*, **97**, 123-138.

Broer, A., Klingel, K., Kowalczuk, S., Rasko, J.E., Cavanaugh, J. and Broer, S. (2004) Molecular cloning of mouse amino acid transport system B0, a neutral amino acid transporter related to Hartnup disorder. *J Biol Chem*, **279**, 24467-24476.
Broer, S. (2002) Adaptation of plasma membrane amino acid transport mechanisms to physiological demands. *Pflugers Arch*, **444**, 457-466.
Broer, S., Cavanaugh, J.A. and Rasko, J.E. (2005) Neutral amino acid transport in epithelial cells and its malfunction in Hartnup disorder. *Biochem Soc Trans*, **33**, 233-236.
Buckingham, S.D., Kidd, J.F., Law, R.J., Franks, C.J. and Sattelle, D.B. (2005) Structure and function of two-pore-domain K+ channels: contributions from genetic model organisms. *Trends Pharmacol Sci*, **26**, 361-367.
Burgess, D.R., Broschat, K.O. and Hayden, J.M. (1987) Tropomyosin distinguishes between the two actin-binding sites of villin and affects actin-binding properties of other brush border proteins. *J Cell Biol*, **104**, 29-40.
Camargo, S.M., Makrides, V., Virkki, L.V., Forster, I.C. and Verrey, F. (2005) Steady-state kinetic characterization of the mouse B(0)AT1 sodium-dependent neutral amino acid transporter. *Pflugers Arch*.
Camargo SMR, Makrides V, Virkki LV, Forster IC and F, a.V. (2005) A Steady-State Kinetic Characterization of the mouse B0AT1 Sodium-dependent Neutral Amino Acid Transporter. *Eur J Physiol*.
Campa, M.J. and Kilberg, M.S. (1989) Characterization of neutral and cationic amino acid transport in Xenopus oocytes. *J Cell Physiol*, **141**, 645-652.
Cariappa, R., Heath-Monnig, E. and Smith, C.H. (2003) Isoforms of amino acid transporters in placental syncytiotrophoblast: plasma membrane localization and potential role in maternal/fetal transport. *Placenta*, **24**, 713-726.
Chaudhry, F.A., Reimer, R.J. and Edwards, R.H. (2002) The glutamine commute: take the N line and transfer to the A. *J Cell Biol*, **157**, 349-355.
Chaudhry, F.A., Reimer, R.J., Krizaj, D., Barber, D., Storm-Mathisen, J., Copenhagen, D.R. and Edwards, R.H. (1999) Molecular analysis of system N suggests novel physiological roles in nitrogen metabolism and synaptic transmission. *Cell*, **99**, 769-780.
Chen, J.G., Liu-Chen, S. and Rudnick, G. (1998) Determination of external loop topology in the serotonin transporter by site-directed chemical labeling. *J Biol Chem*, **273**, 12675-12681.
Chen, N.H., Reith, M.E. and Quick, M.W. (2004) Synaptic uptake and beyond: the sodium- and chloride-dependent neurotransmitter transporter family SLC6. *Pflugers Arch*, **447**, 519-531.
Chesney, R.W. (2001) *in The Metabolic and Molecular Bases of Inherited Diseases*. McGraw-Hill Inc., New York.
Christensen, H.N. (1985) On the strategy of kinetic discrimination of amino acid transport systems. *J Membr Biol*, **84**, 97-103.
Christensen, H.N. (1989) Distinguishing amino acid transport systems of a given cell or tissue. *Methods Enzymol*, **173**, 576-616.
Christensen, H.N. (1990) Role of amino acid transport and countertransport in nutrition and metabolism. *Physiol Rev*, **70**, 43-77.
Coetzee, W.A., Amarillo, Y., Chiu, J., Chow, A., Lau, D., McCormack, T., Moreno, H., Nadal, M.S., Ozaita, A., Pountney, D., Saganich, M., Vega-Saenz de Miera, E.

and Rudy, B. (1999) Molecular diversity of K+ channels. *Ann N Y Acad Sci*, **868**, 233-285.
Dave, M.H., Schulz, N., Zecevic, M., Wagner, C.A. and Verrey, F. (2004) Expression of heteromeric amino acid transporters along the murine intestine. *J Physiol*, **558**, 597-610.
Doyle, D.A., Morais Cabral, J., Pfuetzner, R.A., Kuo, A., Gulbis, J.M., Cohen, S.L., Chait, B.T. and MacKinnon, R. (1998) The structure of the potassium channel: molecular basis of K+ conduction and selectivity. *Science*, **280**, 69-77.
Doyle, F.A. and McGivan, J.D. (1992) The bovine renal epithelial cell line NBL-1 expresses a broad specificity Na(+)-dependent neutral amino acid transport system (System Bo) similar to that in bovine renal brush border membrane vesicles. *Biochim Biophys Acta*, **1104**, 55-62.
Drenckhahn, D. and Dermietzel, R. (1988) Organization of the actin filament cytoskeleton in the intestinal brush border: a quantitative and qualitative immunoelectron microscope study. *J Cell Biol*, **107**, 1037-1048.
Elder, J.H. and Alexander, S. (1982) endo-beta-N-acetylglucosaminidase F: endoglycosidase from Flavobacterium meningosepticum that cleaves both high-mannose and complex glycoproteins. *Proc Natl Acad Sci U S A*, **79**, 4540-4544.
Eulenburg, V., Armsen, W., Betz, H. and Gomeza, J. (2005) Glycine transporters: essential regulators of neurotransmission. *Trends Biochem Sci*, **30**, 325-333.
Evers, J., Murer, H. and Kinne, R. (1976) Phenylalanine uptake in isolated renal brush border vesicles. *Biochim Biophys Acta*, **426**, 598-615.
Fass, S.J., Hammerman, M.R. and Sacktor, B. (1977) Transport of amino acids in renal brush border membrane vesicles. Uptake of the neutral amino acid L-alanine. *J Biol Chem*, **252**, 583-590.
Feliubadalo, L., Arbones, M.L., Manas, S., Chillaron, J., Visa, J., Rodes, M., Rousaud, F., Zorzano, A., Palacin, M. and Nunes, V. (2003) Slc7a9-deficient mice develop cystinuria non-I and cystine urolithiasis. *Hum Mol Genet*, **12**, 2097-2108.
Fernandez, E., Carrascal, M., Rousaud, F., Abian, J., Zorzano, A., Palacin, M. and Chillaron, J. (2002) rBAT-b(0,+)AT heterodimer is the main apical reabsorption system for cystine in the kidney. *Am J Physiol Renal Physiol*, **283**, F540-548.
Fernandez, E., Torrents, D., Chillaron, J., Martin Del Rio, R., Zorzano, A. and Palacin, M. (2003) Basolateral LAT-2 has a major role in the transepithelial flux of L-cystine in the renal proximal tubule cell line OK. *J Am Soc Nephrol*, **14**, 837-847.
Ganapathy, V., Bransch M, and Leibach FH. (1994) *Intestinal transport of amino acids and peptides. In: Physiology of the Gastrointestinal Tract (3rd ed.)*. Johnson LR.
Ganapathy, V., Ganapathy ME, and Leibach FH., edited by Barrett KE, and Donowitz M. (2001) Intestinal transport of peptides and amino acids. In: Current Topics in Membranes. 379-412.
Ganapathy, V., Roesel, R.A., Howard, J.C. and Leibach, F.H. (1983) Interaction of proline, 5-oxoproline, and pipecolic acid for renal transport in the rabbit. *J Biol Chem*, **258**, 2266-2272.
Gasnier, B. (2004) The SLC32 transporter, a key protein for the synaptic release of inhibitory amino acids. *Pflugers Arch*, **447**, 756-759.
Geibel, J., Giebisch, G. and Boron, W.F. (1989) Basolateral sodium-coupled acid-base transport mechanisms of the rabbit proximal tubule. *Am J Physiol*, **257**, F790-797.
Gibson, M.C. and Perrimon, N. (2003) Apicobasal polarization: epithelial form and function. *Curr Opin Cell Biol*, **15**, 747-752.

Giebisch, G. (1998) Renal potassium transport: mechanisms and regulation. *Am J Physiol*, **274**, F817-833.
Gonzalez, C., Almaraz, L., Obeso, A. and Rigual, R. (1994) Carotid body chemoreceptors: from natural stimuli to sensory discharges. *Physiol Rev*, **74**, 829-898.
Gronblad, M. (1983) Function and structure of the carotid body. *Med Biol*, **61**, 229-248.
Halestrap, A.P. and Meredith, D. (2004) The SLC16 gene family-from monocarboxylate transporters (MCTs) to aromatic amino acid transporters and beyond. *Pflugers Arch*, **447**, 619-628.
Hastrup, H., Karlin, A. and Javitch, J.A. (2001) Symmetrical dimer of the human dopamine transporter revealed by cross-linking Cys-306 at the extracellular end of the sixth transmembrane segment. *Proc Natl Acad Sci U S A*, **98**, 10055-10060.
Hediger, M.A., Romero, M.F., Peng, J.B., Rolfs, A., Takanaga, H. and Bruford, E.A. (2004) The ABCs of solute carriers: physiological, pathological and therapeutic implications of human membrane transport proteinsIntroduction. *Pflugers Arch*, **447**, 465-468.
Hernando, N., Forster, I.C., Biber, J. and Murer, H. (2000) Molecular characteristics of phosphate transporters and their regulation. *Exp Nephrol*, **8**, 366-375.
Ishii, T., Nakayama, K., Sato, H., Miura, K., Yamada, M., Yamada, K., Sugita, Y. and Bannai, S. (1991) Expression of the mouse macrophage cystine transporter in Xenopus laevis oocytes. *Arch Biochem Biophys*, **289**, 71-75.
Jan, L.Y. and Jan, Y.N. (1997) Voltage-gated and inwardly rectifying potassium channels. *J Physiol*, **505 (Pt 2)**, 267-282.
Jiang, Y., Lee, A., Chen, J., Ruta, V., Cadene, M., Chait, B.T. and MacKinnon, R. (2003) X-ray structure of a voltage-dependent K+ channel. *Nature*, **423**, 33-41.
Justice, M.J. and Stephenson, D.A. (1994) Mouse chromosome 13. *Mamm Genome*, **5 Spec No**, S196-206.
Kanai, Y. and Hediger, M.A. (2004) The glutamate/neutral amino acid transporter family SLC1: molecular, physiological and pharmacological aspects. *Pflugers Arch*, **447**, 469-479.
Kanai, Y., Lee, W.S., You, G., Brown, D. and Hediger, M.A. (1994) The human kidney low affinity Na+/glucose cotransporter SGLT2. Delineation of the major renal reabsorptive mechanism for D-glucose. *J Clin Invest*, **93**, 397-404.
Kekuda, R., Torres-Zamorano, V., Fei, Y.J., Prasad, P.D., Li, H.W., Mader, L.D., Leibach, F.H. and Ganapathy, V. (1997) Molecular and functional characterization of intestinal Na(+)-dependent neutral amino acid transporter B0. *Am J Physiol*, **272**, G1463-1472.
Kempson, S.A. (1998) Differential activation of system A and betaine/GABA transport in MDCK cell membranes by hypertonic stress. *Biochim Biophys Acta*, **1372**, 117-123.
Kilic, F. and Rudnick, G. (2000) Oligomerization of serotonin transporter and its functional consequences. *Proc Natl Acad Sci U S A*, **97**, 3106-3111.
Kiss, H., Darai, E., Kiss, C., Kost-Alimova, M., Klein, G., Dumanski, J.P. and Imreh, S. (2002) Comparative human/murine sequence analysis of the common eliminated region 1 from human 3p21.3. *Mamm Genome*, **13**, 646-655.
Kiss, H., Kedra, D., Kiss, C., Kost-Alimova, M., Yang, Y., Klein, G., Imreh, S. and Dumanski, J.P. (2001) The LZTFL1 gene is a part of a transcriptional map

covering 250 kb within the common eliminated region 1 (C3CER1) in 3p21.3. *Genomics*, **73**, 10-19.
Kiss, H., Yang, Y., Kiss, C., Andersson, K., Klein, G., Imreh, S. and Dumanski, J.P. (2002) The transcriptional map of the common eliminated region 1 (C3CER1) in 3p21.3. *Eur J Hum Genet*, **10**, 52-61.
Kleta, R., Romeo, E., Ristic, Z., Ohura, T., Stuart, C., Arcos-Burgos, M., Dave, M.H., Wagner, C.A., Camargo, S.R., Inoue, S., Matsuura, N., Helip-Wooley, A., Bockenhauer, D., Warth, R., Bernardini, I., Visser, G., Eggermann, T., Lee, P., Chairoungdua, A., Jutabha, P., Babu, E., Nilwarangkoon, S., Anzai, N., Kanai, Y., Verrey, F., Gahl, W.A. and Koizumi, A. (2004) Mutations in SLC6A19, encoding B0AT1, cause Hartnup disorder. *Nat Genet*, **36**, 999-1002.
Kowalczuk, S., Broer, A., Munzinger, M., Tietze, N., Klingel, K. and Broer, S. (2005) Molecular cloning of the mouse IMINO system: an Na+- and Cl--dependent proline transporter. *Biochem J*, **386**, 417-422.
Kummer, W. and Yamamoto, Y. (2002) Cellular distribution of oxygen sensor candidates-oxidases, cytochromes, K+-channels--in the carotid body. *Microsc Res Tech*, **59**, 234-242.
Kuo, A., Gulbis, J.M., Antcliff, J.F., Rahman, T., Lowe, E.D., Zimmer, J., Cuthbertson, J., Ashcroft, F.M., Ezaki, T. and Doyle, D.A. (2003) Crystal structure of the potassium channel KirBac1.1 in the closed state. *Science*, **300**, 1922-1926.
Leibach, F.H. and Ganapathy, V. (1996) Peptide transporters in the intestine and the kidney. *Annu Rev Nutr*, **16**, 99-119.
Lesage, F. (2003) Pharmacology of neuronal background potassium channels. *Neuropharmacology*, **44**, 1-7.
Lesage, F., Guillemare, E., Fink, M., Duprat, F., Lazdunski, M., Romey, G. and Barhanin, J. (1996) TWIK-1, a ubiquitous human weakly inward rectifying K+ channel with a novel structure. *Embo J*, **15**, 1004-1011.
Lesage, F. and Lazdunski, M. (2000) Molecular and functional properties of two-pore-domain potassium channels. *Am J Physiol Renal Physiol*, **279**, F793-801.
Levy, L.L. (2001) *in The Metabolic and Molecular Bases of Inherited Diseases*. McGraw-Hill Inc., New York.
Liang, R., Fei, Y.J., Prasad, P.D., Ramamoorthy, S., Han, H., Yang-Feng, T.L., Hediger, M.A., Ganapathy, V. and Leibach, F.H. (1995) Human intestinal H+/peptide cotransporter. Cloning, functional expression, and chromosomal localization. *J Biol Chem*, **270**, 6456-6463.
Lill, H. and Nelson, N. (1998) Homologies and family relationships among Na+/Cl- neurotransmitter transporters. *Methods Enzymol*, **296**, 425-436.
Long, S.B., Campbell, E.B. and Mackinnon, R. (2005) Crystal structure of a mammalian voltage-dependent Shaker family K+ channel. *Science*, **309**, 897-903.
Long, S.B., Campbell, E.B. and Mackinnon, R. (2005) Voltage sensor of Kv1.2: structural basis of electromechanical coupling. *Science*, **309**, 903-908.
Loo, D.D., Eskandari, S., Boorer, K.J., Sarkar, H.K. and Wright, E.M. (2000) Role of Cl- in electrogenic Na+-coupled cotransporters GAT1 and SGLT1. *J Biol Chem*, **275**, 37414-37422.
Mackenzie, B. and Erickson, J.D. (2004) Sodium-coupled neutral amino acid (System N/A) transporters of the SLC38 gene family. *Pflugers Arch*, **447**, 784-795.

Madara, J. and Trier, J. (1986) Functional morphology of the mucosa of the small intestine. In LR, J. (ed.), *Physiology of the Gastrointestinal Tract*. Raven Press, New York, p. 44.
Mingarro, I., Nilsson, I., Whitley, P. and von Heijne, G. (2000) Different conformations of nascent polypeptides during translocation across the ER membrane. *BMC Cell Biol*, **1**, 3.
Mitchell, K.J., Pinson, K.I., Kelly, O.G., Brennan, J., Zupicich, J., Scherz, P., Leighton, P.A., Goodrich, L.V., Lu, X., Avery, B.J., Tate, P., Dill, K., Pangilinan, E., Wakenight, P., Tessier-Lavigne, M. and Skarnes, W.C. (2001) Functional analysis of secreted and transmembrane proteins critical to mouse development. *Nat Genet*, **28**, 241-249.
Miyai, A., Yamauchi, A., Moriyama, T., Kaneko, T., Takenaka, M., Sugiura, T., Kitamura, H., Ando, A., Tohyama, M., Shimada, S., Imai, E. and Kamada, T. (1996) Expression of betaine transporter mRNA: its unique localization and rapid regulation in rat kidney. *Kidney Int*, **50**, 819-827.
Moeckel, G.W., Lai, L.W., Guder, W.G., Kwon, H.M. and Lien, Y.H. (1997) Kinetics and osmoregulation of Na(+)-and Cl(-)-dependent betaine transporter in rat renal medulla. *Am J Physiol*, **272**, F100-106.
Mooseker, M.S. (1985) Organization, chemistry, and assembly of the cytoskeletal apparatus of the intestinal brush border. *Annu Rev Cell Biol*, **1**, 209-241.
Mooseker, M.S., Bonder, E.M., Conzelman, K.A., Fishkind, D.J., Howe, C.L. and Keller, T.C., 3rd. (1984) The cytoskeletal apparatus of the intestinal brush border. *Kroc Found Ser*, **17**, 287-307.
Mora, C., Chillaron, J., Calonge, M.J., Forgo, J., Testar, X., Nunes, V., Murer, H., Zorzano, A. and Palacin, M. (1996) The rBAT gene is responsible for L-cystine uptake via the b0,(+)-like amino acid transport system in a "renal proximal tubular" cell line (OK cells). *J Biol Chem*, **271**, 10569-10576.
Munck, B.G. and Munck, L.K. (1994) Phenylalanine transport in rabbit small intestine. *J Physiol*, **480 (Pt 1)**, 99-107.
Munck, B.G., Munck, L.K., Rasmussen, S.N. and Polache, A. (1994) Specificity of the imino acid carrier in rat small intestine. *Am J Physiol*, **266**, R1154-1161.
Munck, L.K. and Munck, B.G. (1994) Chloride-dependent intestinal transport of imino and beta-amino acids in the guinea pig and rat. *Am J Physiol*, **266**, R997-1007.
Munck, L.K. and Munck, B.G. (1995) Amino acid transport in the small intestine. *Physiol Res*, **44**, 335-346.
Murer, H., Evers, J. and Kinne, R. (1976) Polarity of proximal tubular epithelial cells in relation to transepithelial transport. *Curr Probl Clin Biochem*, **6**, 173-189.
Nash, S.R., Giros, B., Kingsmore, S.F., Kim, K.M., el-Mestikawy, S., Dong, Q., Fumagalli, F., Seldin, M.F. and Caron, M.G. (1998) Cloning, gene structure and genomic localization of an orphan transporter from mouse kidney with six alternatively-spliced isoforms. *Receptors Channels*, **6**, 113-128.
Nelson, N. (1998) The family of Na+/Cl- neurotransmitter transporters. *J Neurochem*, **71**, 1785-1803.
Nozaki, J., Dakeishi, M., Ohura, T., Inoue, K., Manabe, M., Wada, Y. and Koizumi, A. (2001) Homozygosity mapping to chromosome 5p15 of a gene responsible for Hartnup disorder. *Biochem Biophys Res Commun*, **284**, 255-260.

Obermuller, N., Kranzlin, B., Verma, R., Gretz, N., Kriz, W. and Witzgall, R. (1997) Renal osmotic stress-induced cotransporter: expression in the newborn, adult and post-ischemic rat kidney. *Kidney Int*, **52**, 1584-1592.

Oxender, D.L. and Christensen, H.N. (1963) Distinct Mediating Systems For The Transport Of Neutral Amino Acids By The Ehrlich Cell. *J Biol Chem*, **238**, 3686-3699.

Pajor, A.M., Hirayama, B.A. and Wright, E.M. (1992) Molecular evidence for two renal Na+/glucose cotransporters. *Biochim Biophys Acta*, **1106**, 216-220.

Palacin, M., Bertran, J. and Zorzano, A. (2000) Heteromeric amino acid transporters explain inherited aminoacidurias. *Curr. Opin. Nephrol. Hypertens.*, **9**, 547-553.

Palacin, M., Estevez, R., Bertran, J. and Zorzano, A. (1998) Molecular biology of mammalian plasma membrane amino acid transporters. *Physiol Rev*, **78**, 969-1054.

Palacin, M. and Kanai, Y. (2004) The ancillary proteins of HATs: SLC3 family of amino acid transporters. *Pflugers Arch*, **447**, 490-494.

Pfeiffer, R., Loffing, J., Rossier, G., Bauch, C., Meier, C., Eggermann, T., Loffing-Cueni, D., Kuhn, L.C. and Verrey, F. (1999) Luminal heterodimeric amino acid transporter defective in cystinuria. *Mol Biol Cell*, **10**, 4135-4147.

Poppe, R., Karbach, U., Gambaryan, S., Wiesinger, H., Lutzenburg, M., Kraemer, M., Witte, O.W. and Koepsell, H. (1997) Expression of the Na+-D-glucose cotransporter SGLT1 in neurons. *J Neurochem*, **69**, 84-94.

Porter, R.K. (2000) Mammalian mitochondrial inner membrane cationic and neutral amino acid carriers. *Biochim Biophys Acta*, **1459**, 356-362.

Potter, S.J., Lu, A., Wilcken, B., Green, K. and Rasko, J.E. (2002) Hartnup disorder: polymorphisms identified in the neutral amino acid transporter SLC1A5. *J Inherit Metab Dis*, **25**, 437-448.

Prabhakar, N.R. (2000) Oxygen sensing by the carotid body chemoreceptors. *J Appl Physiol*, **88**, 2287-2295.

Quan, H., Athirakul, K., Wetsel, W.C., Torres, G.E., Stevens, R., Chen, Y.T., Coffman, T.M. and Caron, M.G. (2004) Hypertension and impaired glycine handling in mice lacking the orphan transporter XT2. *Mol Cell Biol*, **24**, 4166-4173.

Rabito, C.A. and Karish, M.V. (1982) Polarized amino acid transport by an epithelial cell line of renal origin (LLC-PK1). The basolateral systems. *J Biol Chem*, **257**, 6802-6808.

Rabito, C.A. and Karish, M.V. (1983) Polarized amino acid transport by an epithelial cell line of renal origin (LLC-PK1). The apical systems. *J Biol Chem*, **258**, 2543-2547.

Reyes, R., Duprat, F., Lesage, F., Fink, M., Salinas, M., Farman, N. and Lazdunski, M. (1998) Cloning and expression of a novel pH-sensitive two pore domain K+ channel from human kidney. *J Biol Chem*, **273**, 30863-30869.

Ristic, Z., Camargo, S., Romeo, E., Bodoy, S., Bertran, J., Palacin, M., Makrides, V., Furrer, E. and Verrey, F. (2005) Neutral amino acid transport mediated by ortholog of imino acid transporter SIT1/SLC6A20 in opossum kidney cells. *AJP:Renal Phys*.

Roigaard-Petersen, H., Jacobsen, C. and Iqbal Sheikh, M. (1987) H+-L-proline cotransport by vesicles from pars convoluta of rabbit proximal tubule. *Am J Physiol*, **253**, F15-20.

Romeo, E., Dave, M.H., Bacic, D., Ristic, Z., Camargo, S.M.R., Loffing, J., Wagner, C.A. and Verrey, F. (2005) Luminal kidney and intestine SLC6 amino acid transporters of B0AT-cluster and their tissue distribution in Mus musculus. *AJP:Renal Phys*.

Rossier, G., Meier, C., Bauch, C., Summa, V., Sordat, B., Verrey, F. and Kuhn, L.C. (1999) LAT2, a new basolateral 4F2hc/CD98-associated amino acid transporter of kidney and intestine. *J Biol Chem*, **274**, 34948-34954.

Rudnick, G. and Clark, J. (1993) From synapse to vesicle: the reuptake and storage of biogenic amine neurotransmitters. *Biochim Biophys Acta*, **1144**, 249-263.

Samarzija, I. and Fromter, E. (1982) Electrophysiological analysis of rat renal sugar and amino acid transport. III. Neutral amino acids. *Pflugers Arch*, **393**, 119-209.

Sano, Y., Inamura, K., Miyake, A., Mochizuki, S., Kitada, C., Yokoi, H., Nozawa, K., Okada, H., Matsushime, H. and Furuichi, K. (2003) A novel two-pore domain K+ channel, TRESK, is localized in the spinal cord. *J Biol Chem*, **278**, 27406-27412.

Schmid, J.A., Scholze, P., Kudlacek, O., Freissmuth, M., Singer, E.A. and Sitte, H.H. (2001) Oligomerization of the human serotonin transporter and of the rat GABA transporter 1 visualized by fluorescence resonance energy transfer microscopy in living cells. *J Biol Chem*, **276**, 3805-3810.

Seow, H.F., Broer, S., Broer, A., Bailey, C.G., Potter, S.J., Cavanaugh, J.A. and Rasko, J.E. (2004) Hartnup disorder is caused by mutations in the gene encoding the neutral amino acid transporter SLC6A19. *Nat Genet*, **36**, 1003-1007.

Shen, H., Smith, D.E., Yang, T., Huang, Y.G., Schnermann, J.B. and Brosius, F.C., 3rd. (1999) Localization of PEPT1 and PEPT2 proton-coupled oligopeptide transporter mRNA and protein in rat kidney. *Am J Physiol*, **276**, F658-665.

Sigrist-Nelson, K., Murer, H. and Hopfer, U. (1975) Active alanine transport in isolated brush border membranes. *J Biol Chem*, **250**, 5674-5680.

Silbernagl, S., Foulkes, E.C. and Deetjen, P. (1975) Renal transport of amino acids. *Rev Physiol Biochem Pharmacol*, **74**, 105-167.

Smith, Q.R. (2000) Transport of glutamate and other amino acids at the blood-brain barrier. *J Nutr*, **130**, 1016S-1022S.

Snutch, T.P. (1988) The use of Xenopus oocytes to probe synaptic communication. *Trends Neurosci*, **11**, 250-256.

Solbu, T.T., Boulland, J.L., Zahid, W., Lyamouri Bredahl, M.K., Amiry-Moghaddam, M., Storm-Mathisen, J., Roberg, B.A. and Chaudhry, F.A. (2005) Induction and targeting of the glutamine transporter SN1 to the basolateral membranes of cortical kidney tubule cells during chronic metabolic acidosis suggest a role in pH regulation. *J Am Soc Nephrol*, **16**, 869-877.

Sorkina, T., Doolen, S., Galperin, E., Zahniser, N.R. and Sorkin, A. (2003) Oligomerization of dopamine transporters visualized in living cells by fluorescence resonance energy transfer microscopy. *J Biol Chem*, **278**, 28274-28283.

Souba, W.W., Pan, M. and Stevens, B.R. (1992) Kinetics of the sodium-dependent glutamine transporter in human intestinal cell confluent monolayers. *Biochem Biophys Res Commun*, **188**, 746-753.

Steffgen, J., Koepsell, H. and Schwarz, W. (1991) Endogenous L-glutamate transport in oocytes of Xenopus laevis. *Biochim Biophys Acta*, **1066**, 14-20.

Stevens, B.R., Kaunitz, J.D. and Wright, E.M. (1984) Intestinal transport of amino acids and sugars: advances using membrane vesicles. *Annu Rev Physiol*, **46**, 417-433.

Stevens, B.R., Ross, H.J. and Wright, E.M. (1982) Multiple transport pathways for neutral amino acids in rabbit jejunal brush border vesicles. *J Membr Biol*, **66**, 213-225.

Stevens, B.R. and Wright, E.M. (1985) Kinetic model of the brush-border proline/sodium (IMINO) cotransporter. *Ann N Y Acad Sci*, **456**, 115-117.

Stevens, B.R. and Wright, E.M. (1985) Substrate specificity of the intestinal brush-border proline/sodium (IMINO) transporter. *J Membr Biol*, **87**, 27-34.

Stevens, B.R. and Wright, E.M. (1987) Kinetics of the intestinal brush border proline (Imino) carrier. *J Biol Chem*, **262**, 6546-6551.

Stoll, J., Wadhwani, K.C. and Smith, Q.R. (1993) Identification of the cationic amino acid transporter (System y+) of the rat blood-brain barrier. *J Neurochem*, **60**, 1956-1959.

Takanaga, H., Mackenzie, B., Suzuki, Y. and Hediger, M.A. (2005) Identification of mammalian proline transporter SIT1 (SLC6A20) with characteristics of classical system imino. *J Biol Chem*, **280**, 8974-8984.

Taylor, P.M., Hundal, H.S. and Rennie, M.J. (1989) Transport of glutamine in Xenopus laevis oocytes: relationship with transport of other amino acids. *J Membr Biol*, **112**, 149-157.

Torrents, D., Mykkanen, J., Pineda, M., Feliubadalo, L., Estevez, R., de Cid, R., Sanjurjo, P., Zorzano, A., Nunes, V., Huoponen, K., Reinikainen, A., Simell, O., Savontaus, M.L., Aula, P. and Palacin, M. (1999) Identification of SLC7A7, encoding y+LAT-1, as the lysinuric protein intolerance gene. *Nat Genet*, **21**, 293-296.

Torres, G.E., Carneiro, A., Seamans, K., Fiorentini, C., Sweeney, A., Yao, W.D. and Caron, M.G. (2003) Oligomerization and trafficking of the human dopamine transporter. Mutational analysis identifies critical domains important for the functional expression of the transporter. *J Biol Chem*, **278**, 2731-2739.

Verrey, F., Closs, E.I., Wagner, C.A., Palacin, M., Endou, H. and Kanai, Y. (2004) CATs and HATs: the SLC7 family of amino acid transporters. *Pflugers Arch*, **447**, 532-542.

Verrey, F., Ristic, Z., Romeo, E., Ramadan, T., Makrides, V., Dave, M.H., Wagner, C.A. and Camargo, S.M. (2005) Novel renal amino acid transporters. *Annu Rev Physiol*, **67**, 557-572.

Wang, W., Hebert, S.C. and Giebisch, G. (1997) Renal K+ channels: structure and function. *Annu Rev Physiol*, **59**, 413-436.

Warth, R., Barriere, H., Meneton, P., Bloch, M., Thomas, J., Tauc, M., Heitzmann, D., Romeo, E., Verrey, F., Mengual, R., Guy, N., Bendahhou, S., Lesage, F., Poujeol, P. and Barhanin, J. (2004) Proximal renal tubular acidosis in TASK2 K+ channel-deficient mice reveals a mechanism for stabilizing bicarbonate transport. *Proc Natl Acad Sci U S A*, **101**, 8215-8220.

Wasserman, J.C., Delpire, E., Tonidandel, W., Kojima, R. and Gullans, S.R. (1994) Molecular characterization of ROSIT, a renal osmotic stress-induced Na(+)-Cl(-)-organic solute cotransporter. *Am J Physiol*, **267**, F688-694.

Wright M. W., El-Mehidi N. S., Bruford E. A., Khodiyar V. K., Lovering R. C., Lush M. J., C. C. Talbot Jr., Wain H. M. and Povey S. (2003) Family matters - naming genes within families. *European Journal of Biochemistry*, **Supplement 1**.

Yamamoto, Y., Kummer, W., Atoji, Y. and Suzuki, Y. (2002) TASK-1, TASK-2, TASK-3 and TRAAK immunoreactivities in the rat carotid body. *Brain Res*, **950**, 304-307.

Yamashita, A., Singh, S.K., Kawate, T., Jin, Y. and Gouaux, E. (2005) Crystal structure of a bacterial homologue of Na(+)/Cl(-)-dependent neurotransmitter transporters. *Nature*.

Yamauchi, A., Kwon, H.M., Uchida, S., Preston, A.S. and Handler, J.S. (1991) Myo-inositol and betaine transporters regulated by tonicity are basolateral in MDCK cells. *Am J Physiol*, **261**, F197-202.

Yamauchi, A., Uchida, S., Kwon, H.M., Preston, A.S., Robey, R.B., Garcia-Perez, A., Burg, M.B. and Handler, J.S. (1992) Cloning of a Na(+)- and Cl(-)-dependent betaine transporter that is regulated by hypertonicity. *J Biol Chem*, **267**, 649-652.

You, G., Lee, W.S., Barros, E.J., Kanai, Y., Huo, T.L., Khawaja, S., Wells, R.G., Nigam, S.K. and Hediger, M.A. (1995) Molecular characteristics of Na(+)-coupled glucose transporters in adult and embryonic rat kidney. *J Biol Chem*, **270**, 29365-29371.

Zhou, Y., Morais-Cabral, J.H., Kaufman, A. and MacKinnon, R. (2001) Chemistry of ion coordination and hydration revealed by a K+ channel-Fab complex at 2.0 A resolution. *Nature*, **414**, 43-48.

CURRICULUM VITAE

First name: ELISA

Family name: ROMEO

Place and date of birth: Busto Arsizio (VA), Italy, 31st December 1978

Nationality: Italian

Previous studies:

September 1984-June 1992: Elementary and Middle schools, Gallarate (VA), Italy.

September 1992-July 1997: High school I.P.S.S.C. “Giovanni Falcone”, Gallarate (VA), Italy.

July 1997: Maturità (Diploma) (58 out of 60)

September 1997- July 2002: Biological Sciences at University of Insubria, Varese (VA), Italy.

May 2001-July 2002: Thesis project at DBSF University of Insubria, Varese (VA), Italy. Group Prof. A. Peres, Cellular and Molecular Physiology Laboratory. Title of the thesis: “Loop extracitoplasmatici dei trasportatori Na^+/Cl^- -dipendenti coinvolti nella selettività del substrato” (English translation: “Extracitoplasmatic loops of Na^+/Cl^- -dependent transporters involved in the substrate selectivity”).

Subject: cellular and molecular physiology.

July 2002:	Laurea degree (mark: 107 out of 110) at University of Insubria, Varese (VA), Italy. Master Degree in Biological Sciences.
Since September 2002:	PhD Student at University of Zurich, Institute of Physiology, Winterthurerstrasse 190, 8057 Zürich. Group Prof. Dr. F. Verrey “Epithelial Transports”. Project title: Sodium/amino acid cotransporters from the SLC6 family localizing to the luminal membrane of kidney and intestine
	PhD Supervisors: Prof. Dr. François Verrey Prof. Dr. Esther Stoeckli Prof. Dr. Richard Warth

ACKNOWLEDGEMENTS

There are many people I want to acknowledge for this three-year PhD.

Starting from the supervisors I had during this time I want to thank Richard and François for the support in my work, the fruitful discussions and the patience in reading the thesis and the manuscript of my first paper. Thanks also to Carsten who helped me in the regulation studies in mice.

A special thank also to Prof. Stoeckli who decided to take the responsibility of my thesis in front of the Faculty of Science and for showing great interest in our research.

I had a great time at the Institute of Physiology thanks to the nice people working there with me. I want to acknowledge all of them…
…thanks to Mital, Tamara, Simone, Vicky, Panos, Raffaella, Gabi, Esther, Markus, Emiljia, Zorica, Thomas, Dustin, Katja, Mirate, Mirko, Brigitte, Helen and Martin (I hope I did not forget anybody) in the Verrey group.
…moreover, thanks to Paola, Nati, Eva, Gerti, Ian for giving always good suggestions and support.

In general, thanks to all the people of the J-floor I did not mention above